

COMPARATIVE FUNDAMENTAL CRYOBIOLOGY OF MOUSE EMBRYONIC STEM CELLS

A Dissertation
presented to
the Faculty of the Graduate School
at the University of Missouri-Columbia

In Partial Fulfillment
of the Requirements for the Degree
Doctor of Philosophy

by
CORINNA MARY KASHUBA BENSON
Dr. John K. Critser, Dissertation Supervisor
DECEMBER 2009

© Copyright by Corinna Mary Kashuba Benson 2009

All Rights Reserved

The undersigned, appointed by the dean of the Graduate School, have examined the
dissertation entitled

**COMPARATIVE FUNDAMENTAL CRYOBIOLOGY OF MOUSE EMBRYONIC
STEM CELLS**

presented by Corinna Mary Kashuba Benson,
a candidate for the degree of doctor of philosophy,
and hereby certify that, in their opinion, it is worthy of acceptance.

John K. Critser, Ph.D.
Dissertation Supervisor

Yuksel Agca, D.V.M., Ph.D.

Elizabeth Bryda, Ph.D.

Mark Kirk, Ph.D.

Erik J. Woods, Ph.D.

The past several years were a wonderful journey.

Not only were my academic goals fulfilled, I gained a second half, my husband, James,
and a beautiful son, Jonathan William.

They make my life complete, and I am very happy.

ACKNOWLEDGEMENTS

I would like to extend my sincere gratitude to my advisor, Dr. John K. Critser, for his scientific and philosophic insights, his patience, and unwavering support throughout my time at MU. Dr. Critser gave me a renewed appreciation for statistics and experimental design, not to mention fantastic opportunities for travel, collaboration, and collegiality through the Society for Cryobiology Annual Meetings. It was amazing to watch him somehow transform awkward gatherings of multidisciplinary minds into collaborative, patent generating, research machines. It was an honor to be in his laboratory.

I also owe a depth of gratitude to my Ph.D. committee members. To Dr. Yuksel Agca, thank you for many long conversations over the years and for giving me much perspective on life during and beyond graduate school. To Dr. Elizabeth Bryda, thank you for being a good listener and for making things shine when they needed considerable buffing. To Dr. Mark Kirk, thank you also for your ear, and for being my stem cell expert – I loved your stem cell course and the people in it. To Dr. Erik Woods, thanks also for scientific insights, for making Cryo meetings fun, for your reassurances on life beyond graduate school, and for jumping on board my committee at last minute.

To my fellow Critser labmates, past and present, thank you for your positivity and friendship. Thanks, Jenn, for making me laugh and for watching Jack, and to Janelle for your good cheer and ability to seemingly handle anything. To Dr. Hongsheng Men, thanks for your wit, knowledge, and willingness to help. Thanks to Dr. Xu Han for your cryomicroscopy skills and congeniality. Thanks to Chongbei and Katie for your ES cell

conversations and energy. Thanks to Steve Mullen, now basking in the California sun, for his statistical skills at odd hours.

While life as a graduate student is interesting enough on its own, I have been fortunate to also be part of a dynamic and innovative group of individuals in the Comparative Medicine Residency Program. To these people, Craig Franklin, Cindy Besch-Williford, Robert S. Livingston, Lela Riley, Earl Steffen, Matt Myles, Beth Bauer, Lon Dixon, Bart Carter, Shari Hamilton, Sherrie Neff, Judy Green, all the OAR and RADIL staff, the Comparative Medicine Post-doctoral Research Fellows, and people too numerous to mention, I extend my sincere gratitude for their academic and personal support, good humor, and seemingly boundless energy. I must single out Dr. Craig Franklin to thank him for getting me here in the first place, for his sense of humor and scientific curiosity, and for being a constant source of encouragement. I must also single out Dr. Cindy Besch-Williford, in appreciation of her extreme listening skills and steadiness, not to mention encyclopedia-like knowledge. Thanks also to Bob Livingston, not only for his diagnostic prowess, but his volleyball skills. Thanks to all the RADIL-associated softball, volleyball, and dodgeball players for providing an entertainment outlet (for me, either as a spectator or as a participant) and reminding me why I never want to actually play dodgeball, and in particular, Greg Purdy, for taking the occasional volleyball in the face with good humor. Thanks also to Roseanne Mayfield for her warm spirit and versatility, for being the person I go to first with random questions and tasks, and for her friendship.

To Trina, Idelle, and DeShayda Martin, thank you for your warm hearts and for providing a stimulating and safe day-home for my son since he was 3 months old. Words

cannot express how fortunate we are to find someone we trust so much with a most precious person.

To my mother- and father-in-law, Barb and Dale Benson, thank you for your support and perspective, great dinners, cruises, Christmases, your excellent painting skills, and for being such loving grandparents. I am very lucky to have you.

To my brother and sister, Sheldon Kashuba and Shauna Kashuba Garrow, thanks for being your unique selves, for your strange senses of humor, for bringing me down to earth, for your encouragement, your conversations at all hours of the day, and the dimensions you and your families add to my life.

To my mother, Anna Kashuba, one of my favorite memories of my time in Missouri is the car trip down here, because it was with you. Thank you for all the telephone calls, the letters, the emails, the trips back and forth, the babysitting, and your unique and broad perspective on all things in life. I am who I am because of you.

To my son, Jonathan William, thank you for your laughter, the countless hours of rocking in the middle of the night, the way your face lights up, your boundless curiosity, energy, and love. You are pure joy.

Finally, to my husband, James, thank you for your calm spirit, your unusual sense of humor, the music you bring to my life, for being such a great dad to Jack, and for your analytical mind. Thank you for being someone I can spend twenty-four hours a day with, seven days a week, and still find it hard to part with you when we temporarily go our separate ways. You have contributed so much to this dissertation, not only in hours of data analysis but in simply being there for me. I love you and I owe you big!

TABLE OF CONTENTS

ACKNOWLEDGEMENTS	ii
LIST OF FIGURES	viii
LIST OF TABLES	ix
ABSTRACT	x
Chapter	
1. INTRODUCTION	1
Purpose.....	1
Significance.....	2
Cryobiology Fundamentals	5
Osmotic Tolerance Limits.....	8
Warming and Thawing	9
Fundamental Cryobiology of Mouse Embryonic Stem Cells	10
References.....	11
2. AN IMPROVED CRYOPRESERVATION METHOD FOR A MOUSE EMBRYONIC STEM CELL LINE	15
Introduction.....	15
Materials and Methods.....	20
Results.....	32
Discussion	37
References.....	44

3. COMPARATIVE FUNDAMENTAL CRYOBIOLOGY OF MULTIPLE MOUSE EMBRYONIC STEM CELL LINES AND THE IMPLICATIONS FOR EMBRYONIC STEM CELL CRYOPRESERVATION PROTOCOLS	50
Introduction.....	50
Materials and Methods.....	54
Results.....	61
Discussion	70
References.....	74
4. OPTIMIZED MOUSE EMBRYONIC STEM CELL CRYOPRESERVATION PROTOCOLS: A COMPARISON OF PREDICTED OPTIMAL COOLING RATES AND PLUNGE TEMPERATURES ACROSS FOUR MOUSE EMBRYONIC STEM CELL LINES AND EMPIRICAL VALIDATION OF PREDICTED OPTIMA.....	78
Introduction.....	78
Materials and Methods.....	80
Results.....	86
Discussion	92
References.....	104
5. THE INFLUENCE OF TEMPERATURE, CRYOPROTECTIVE AGENTS, AND LATRUNCULIN ON FUNDAMENTAL CRYOBIOLOGICAL PARAMETERS AND THEIR IMPLICATIONS TO IMPROVING CRYOPRESERVATION METHODS	107
Introduction.....	107
Materials and Methods.....	111
Results.....	121
Discussion	130
References.....	140

6. GENERAL DISCUSSION AND FUTURE DIRECTIONS	144
Overview.....	144
Conclusion	150
Future Studies	151
References.....	154
APPENDIX A.....	157
VITA	159

LIST OF FIGURES

Figure

2.1 Representative plots of calibrated cell volume versus time data from the Coulter counter.....	24
2.2 Plot of theoretical cell volume versus temperature during cooling and warming, and versus time at room temperature for cells in cryoprotectant.....	30
2.3 Boyle Van't Hoff relationship for C57BL/6 mouse embryonic stem cell line	33
2.4 Mean osmotic tolerance limits of C57BL/6 mouse embryonic stem cells as determined by plasma membrane integrity.....	34
2.5 An improved freezing protocol for C57BL/6 mouse embryonic stem cells.....	43
3.1 Percent post-thaw recoveries of four mouse embryonic stem cell lines frozen in cryovials in standard freezing conditions	62
3.2 Osmotic tolerance limits of five mouse embryonic stem cell lines as determined by plasma membrane integrity.....	64
4.1 A new standard protocol for mouse embryonic stem cells	103
5.1 Minimal cell volume of C57BL/6 mouse embryonic stem cells during preliminary subzero permeability experiments	109
5.2 When estimating spherical volumes, the magnitude of error changes according to the true shape of the measured area	110
5.3 Typical output plots of the method used to find population mean volumes in “noisy” data with the Coulter counter	117
5.4 Determining the minimum concentration of Latrunculin A for depolymerization of the actin cytoskeleton of C57BL/6 mouse embryonic stem cells	122
5.5 The effect of Latrunculin A on cell count and membrane integrity of C57BL/6 mouse embryonic stem cells.....	124
5.6 The effect of Latrunculin A on the post-thaw recovery of C57BL/6 mouse embryonic stem cells.....	125
5.7 Volume response of 1.5 M dimethyl sulfoxide-equilibrated cells in different osmolalities at -3°C.....	136

LIST OF TABLES

Table

2.1 Definition of major symbols and terms	19
2.2 Room temperature solute permeabilities and hydraulic conductivities, and their associated activation energies for C57BL/6 mouse embryonic stem cells with respect to four cryoprotective agents	35
2.3 Predicted optimal freezing rates for the C57BL/6 mouse embryonic stem cell line ...	35
3.1 Definition of major symbols and terms	53
3.2 Osmotically inactive cell volume of four mouse embryonic stem cell lines	63
3.3 Room temperature hydraulic conductivity, cryoprotectant permeability, and their associated activation energies for five mouse embryonic stem cell lines in the presence of 1.0 M cryoprotectant.....	69
4.1 Predicted optimal cooling rates for the BALB/c, CBA, FVB, and 129R1 mouse embryonic stem cell lines for three cryoprotectants	86
4.2 Experimental cryopreservation protocols that improved percent post-thaw recovery of BALB/c mouse embryonic stem cells.....	88
4.3 Experimental cryopreservation protocols that improved percent post-thaw recovery of CBA mouse embryonic stem cells	88
4.4 Experimental cryopreservation protocols that improved percent post-thaw recovery of FVB mouse embryonic stem cells	88
4.5 Experimental cryopreservation protocols that improved percent post-thaw recovery of 129R1 mouse embryonic stem cells	89
5.1 Isosmotic cell volumes of Latrunculin A-treated and untreated mouse embryonic stem cells in the presence or absence of dimethyl sulfoxide at 22°C and -3°C	127
5.2 Osmotically inactive cell volume of Latrunculin A-treated and untreated mouse embryonic stem cells in the presence or absence of dimethyl sulfoxide at 22°C and -3°C	128
5.3 The effects of Latrunculin A treatment on the hydraulic conductivity and cryoprotectant permeability of C57BL/6 mouse embryonic stem cells at 22°C and -3°C	129

COMPARATIVE FUNDAMENTAL CRYOBIOLOGY OF MOUSE

EMBRYONIC STEM CELLS

Corinna Mary Kashuba Benson

Dr. John K. Critser, Dissertation Supervisor

ABSTRACT

Mouse embryonic stem cell (mESC) lines are central to projects such as the Knock-Out Mouse Project, North American Conditional Mouse Mutagenesis Program, and European Conditional Mouse Mutagenesis Program, which seek to create thousands of mutant mouse strains using mESCs for the production of human disease models in biomedical research. Crucial to the success of these programs is the ability to efficiently cryopreserve these cell lines for banking and transport. Although the post-thaw recovery of mESCs is often assumed to be adequate with current methods, as this dissertation will show, the post-thaw recovery of viable cells actually varies significantly by genetic background. Therefore there is a need to improve the efficiency and reduce the variability of current mESC cryopreservation methods. To address this need, we employed the principles of fundamental cryobiology to improve the cryopreservation protocol of five mESC lines from different genetic backgrounds (BALB/c, C57BL/6, CBA, FVB, and 129R1 mESCs) through a comparative study characterizing the membrane permeability characteristics and osmotic tolerance limits of each cell line. These values were in turn used to predict optimal cryoprotectants, cooling rates, warming rates, and plunge temperatures, which were then verified experimentally for their effects

on post-thaw recovery. From this study we determined that a cryopreservation protocol utilizing 1 M propylene glycol, a cooling rate of 1°C/minute, and plunge into liquid nitrogen at -41°C, combined with subsequent warming in a 22°C water bath with agitation would significantly improve post-thaw recovery for most mESC lines, the exception being the CBA cell line for which a cooling rate of 5°C/minute in the presence of 1.0 M dimethyl sulfoxide or 1.0 M propylene glycol, combined with plunge temperature of -80°C was optimal. It is expected that this protocol can be applied to most mESC lines beyond those included within this study. Mouse ESC lines that cryopreserve poorly using this method can be approached on a case-by-case basis using the methods outlined in this dissertation. We also examined the effects of Latrunculin A (LATA), 1.5 M dimethyl sulfoxide, and temperature on C57BL/6 mESC osmotic response and permeability parameters, and explored the potential use of Latrunculin A as a cryoprotectant for these cells as well as a method to allow spherical shrinkage during subzero permeability studies. Latrunculin A did not significantly improve post-thaw recovery of C57BL/6 mESCs. Temperature, CPA, and LATA significantly influenced isosmotic cell volume (V_{iso}), and LATA significantly affected adjusted osmotically inactive cell volume (V_b) as well as permeability parameters for the C57BL/6 mESC line. These findings suggest that LATA is inappropriate for use in subzero measurement of permeability parameters. Additionally, the effects of temperature and CPA on V_{iso} have a significant role in the assumptions of the two parameter mass transport model for determining hydraulic conductivity and solute permeability.

CHAPTER 1

INTRODUCTION AND BACKGROUND

Purpose

The overall goal of this dissertation was to study the fundamental cryobiology of mouse embryonic stem cells (mESCs) in order to establish improved cryopreservation approaches. Specifically, the aims were to (1) determine fundamental cryobiological characteristics of five mESC lines, including osmotic tolerance limits (OTL), osmotically inactive cell volume (V_b), hydraulic conductivity (L_p), the permeability of the cells to cryoprotectant agents (CPAs) (P_{CPA}), the temperature dependence of these values (activation energy, E_a), and intracellular ice formation model parameters; (2) use these characteristics to predict optimal CPAs and approaches for CPA addition and removal for each mESC line; and (3) predict, and experimentally verify, optimal cooling and warming rates to minimize cellular volume excursions and preclude damaging intracellular ice formation.

Chapters 2, 3, 4, and 5 are stand-alone manuscripts that were published or will be submitted to peer-reviewed journals. Chapter 2 is a primary study of the fundamental cryobiological characteristics of the C57BL/6 mESC cell line; this research verified the fundamental cryobiological approach to improving mESC cryopreservation and recovery and resulted in greater than a two-fold recovery of membrane-intact C57BL/6 mESC.

Chapter 3, the method established with the C57BL/6 mESC line was extended to a comparative study in order to determine whether there were in fact differences in fundamental cryobiological parameters among four inbred mESC lines, including a BALB/c mESC line, a CBA mESC line, an FVB mESC line, and the 129R1 mESC cell line. It was important to determine whether a single common cryopreservation protocol could be applied to all mESC lines, or whether each individual cell line would require a customized cryopreservation protocol. In Chapter 4, these fundamental cryobiological parameters were applied to predict optimal cooling rates and the corresponding optimal plunge temperatures for the same four mESC lines, and the predicted optimal protocols were experimentally validated. New cryopreservation protocols were generated for each of the four mESC lines that resulted in greatly improved post-thaw recovery. In Chapter 5, basic fundamental cryobiological assumptions were investigated with regards to the osmotic response of C57BL/6 mESCs, namely the effects of Latrunculin A-induced cytoskeletal depolymerization, CPA, and temperature on V_b . The final chapter of this manuscript is a summary of the collective meaning of these chapters and discusses future directions of research in mESC cryopreservation.

Significance

The focus of this dissertation was to determine the fundamental cryobiological parameters of multiple mESC lines in order to establish improved cryopreservation techniques. The fundamental cryobiological parameters of a cell are the intrinsic properties that govern the cellular response to freezing and thawing. They include OTL

(defined as the osmotic range within which mESC retain membrane integrity and mESC characteristics, including pluripotency and proliferative potential), V_b , L_p (cell membrane permeability to water), P_{CPA} (the permeability of the cells to cryoprotective agents (CPAs), and the E_a of L_p and P_{CPA} . In comparing the parameters of multiple mESC lines, the goal was to determine whether a single, optimized cryopreservation protocol can be applied to all mESC lines, or whether cryopreservation protocols must be optimized to individual mESC lines. A third alternative would be that mESC lines can be categorized according to fundamental cryobiological parameters, thus making it possible to optimize cryopreservation protocols to individual categories of mESCs.

Embryonic stem cells (ESCs) are pluripotent cells derived from the inner cell mass of mammalian blastocysts. In 1998, Thomson et al. [1] outlined the criteria to define an ESC line, and these include (i) derivation from the pre- or peri-implantation embryo, (ii) prolonged undifferentiated proliferation, and (iii) stable developmental potential, including the ability to differentiate into all three embryonic germ layers after prolonged culture. Mouse ESCs satisfy all three criteria, and correspondingly have revolutionized biomedical research due to their broad applications in the areas of transgenics, comparative medicine, comparative genomics, pharmacology, embryogenesis, and regenerative medicine.

The use of mESCs in transgenic mouse production has contributed to a virtual explosion in the number of existing transgenic mouse models that are vital for human biomedical research due to their ease of genetic manipulation, wide accessibility to researchers, and the existence of ESC lines of multiple genetic backgrounds [2][3]. Coordinated projects to systematically knock out all mouse genes, such as the Knockout

Mouse Project (KOMP) [4], Canada's North American Conditional Mouse Mutagenesis Program (NorCOMM, <http://norcomm.phenogenomics.ca>), the European Conditional Mouse Mutagenesis Program (EUCOMM, <http://www.eucomm.org>) [5], and Bay Genomics' use of *N*-ethyl-*N*-nitrosurea (ENU) (<http://baygenomics.ucsf.edu>) [6], will create thousands of mutant mESC lines as a step towards producing mutant mice that serve as important models of human biology and disease [7]. Storage and maintenance of valuable genotypes as live animal lines would be wholly impractical [8]. On the other hand, banking lines as ESCs is cost-effective and space-efficient; restoration of mESCs into live, reproductively viable mice is routine in many laboratories across the world. Efficiency of this restoration is greatly improved when freezing and thawing methods produce healthy, rapidly dividing, germ-line competent cells. Accessibility to banked mESC lines is greater when mESCs are easily recovered post-thaw using technically simple, but optimal cryopreservation methods.

Post-thaw recovery of viable mESCs varies dramatically from one cell line to the next, ranging anywhere from 10% to 90% (D. Nielsen, personal communication, Stem Cell Technologies, 2004) (X. Yu, personal communication, University of California-Davis, 2004) [9][10]. Based on our experience, fewer than 50% of all cells in most mESC lines survive cryopreservation, which calls into question the efficacy of current methods. Cryopreservation protocols optimized to individual cell lines, if necessary, would allow for the full exploitation of mESCs from all strains, reducing the need for backcrossing in the production of mutant mice as individual backgrounds would be more accessible as viable ESC lines. Optimized cryopreservation protocols maximize post-thaw recovery of intact, pluripotent cells, reducing the time it takes to expand cultures

post-thaw and increasing the number of aliquots one can cryopreserve from a single plate.

Cryobiology Fundamentals

By exploring the fundamental cryobiology of mESCs from different genetic backgrounds, we were able to model the effects of cooling and warming conditions on cell volume and use this information to develop optimized protocols. The cryobiological approach currently used to preserve mESCs is an equilibrium cooling approach, and this is the approach we elected to pursue. Essentially, we designed a protocol that cooled cells at an optimal rate to a point at which they were plunged into liquid nitrogen for vitrification and long-term storage. The cells were then thawed at a prescribed rate that was optimized for maximum cell membrane integrity.

Importantly, cell damage is not due to ability or inability of the cell to withstand very low temperatures [11]. At -196°C, the temperature of liquid nitrogen, which is typically used for long term storage, solute effects are negligible due to the lack of available thermal energy for chemical reactions to occur [12]; at this point, only photophysical events, such as free radical formation and damage to macromolecules due to background ionizing radiation or cosmic rays, occur, and it is generally accepted that appreciable damage would take centuries or millennia at these temperatures [11].

The major damage due to the freezing and thawing process is theorized to be due to two major factors: intracellular ice crystal formation, which causes mechanical disruption of the cell, and solute effects, generally described as chemical damage that occurs due to a increase in the concentration of intracellular ions that occurs during

cryopreservation [13]. The degree of damage caused by these factors varies with temperature and cooling rate. Cells and the extracellular medium (containing ~1 M of solute) do not freeze until they reach a temperature of approximately -5°C [11]. This is due to freezing point depression by the presence of solutes such as CPAs, as well as the physics of a process called supercooling, with supercooling defined as the cooling of a liquid to a temperature below its freezing point in the absence of ice crystal nucleation. From approximately -5 to -15°C, ice formation occurs in the extracellular solution, either spontaneously or via induced nucleation with ice crystals, but the cell itself remains unfrozen and supercooled [11]. In this temperature range, due to the higher chemical potential of the supercooled intracellular water, water moves extracellularly across the cell membrane, freezing externally and effectively dehydrating the cell. Most damage during the cell freezing process occurs during an intermediate zone of temperature, from approximately -15 to -60°C [11]. Of course, cells experience these temperatures during both the cooling and thawing process. Over this temperature range, cooling velocity becomes critical to the degree of damage a cell sustains. If cooling velocity is ideal, dehydration continues through exosmosis to concentrate the intracellular solutes sufficiently to maintain chemical equilibrium; that is, supercooling is eliminated, the cell dehydrates and intracellular ice crystal formation does not occur. However, if the cell is cooled too rapidly, chemical equilibrium is not maintained due to insufficient exosmosis. The cell becomes increasingly supercooled and eventually reaches chemical equilibrium by freezing intracellularly, causing damaging ice crystals to form. Conversely, if the cell is cooled too slowly, dehydration occurs, minimizing intracellular ice formation, but the

cell is exposed to concentrated ions for unnecessary lengths of time at temperatures during which damaging thermally dependent chemical reactions can take place [13].

There are two approaches to minimizing intracellular ice formation and solute effects, namely vitrification and equilibrium cooling. Vitrification is a physical process during which a solution solidifies during cooling without crystallization, forming a glass. The molecular and ionic distributions found in the liquid solution remain the same in the glass state [14]. Vitrification typically requires very high concentrations of CPA, which can be toxic to the cell, but avoids the damaging effects of intracellular ice formation. Vitrification can also be technically challenging, requiring cooling rates on the order of hundreds of degrees per minute at high CPA concentrations; vitrification at 1-2 M CPA requires cooling rates on the order of 10^5 to 10^6 K/min [15].

Equilibrium cooling, on the other hand, relies on the formation of extracellular ice, which leads to progressive cell dehydration and effectively concentrates the intracellular solution to a vitrifiable state [16]. Fundamental cryobiology, as it is applied to equilibrium cooling, defines basic cell membrane permeability coefficients such as hydraulic conductivity (L_p), solute permeability (in our case, the permeability of cryoprotectants, P_{CPA}) and their temperature dependence in order to predict optimal cooling and warming rates for that cell type. Osmotic tolerance limits, nominal limits to which a cell can shrink or swell in response to osmotic stress without significant loss of function, are also defined. Each of these parameters can vary greatly according to cell type, species, and even individual (e.g. canine erythrocytes vs. spermatozoa of mice vs. chimpanzee spermatozoa) [17][18][19]. Correspondingly, optimal cooling and warming rates can also vary greatly between these groups, by even a thousand fold, from less than

1°C/minute for bovine embryos [20-23] to greater than or equal to 1000°C/minute for human erythrocytes [24].

Osmotic Tolerance Limits

While the use of permeating CPAs is a necessary component of most cryopreservation procedures and protects against solute damage, it introduces another complication: cells undergo osmotic shrinkage during their introduction, and osmotic swelling during their removal [8]. As Critser and Mobraaten explain in their 2000 review paper, the magnitude of the volume excursions depends primarily on the cell permeability to the CPA and secondarily on the time over which the CPA is added and removed. If the excursions are too extensive, cell damage will occur. The definition of “too extensive” depends on the susceptibility of the particular cell type, which is partly determined by its surface to volume (S/V) ratio [8]. The effects of osmolality on mESCs can be directly translated into effects related to the corresponding change in cell volume. If the values for P_{CPA} and corresponding L_p^{CPA} are known and are coupled with the knowledge of the OTL, changes in cell volume occurring with cell exposure to anisosmotic conditions can be predicted in addition to the conditions that will allow the cells to be maintained within their OTL [8]. This method has been successfully applied to a number of cell types in the past with resulting significantly higher survival rates [8], including human [25] and mouse [26] spermatozoa. An important part of our study was to compare osmotic tolerance limits of cell lines with different genetic backgrounds in order to determine whether one protocol would suit all genetic backgrounds. Variation of

OTL within species and between strains has been identified in the past in spermatozoa, for example, and it was prudent to observe for this trend in mESC lines as well.

Warming and Thawing

Cells that have survived cooling to low temperatures are subsequently challenged to the effects of warming and thawing, which exert similar effects on survival to those of cryopreservation. The type of damage that occurs is dependent on whether damaging ice crystals or dehydration has occurred during cooling [8]. If the cells are not irreversibly damaged from intracellular ice crystal formation, the ice crystals tend to be small, but small crystals can form larger crystals during low warming rates [8]. Additionally, successfully vitrified cells can de-vitrify and form ice crystals during warming, a damaging process called re-crystallization [27][28][11]. The response to warming rate is highly variable if the cells are cooled slowly enough to preclude intracellular freezing [8], in that it can make little or no difference in some cell types while in other cells, rapid warming is imperative [29][8].

Warming rates are classically optimal if they mimic their cooling rate counterparts [11][30][31]. However, as long as warming rates are greater than those that allow devitrification, intracellular ice formation is not a factor. In this case the concern is only with the osmotically driven volume changes after temperature equilibration occurs. When cells are warmed rapidly, water and solute permeability is not high enough to allow for equilibration during rapid warming. The subsequent osmotic pressure across

the membrane that is proportional to the warming rate can cause a damaging influx of water [11].

Fundamental Cryobiology of Mouse Embryonic Stem Cells

Thus, the optimal cooling rate for each mESC line was determined to be the most rapid rate at which a cell suspension could be cooled without causing a large difference (supercooling) between the intracellular freezing point and the intracellular temperature. Using principles of the Boyle–Van’t Hoff relation [32], the Arrhenius relation [33], a two parameter mass transport model [34][35], and Mazur’s two factor hypothesis [13], the fundamental cryobiological parameters of multiple mESC lines were explored in order to improve existing cryopreservation protocols and to define methods for the routine assessment of cryopreservation methods in a repository setting. Permeability of cryoprotectant and L_p in the presence of CPA (L_p^{CPA}), and the temperature dependence of these values was assessed in the presence of four commonly used CPA, namely ethylene glycol (EG), 1,2-propanediol (PG), dimethyl sulfoxide (Me₂SO), and glycerol (GLY). The V_b was calculated and OTL were established per cell line using membrane integrity as an endpoint. These parameters were in turn used to predict theoretically optimized cryopreservation protocols that improved post-thaw recovery.

The improved cryopreservation protocols and the standard cryopreservation protocol are based on a two-step, interrupted slow freezing process. The initial step involves equilibrium cooling at a controlled rate to a temperature where, in the second

step, the initial cooling rate is halted (i.e., “interrupted”) and the sample is plunged into liquid nitrogen. The final plunge into liquid nitrogen results in very rapid cooling and intracellular vitrification. Vitrification avoids lethal intracellular freezing and takes the cell to a low temperature such that solution effects are virtually eliminated due to greatly reduced kinetic energy of chemical reactions [36][37], enabling long-term storage.

References

1. Thomson, J.A., et al., *Embryonic stem cell lines derived from human blastocysts*. Science, 1998. **282**(5391): p. 1145-7.
2. Bedell, M.A., N.A. Jenkins, and N.G. Copeland, *Mouse models of human disease. Part I: techniques and resources for genetic analysis in mice*. Genes Dev, 1997. **11**(1): p. 1-10.
3. Bedell, M.A., et al., *Mouse models of human disease. Part II: recent progress and future directions*. Genes Dev, 1997. **11**(1): p. 11-43.
4. Austin, C.P., et al., *The knockout mouse project*. Nat Genet, 2004. **36**(9): p. 921-4.
5. Auwerx, J., et al., *The European dimension for the mouse genome mutagenesis program*. Nat Genet, 2004. **36**(9): p. 925-7.
6. Munroe, R.J., et al., *Mouse mutants from chemically mutagenized embryonic stem cells*. Nat Genet, 2000. **24**(3): p. 318-21.
7. *Touching base*. Nat Genet, 2006. **38**(10): p. 1107.
8. Critser, J.K. and L.E. Mobraaten, *Cryopreservation of murine spermatozoa*. Ilar J, 2000. **41**(4): p. 197-206.
9. Kashuba Benson, C.M., J.D. Benson, and J.K. Critser, *An improved cryopreservation method for a mouse embryonic stem cell line*. Cryobiology, 2008. **56**(2): p. 120-30.

10. Miszta-Lane, H., et al., *Effect of slow freezing versus vitrification on the recovery of mouse embryonic stem cells*. Cell preservation technology, 2007. **5**(1): p. 16-24.
11. Mazur, P., *Freezing of living cells: mechanisms and implications*. Am J Physiol, 1984. **247**(3 Pt 1): p. C125-42.
12. McGee, H.A., Jr. and W.J. Martin, *Cryochemistry*. Cryogenics, 1962. **2**: p. 257-267.
13. Mazur, P., S.P. Leibo, and E.H. Chu, *A two-factor hypothesis of freezing injury. Evidence from Chinese hamster tissue-culture cells*. Exp Cell Res, 1972. **71**(2): p. 345-55.
14. MacFarlane, D.R., *Physical aspects of vitrification in aqueous solutions*. Cryobiology, 1987. **24**: p. 181-195.
15. Boutron, P., *Comparison with the theory of the kinetics and extent of ice crystallization and of the glass-forming tendency in aqueous cryoprotective solutions*. Cryobiology, 1986. **23**(1): p. 88-102.
16. Pegg, D.E. and M.P. Diaper, *Freezing versus vitrification: Basic principles*, in *Cryopreservation and Low Temperature Biology in Blood Transfusion*, C.T. Smit Sibinga, P.C. Das, and H.T. Meryman, Editors. 1990, Kluwer Academic Publishers: Dordrecht. p. 55-69.
17. Agca, Y., et al., *Chimpanzee (*Pan troglodytes*) spermatozoa osmotic tolerance and cryoprotectant permeability characteristics*. J Androl, 2005. **26**(4): p. 470-7.
18. Devireddy, R.V., et al., *Subzero water permeability parameters of mouse spermatozoa in the presence of extracellular ice and cryoprotective agents*. Biol Reprod, 1999. **61**(3): p. 764-75.
19. Liu, J., J.A. Christian, and J.K. Critser, *Canine RBC osmotic tolerance and membrane permeability*. Cryobiology, 2002. **44**(3): p. 258-68.
20. Fair, T., et al., *Ultrastructure of bovine blastocysts following cryopreservation: effect of method of blastocyst production*. Mol Reprod Dev, 2001. **58**(2): p. 186-95.
21. Nedambale, T.L., et al., *Comparison on in vitro fertilized bovine embryos cultured in KSOM or SOF and cryopreserved by slow freezing or vitrification*. Theriogenology, 2004. **62**(3-4): p. 437-49.

22. Mucci, N., et al., *Effect of estrous cow serum during bovine embryo culture on blastocyst development and cryotolerance after slow freezing or vitrification*. Theriogenology, 2006. **65**(8): p. 1551-62.
23. Visintin, J.A., et al., *Cryopreservation of Bos taurus vs Bos indicus embryos: are they really different?* Theriogenology, 2002. **57**(1): p. 345-59.
24. Fujikawa, S., *The effect of various cooling rates on the membrane ultrastructure of frozen human erythrocytes and its relation to the extent of haemolysis after thawing*. J Cell Sci, 1981. **49**: p. 369-82.
25. Gilmore, J.A., et al., *Effect of cryoprotectant solutes on water permeability of human spermatozoa*. Biol Reprod, 1995. **53**(5): p. 985-95.
26. Phelps, M.J., et al., *Effects of Percoll separation, cryoprotective agents, and temperature on plasma membrane permeability characteristics of murine spermatozoa and their relevance to cryopreservation*. Biol Reprod, 1999. **61**(4): p. 1031-41.
27. Rall, W. and C. Polge, *Effect of warming rate on mouse embryos frozen and thawed in glycerol*. J Reprod Fertil., 1984. **70**(1): p. 285-92.
28. Rall, W.F., D.S. Reid, and C. Polge, *Analysis of slow-warming injury of mouse embryos by cryomicroscopical and physiochemical methods*. Cryobiology, 1984. **21**(1): p. 106-21.
29. Mazur, P., *Equilibrium, quasi-equilibrium, and nonequilibrium freezing of mammalian embryos*. Cell Biophys, 1990. **17**(1): p. 53-92.
30. Gao, D., P. Mazur, and J.K. Critser, *Fundamental Cryobiology of Mammalian Sperm*, in *Reproductive Tissue Banking: Scientific Principles*, A.M. Karow and J.K. Critser, Editors. 1997, Academic Press: San Diego. p. 263-328.
31. Agca, Y., et al., *Osmotic tolerance and membrane permeability characteristics of rhesus monkey (*Macaca mulatta*) spermatozoa*. Cryobiology, 2005. **51**(1): p. 1-14.
32. Nobel, P.S., *The Boyle-Van't Hoff relation*. Journal of Theoretical Biology, 1969. **23**(3): p. 375-9.
33. Mazur, P., *Kinetics Of Water Loss From Cells At Subzero Temperatures And The Likelihood Of Intracellular Freezing*. J Gen Physiol, 1963. **47**: p. 347-69.

34. Jacobs, M.H., *The simultaneous measurement of cell permeability to water and to dissolved substances*. Journal of Cellular and Comparative Physiology, 1933. **2**(4): p. 427-444.
35. Katkov, II, *A two-parameter model of cell membrane permeability for multisolute systems*. Cryobiology, 2000. **40**(1): p. 64-83.
36. Muldrew, K., et al., *The Water to Ice Transition: Implications for Living Cells*, in *Life in the Frozen State*, B.J. Fuller, N. Lane, and E.E. Benson, Editors. 2004, CRC Press LLC: Boca Raton, Florida. p. 67-108.
37. Woods, E.J., et al., *A theoretically optimized method for cord blood stem cell cryopreservation*. J Hematother Stem Cell Res, 2003. **12**(3): p. 341-50.

CHAPTER 2

AN IMPROVED CRYOPRESERVATION METHOD FOR A MOUSE EMBRYONIC STEM CELL LINE

Introduction

The use of mouse embryonic stem (ES) cells in transgenic mouse production has contributed to a virtual explosion in the number of existing transgenic mouse models that are vital for human biomedical research [1][2]. Coordinated projects to systematically knock out all mouse genes, such as the Knockout Mouse Project (KOMP) [3], Canada's North American Conditional Mouse Mutagenesis Program (NorCOMM, <http://norcomm.phenogenomics.ca/index.htm>), the European Conditional Mouse Mutagenesis Program (EUCOMM, <http://www.eucomm.org>) [4], and Bay Genomics' use of *N*-ethyl-*N*-nitrosurea (ENU) (<http://baygenomics.ucsf.edu/>) [5], will create thousands of mutant mESC lines as a step towards producing mutant mice that serve as important models of human biology and disease [6]. The C57BL/6 mouse lineage is central to these projects, due to its ease of genetic manipulation, wide accessibility to researchers, and the existence of mESC lines of this genotype. Storage and maintenance of valuable

This chapter was published as a full manuscript in the journal, *Cryobiology*. The full citation is as follows: C.M. Kashuba Benson, J.D. Benson, and J.K. Critser. 2008. An improved cryopreservation method for a mouse embryonic stem cell line. *Cryobiology* 56:120-130.

genotypes as live animal lines would be wholly impractical [7]. On the other hand, banking lines as mESCs is cost-effective and restoration of the mESCs into live, reproductively viable mice is routine in many laboratories across the world. Efficiency of this restoration is greatly improved when freezing and thawing methods produce healthy, rapidly dividing, germ line competent cells.

To our knowledge, there are no published reports quantifying post-thaw recovery of cryopreserved C57BL/6 mESCs. Post-thaw recovery of viable mESCs varies dramatically from one cell line to the next, ranging anywhere from 10-90% (personal communication, Deanna Nielsen, Stem Cell Technologies technical support, 2004; personal communication, Xin Yu, University of California-Davis, 2004). Based on our experience, fewer than 50% of all cells in most mESC lines survive cryopreservation, which calls into question the efficacy of current methods. Cryopreservation protocols optimized to individual cell lines, if necessary, would allow for the full exploitation of ESCs from all strains, reducing the need for backcrossing in the production of mutant mice as individual backgrounds would be accessible as viable ESC lines. Optimized cryopreservation protocols maximize post-thaw recovery of intact, pluripotent cells, reducing the time it takes to expand cultures post-thaw and increasing the number of aliquots one can cryopreserve from a single plate

The cryobiological approach currently used to preserve mESCs is an equilibrium cooling approach. Equilibrium cooling relies on the formation of extracellular ice, which leads to progressive cell dehydration, effectively concentrating the intracellular solution to a vitrifiable state in which, upon further cooling, the cytoplasm becomes a glass [8]. The term, “vitrification” is most often used to describe cooling protocols which bring

about an extreme elevation in viscosity of an extracellular solution, *i.e.* the formation of a glass in the absence of ice crystallization [9]. Typically, this requires rapid cooling protocols in the presence of high concentrations of cryoprotective agents (CPAs). However, the use of equilibrium cooling to render a cell to a more vitrifiable state through controlled dehydration, an idea elucidated by Pegg and Diaper in 1990 [8], has only recently gained consistent and systematic support [10][11][12]. Major damage during a cryobiological protocol using the equilibrium cooling approach is theorized to be due to three major factors: osmotic damage due to water influx and efflux during the addition and removal of CPAs (*e.g.* Me₂SO [13]), mechanical damage due to intracellular ice crystal formation, and solute effects, generally described as chemical damage that occurs due to a increase in the concentration of intracellular ions that occurs during freezing [14]. The degree of damage caused by these factors varies with CPA and cooling and warming profiles.

A direct means to derive optimal cryopreservation protocols for a given cell type is via an exploration of the cell's fundamental cryobiological parameters and how they relate to the major physical events that occur during the freezing process [14]. Fundamental cryobiology, as it is applied to equilibrium cooling, seeks to define basic cell membrane permeability coefficients such as hydraulic conductivity (L_p), solute permeability (in our case, the permeability of cryoprotectants, P_{CPA}) and their temperature dependence (defined by an Arrhenius equation with activation energy E_a) in order to predict optimal cooling and warming rates for that cell type. To avoid damage during the addition and removal of CPA, osmotic tolerance limits, nominal limits to which a cell can shrink or swell in response to osmotic stress without significant loss of function, are also

defined. Each of these parameters can vary greatly according to cell type, species, and even individual (*e.g.* canine erythrocytes *vs.* spermatozoa of mice *vs.* chimpanzee spermatozoa [15][16][17]). Correspondingly, optimal cooling and warming rates can also vary greatly between these groups (*e.g.* human cord blood stem cells *vs.* erythrocytes [18][19]).

Optimal cooling rates are defined as those that cool cell suspensions as rapidly as possible without causing a large difference between the intracellular freezing point and the intracellular temperature, and warming rates are classically optimal if they mimic their cooling rate counterparts [20]. Using principles of the Boyle Van't Hoff relation [21], the Arrhenius relation [22], a two-parameter mass transport model [23], and Mazur's two factor hypothesis [24], we explored the fundamental cryobiological parameters of a C57BL/6 mESC line in order to improve existing cryopreservation protocols and define methods by which cryopreservation methods would be routinely assessed in a repository setting. P_{CPA} and L_p in the presence of CPA (L_p^{CPA}), and the temperature dependence of these values were assessed in the presence of four commonly used CPA, namely ethylene glycol (EG), propylene glycol (PG), Me₂SO, and glycerol (GLY). The osmotically inactive fraction of the cell, V_b , was calculated and osmotic tolerance limits were established using membrane integrity as the endpoint. These parameters were in turn used to predict a theoretically optimized cryopreservation protocol that improved the efficiency of cryopreservation for the C57BL/6 mESC line by greater than 2-fold. Finally, this protocol will provide an experimental basis to improve cryopreservation methods for other mESC lines, and will allow optimization accounting for other endpoints such as gene expression profiles associated with differentiation.

Table 2.1 Definition of major symbols and terms

Symbol or abbreviation	Description	Units	Value
e, i	Superscripts: e, external; i, internal	None	None
s, n, w	Subscripts: s, solute; n, non-permeating; w, water	None	None
L_p^{CPA}	Hydraulic conductivity in the presence of cryoprotectant	$\mu\text{m min}^{-1} \text{ atm}^{-1}$	Parameter
P_{CPA}	Solute permeability	$\mu\text{m min}^{-1}$	Parameter
E_a	Activation energy	kcal mol^{-1}	Parameter
T	Temperature	K	295
A	Cell surface area	μm^2	Parameter
V	Cell volume	μm^3	Variable
V_b	Osmotically inactive cell volume	μm^3	Parameter
$V_w(t)$	Intracellular water volume at time t	μm^3	Variable
$n_s^i(t)$	Moles of internal permeating solute at time t	Moles	Variable
t	Time	Seconds	Variable
M_{iso}	Osmolality of initial (isotonic) intracellular salts	$\text{Osm kg}^{-1} \text{ H}_2\text{O}$	0.290
M_n^e	Osmolality of extracellular salts	$\text{Osm kg}^{-1} \text{ H}_2\text{O}$	0.290
n_n^i	Osmoles of intracellular salts	Osm	Variable
M	Molality	$\text{mol kg}^{-1} \text{ H}_2\text{O}$	Variable
\bar{V}	Partial molal volume of solute	L mole^{-1}	Variable
R	The universal gas constant	$\text{kcal mole}^{-1} \text{ K}^{-1}$	1.987×10^{-3}

Materials and Methods

Embryonic stem cells

The C57BL/6 mESC line was acquired at passage 11 from Specialty Media Group (Chemicon International, Temecula, California, now part of Millipore, Billerica, Massachusetts). C57BL/6 mESC cultures were negative for all pathogens (IMPACT I test, Research Animal Diagnostic Laboratory, Columbia, Missouri; www.radil.missouri.edu/info/index.asp).

Cell culture and standard freezing method

Mouse ESCs were cultured on primary mouse embryonic fibroblast cells (PMEF) (Chemicon International) at 37°C and 5% CO₂. Culture media contained 15% Defined FBS (Hyclone, Logan, UT), 0.1mM non-essential amino acids (GIBCO/ Invitrogen, Carlsbad, CA), 1.0 mM sodium pyruvate (GIBCO), 100 µM beta-mercaptoethanol (Sigma Aldrich, St. Louis, MO), 50 IU/mL penicillin (GIBCO), 50 µg/mL streptomycin (GIBCO), and 1000 U ESGRO/mL (Chemicon International) in high glucose DMEM (Chemicon International). Mouse ESCs were passaged and/or collected every 2 days or at 80% confluence.

For the standard slow cooling freezing method, cells were resuspended in freezing medium (1.3 M (10%) Me₂SO (Sigma Aldrich), 50% defined fetal bovine serum (Hyclone), and 40% culture medium) in 1mL aliquots in cryovials (Nalgene Nunc

International, Rochester, NY). Cryovials were transferred to a commercially available freezing kit (Nalgene), refrigerated at -80°C overnight (a process which cools at a rate of 1°C/minute), and subsequently transferred to liquid nitrogen (LN₂).

Mouse ESCs were used within 10 passages from the original, and were of normal karyotype at highest passage. Cell counts were performed using a hemacytometer and Trypan blue stain (Sigma Aldrich) for membrane integrity.

Separation of mESCs from feeders

For Coulter counter and osmotic tolerance experiments, mESCs were separated from the feeder cells using a differential sedimentation technique previously described by Doetschman [25]. The separation of PMEF from mESCs is routine, and there are many variations of the basic method exploiting the difference in the rate at which fibroblast feeder cells and mESCs settle and adhere to culture dishes [26][27][28]. Briefly, trypsinized mESC cultures containing PMEF were centrifuged, resuspended in 10 mL of culture medium, and plated on the original 100mm cell culture dish for 30 minutes at 37°C. Following incubation, culture medium containing mostly mESCs was transferred to a second culture dish for one hour incubation at 37°C in order to remove remaining fibroblast feeders. Following the second incubation, culture medium containing the mESCs was removed, and the mESCs were counted, centrifuged, and resuspended in either DPBS or culture medium for experimentation. In our hands, the Doetschman

sedimentation method resulted in the removal of greater than 99% of contaminating feeder cells from the mESC suspension (data not shown).

Electronic particle counter

A modified electronic particle counter (EPC) (Coulter Counter model ZM, Beckman Coulter, Inc., Fullerton, CA), equipped with a standard 50 μm aperture tube and computer interface [29], and modified to operate without a mercury-filled manometer as per Benson *et al.* [30] was used for all cellular volumetric measurements. Raw volumetric data were exported into Mathematica (Wolfram Research Inc., Champaign, Illinois) computing package for processing and analysis. Volume was calibrated using standard nominal 10 μm polystyrene latex particles (Beckman Coulter, Inc., Fullerton, CA) at 0, 6, 12, and 22°C. The relationship between conductivity and latex bead volume was assumed to be the same as that between conductivity and mESC volume.

Determination of osmotic tolerance limits

Osmotic tolerance limits were defined by the maintenance of plasma membrane integrity, as indicated by propidium iodide exclusion in 80% of the mESC population following exposure to anisosmotic conditions using sodium chloride as an impermeable solute. Solutions of varying osmolality were prepared using Dulbecco's Phosphate Buffered Saline (PBS) that was adjusted to the appropriate osmolality by the addition of either double distilled water or sodium chloride (Sigma Aldrich). The solutions were

adjusted to pH 7.1 using NaOH or HCl as necessary. The osmolality of each solution was verified using a vapor pressure osmometer (Wescor, Logan, UT). On three separate days, 80% confluent C57BL/6 mESCs were trypsinized and separated from fibroblast feeders. Equal numbers of cells were then exposed to solutions of 37, 75, 150, 600, 1200, 2400 and 4800 mOsm (n=3 for each solution) for 10 minutes at room temperature. Conditions were abruptly returned to isosmotic by the abrupt addition of appropriate volumes of hyperosmotic solution in the case of hyposmotic conditions, and hypoosmotic solution in the case of hyperosmotic conditions. Cells were then centrifuged for five minutes at 200g and resuspended in isosmotic solution. Cells exposed to anisosmotic conditions were compared to controls in which the same quantities of cells were exposed to isosmotic conditions (285 mOsm) following the same protocol. Plasma membrane integrity was assessed by flow cytometry analysis (FACScan, Becton Dickinson, San Jose, CA) of propidium iodide exclusion.

Measurement of cell osmotic response

Mouse ESC volumetric response to variable osmotic stresses was measured at 22°C using an EPC, as previously described [29][31][32][33][34]. Mean cell volume response was measured in real time following abrupt exposure to 206, 285, 600, 900, 1350, and 2880 mOsm solutions prepared from 10X PBS (Sigma) and Milli-Q water and adjusted to pH 7.1 with hydrochloric acid. The osmolality of the solutions was verified using a vapor pressure osmometer (Wescor). Data were averaged over 100 ms intervals prior to analysis. Three replicates were performed for each experimental condition and a

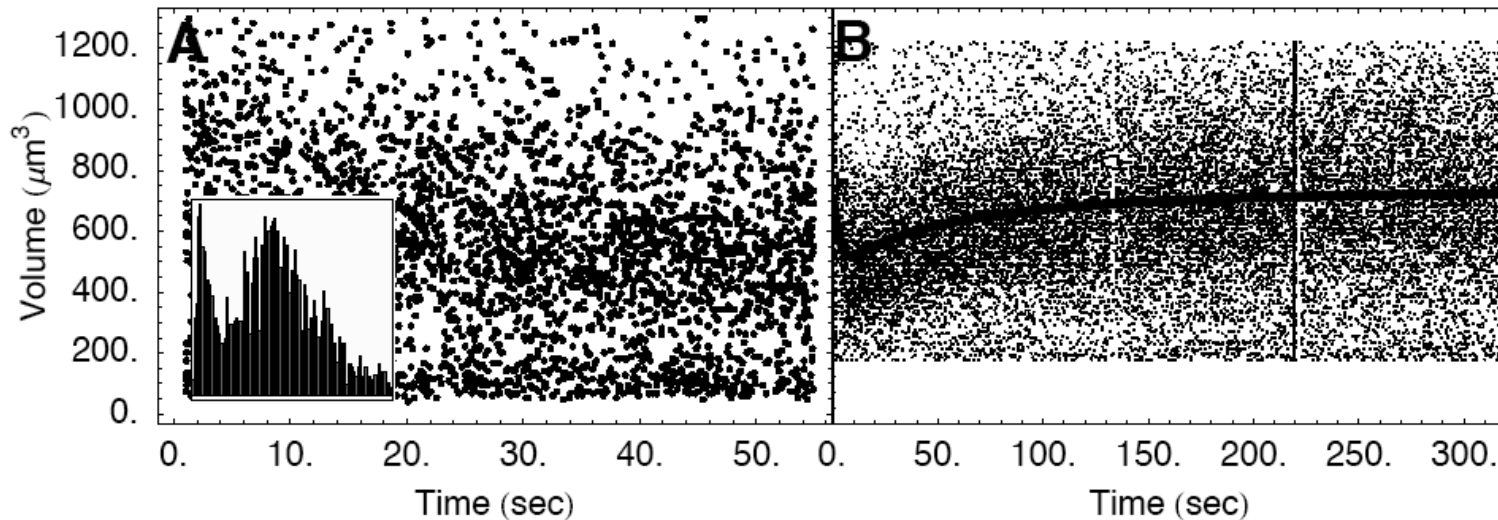


Figure 2.1. Representative plots of calibrated cell volume versus time data from the coulter counter. (A) Representative plot of calibrated cell volume versus time data from the Coulter counter and (inset) a histogram of the equilibrated volume distribution. Cells equilibrated in isosmotic media were abruptly injected into anisosmotic media, the resulting equilibrated volumes were recorded, noise was filtered out digitally, and mean volumes were recorded. (B) Representative plot of calibrated cell volume versus time data from the Coulter counter and a representative two parameter model fit. Cells equilibrated in isosmotic media were abruptly injected into media containing 1M CPA in isotonic buffer. The resulting "shrink-swell" volume versus time data were fit to a two parameter solute solvent flux model.

representative plot of the output can be seen in Figure 2.1A.

Equilibrated cell volumes were normalized to their respective isotonic values, and plotted against the reciprocal of normalized osmolality in accordance with the Boyle Van't Hoff relationship [21]. Linear regression was calculated using Mathematica to fit the Boyle Van't Hoff equation to the data. This equation is defined by

$$V = V_{w,iso} M_{iso} / M + V_b,$$

where V is cell volume at osmolality M , $V_{w,iso}$ is isotonic cell water volume, M_{iso} is isotonic osmolality, and V_b is the osmotically inactive cell volume. V_b was determined by performing a linear regression of volume as a function of the reciprocal of osmolality and extrapolating to infinite osmolality (i.e. $1/M = 0$).

Determination of permeability parameters

Volume changes over time were measured by an EPC following abrupt addition of cells to 1.0 M CPA in 1x PBS. Volumetric changes in the presence of 1.0 M Me₂SO, 1.0 M EG, and 1.0 M PG were measured at 0, 6, 12, 22, and 34°C, and a representative plot of the experimental output can be seen in Figure 2.1B. Measurements of cells in the presence of 1.0 M GLY were determined at 22 °C only. Three replicates were performed for each treatment on three different days.

Data were fit to the following two-parameter mass transport model [35] to determine membrane permeability coefficients for cryoprotective agents (P_{CPA}) and hydraulic conductivity in the presence of cryoprotectants (L_p^{CPA}) at all temperatures:

$$\frac{dV_w}{dt} = -L_p A R T \left(M_s^e + M_n^e - \frac{n_s^i + n_n^i}{V_w} \right),$$

$$\frac{dn_s^i}{dt} = P_s A \left(M_s^e - \frac{n_s^i}{V_w} \right).$$

Here, superscripts e and i indicate extra- and intracellular quantities, respectively, subscripts s and n indicate permeating and non-permeating quantities, respectively, and A is the volume independent spherical surface area at V_{iso} . Finally, we assume the relationship $n^i = V_w M^i$ where V_w is the intracellular water volume.

The Arrhenius relationship^{c,f.} [14] was used to determine the activation energies, E_a , for the parameters L_p^{CPA} and P_{CPA} by plotting the permeability value (L_p^{CPA} or P_{CPA}) at any absolute temperature T as $R \ln(P(T))$ versus $1/T$:

$$P(T) = P_0 \exp \left[\frac{E_a}{R} \left(\frac{1}{T_0} - \frac{1}{T} \right) \right],$$

where P_0 is the value at some reference temperature T_0 , R is the gas constant and E_a is the activation energy for the process, expressed in kcal/mol and determined by the slope of the linear regression.

Theoretical simulations

Theoretical simulations were performed to determine optimal CPA addition and removal protocols of a 1.0 M solution of Me₂SO, PG, or EG for C57BL/6 mESCs. A protocol was defined to be optimal if it minimized the number of addition and dilution steps while maintaining mESCs within the defined range of osmotic tolerance. The overall goal was to minimize cell volume excursion and cryoprotectant exposure time at ambient temperatures. A computer model was used for these procedures. In given experimental conditions, which included osmotic tolerance limits, initial intracellular concentration, and temperature, the program automatically optimized addition and removal steps, and also provided the appropriate diluent concentration.

Theoretical optimization of cryopreservation protocols based on Mazur's two factor hypothesis was also performed. Briefly, Mazur's two factor hypothesis [24] states that sub-optimal cooling rates cause damage due to unnecessarily prolonged exposure to the high concentrations of solutes that occur at low temperatures, and super-optimal cooling rates cause damage due to insufficient cellular dehydration, leading to deleterious intracellular ice formation. Mazur suggests that the optimal cooling rate is that which minimizes cooling exposure time while maintaining at most two degrees of supercooling [24]. In other words, he suggests that cells are cooled as quickly as possible without causing the intracellular concentration to be such that the freezing point is more than two degrees above the cellular environment. This optimization can be achieved by pairing solute-solvent flux models with the appropriate ternary phase diagram (NaCl-CPA-Water) to determine to what degree supercooling would occur.

In a two-step freezing protocol, cells are cooled at a controlled rate to a temperature, termed the “plunge temperature”, at which point they are plunged into liquid nitrogen. The purpose of this procedure is to minimize intracellular ice formation and promote vitrification. Optimal plunge temperatures were calculated using computer simulations based on the above model that estimated the temperature at which the combination of cooling rate and initial CPA concentration would result in an intracellular CPA concentration of 40% by weight. Computer simulations of freezing for all cell lines and CPAs were performed iteratively until optimal cooling rates were determined, i.e. simulations were run at increasing cooling rates until more than two degrees of supercooling occurred before the intracellular concentration of CPA reached 40%. For an illustrative curve of determination of optimal cooling rates, please refer to Figure 2.2.

Warming was simulated using the two parameter mathematical model [35] described above, and the subsequent volume excursion upon equilibration was compared to the predicted osmotic tolerance limits. Warming rates up to 1×10^4 °C/min were simulated to verify that damage due to volume changes would not occur. An optimal warming rate is that which is fast enough to prevent devitrification, yet not too fast that after warming, the influx of water causes the cell to exceed osmotic tolerance limits (see [12] for a discussion on the avoidance of devitrification using rapid warming rates, and [36] for a discussion of the damaging effects of volume change from overly rapid warming rates). Since the fastest practical method for warming is placing a straw in room temperature or 37°C water (the difference in cooling rates is reasonably negligible) it remains only to verify that cell volume excursions are within the osmotic tolerance limits. For an illustrative curve of optimal warming rates, please refer to Figure 2.2.

Empirical validation of predicted optima

Empirical validation of predicted freezing rates was conducted with 1.0 M PG and 1.0 M Me₂SO. C57BL/6 mESCs, cultured in standard conditions, were separated from fibroblast feeders and resuspended in freezing medium at a concentration of 1 x 10⁶ cells/mL. Propylene glycol freezing medium consisted of 1.0 M PG (Sigma), suspended in culture medium and 50% v/v defined fetal bovine serum (FBS) (Hyclone). Dimethyl sulfoxide freezing medium consisted of 1.0 M Me₂SO (Sigma), suspended in culture medium and 50% v/v FBS. Cells were cooled in sealed 250 µL cryostraws (IMV International, Maple Grove, MN) in a Planer Kryo 10 Series III programmable freezer (TS Scientific). Comparisons were made with standard conditions (Me₂SO, 1°C/minute, -80°C plunge temperature) and predicted optimal conditions that included cooling rate (4°C/minute, Me₂SO; 1°C/minute, PG) and two plunge temperatures of predicted optimal (-32.5 ± 0.5°C, Me₂SO; -40.5 ± 0.5°C, PG) vs. low (-80°C). Initial studies comparing the effects of seeding (the induced nucleation of intracellular ice crystals by applying a LN₂-cooled forceps to the freezing vessel until visible ice crystals form, theorized to increase the uniformity of sample cooling [37][38]) vs. not seeding revealed no significant difference (data not shown); therefore these comparisons were not included in additional studies. Finally, mESC recovery using cryostraws in conditions mimicking standard mESC freezing conditions were compared to mESC recovery in standard conditions using cryovials (Nalge Nunc International, Rochester, NY) that are commonly used to freeze and distribute mESCs.

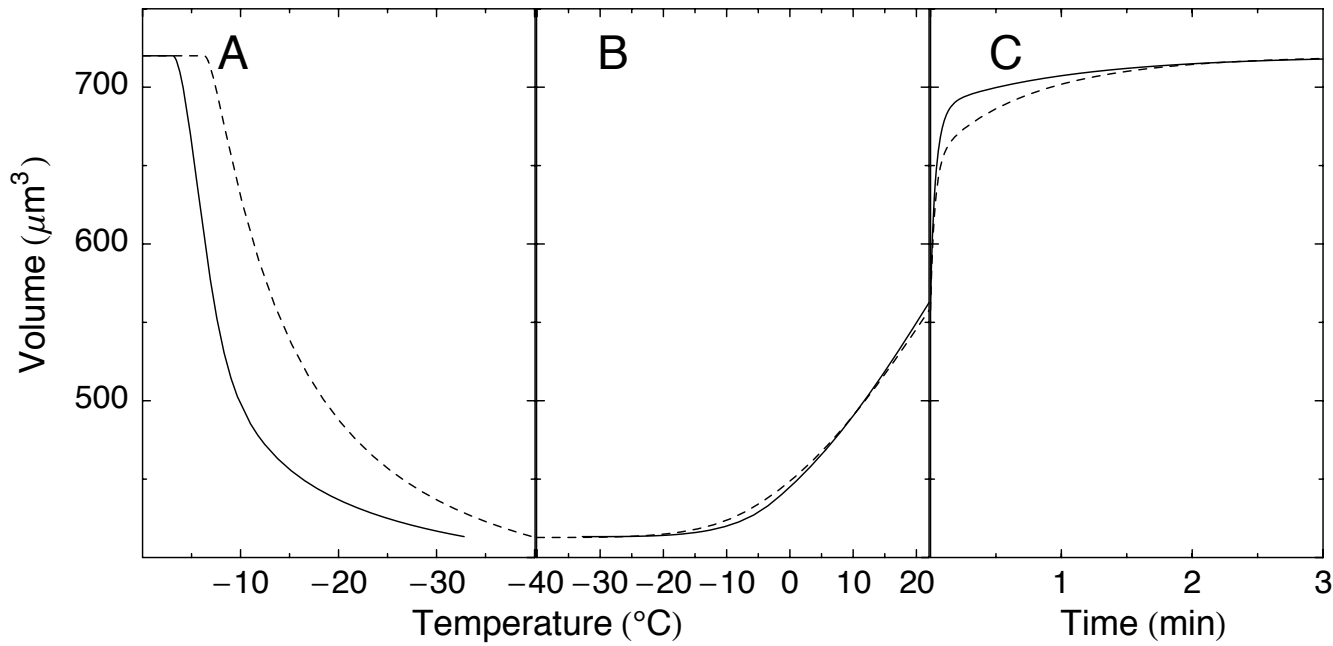


Figure 2.2. Plot of theoretical cell volume versus temperature during cooling (A), warming (B), and versus time at room temperature (C) for cells in Me_2SO (solid line) and in PG (dashed line). In (A), cooling rates were $4^\circ\text{C}/\text{min}$ and $1^\circ\text{C}/\text{min}$ for Me_2SO and PG, respectively, and plunge temperatures were -32.5°C and -40.5°C for Me_2SO and PG, respectively.

Theoretical simulations predicted that warming rates between 10 and 1 x 10⁴°C/minute would have negligible effects on cell survival. Therefore, cryo-straws were thawed in a room temperature water bath (22 ± 1°C), resulting in a measured warming rate of approximately 700°C/minute (data not shown). Immediately post-thaw, mESCs were diluted, drop-wise, by 5 volumes of culture media, centrifuged, resuspended in 1x PBS, stained with propidium iodide, and passed through a FACScan flow cytometer (BD Biosciences, San Jose, CA) for analysis of percent post-thaw recovery (PTR).

Statistical analysis

A *t*-test was used to compare percent PTR in standard conditions using cryo-straws and cryovials. A Dunnett's test was used in the analysis of experimental validation studies of predicted optimal cooling rates and plunge temperatures as compared to standard conditions [39]. For all other comparisons, standard analysis of variance (ANOVA) was performed with the SAS General Linear Models program (SAS Institute, Inc., Cary, NC). An alpha value of p<0.05 was used for all tests. All values are stated as mean ± SEM, unless stated otherwise.

Results

Osmotically inactive cell volume

C57BL/6 mESCs behaved as ideal linear osmometers over a range of 200 mOsm to 2800 mOsm. The calibrated measurements with the Coulter counter gave a mean isosmotic volume of $695 \pm 3.4 \mu\text{m}^3$. Extrapolation of the regression line to infinite osmolality gave an osmotically inactive cell volume of $49.7 \pm 1.3\%$ of isosmotic cell volume with an r^2 value of 0.945. These values are depicted in Figure 2.3.

Osmotic tolerance

The effects of anisosmotic conditions on C57BL/6 mESC membrane integrity, as represented by propidium iodide (PI) exclusion, are shown in Figure 2.4. There was a significant main effect of osmolality on mESC plasma membrane integrity ($p<0.05$). Post-anisosmotic exposure cell membrane integrity varied by day of experiment ($p<0.05$). Overall, an increase in the proportion of cells staining positive for PI, indicating decreased membrane integrity, was observed as conditions departed from isosmotic. As shown in Figure 2.4, as compared to isosmotic conditions, the membrane integrity of mESCs was decreased significantly in anisosmotic conditions of 37.5, 75, 1200, 2400, and 4800 mOsm ($p<0.05$). Ninety percent or greater of C57BL/6 mESCs excluded propidium iodide, *i.e.* maintained cell membrane integrity, following exposure to

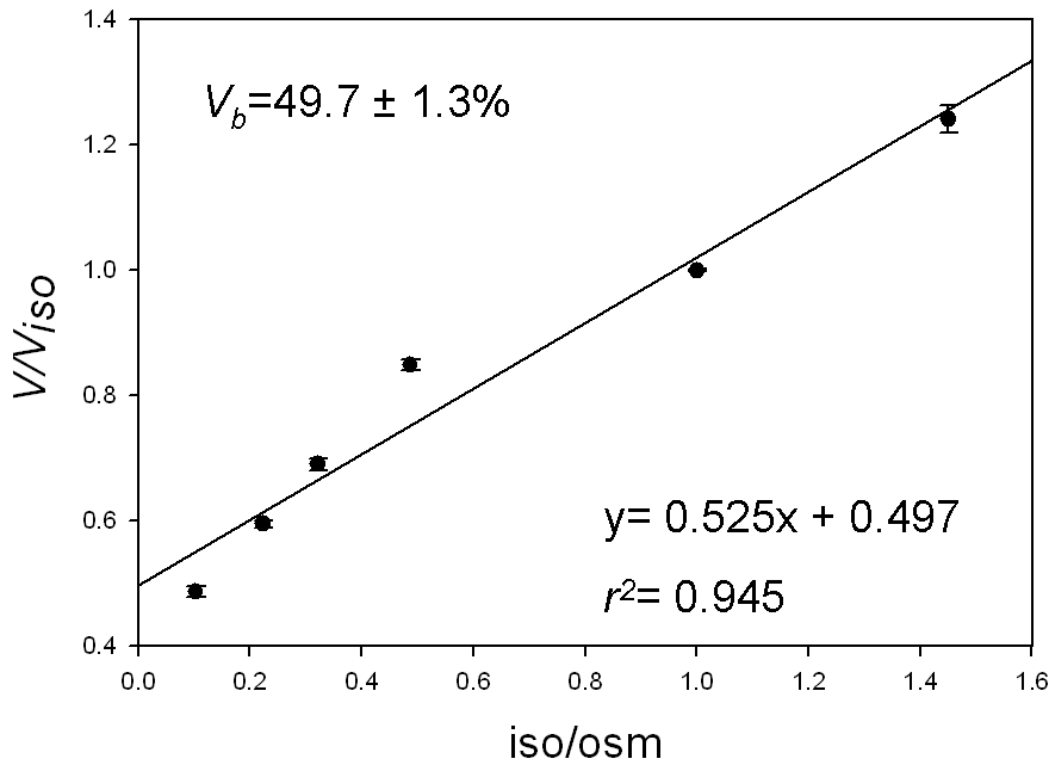


Figure 2.3. Boyle Van't Hoff relationship for C57BL/6 mouse embryonic stem cell (ESC) line. Mouse ESC volumetric response to different osmolalities was measured at 22°C using an electronic particle counter. Cell volume response was measured in real time following abrupt exposure to 206, 290, 600, 900, 1300, and 2800 mOsm solutions, n=6. Error bars represent SEM. V , equilibrated cell volume; V_{iso} , isosmotic cell volume; iso, isosmotic; osm, osmolality of treatment. V_b is expressed as mean percent of isosmotic cell volume \pm SEM.

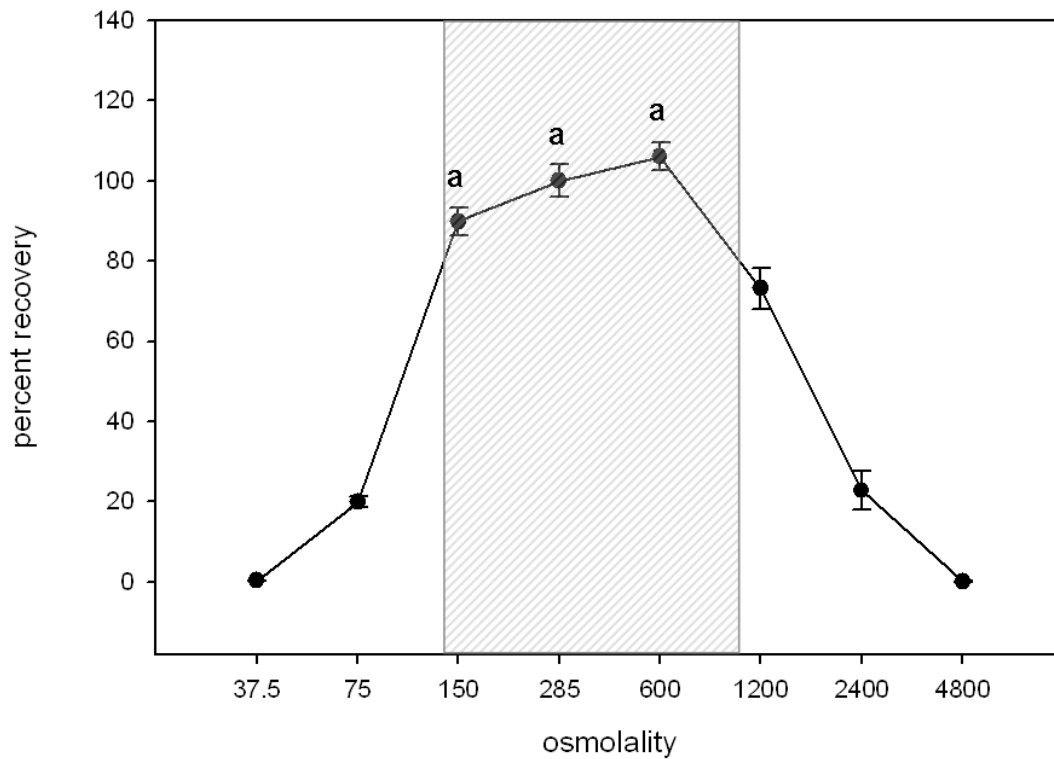


Figure 2.4. Mean (\pm SEM) osmotic tolerance limits of C57BL/6 mouse embryonic stem cells (mESCs) as determined by plasma membrane integrity. Equal numbers of mESCs were exposed to solutions of 38, 75, 150, 600, 1200, 2400 and 4800 mOsm ($n=6$ for each solution) for 10 minutes at room temperature, and compared with controls in which the same quantities of cells were exposed to isosmotic solution (285 mOsm) in the same manner. Plasma membrane integrity was assessed by flow cytometry analysis of propidium iodide exclusion. The shaded area of the graph represents the osmotic range in which 80% of cells maintain plasma membrane integrity. Data points with similar subscripts are not significantly different as compared to isosmotic solution ($p<0.05$).

osmolalities [35] between 150 mOsm and 600 mOsm. Extrapolation from the regression line between data points indicated that 80% of the C57BL/6 mESC population retains membrane integrity between 139 mOsm and 1075 mOsm, or 63% and 153% of isosmotic cell volume, respectively.

Permeability parameters for C57BL/6 mESCs

Changes in mESC volume in the presence of 1.0 M CPA, measured over time EPC at 0, 6, 12, 22, and 34°C, were fitted to compute P_{CPA} and L_p^{CPA} . Room temperature values of P_{CPA} , L_p^{CPA} , and their associated activation energies are shown in Table 2.2.

Table 2.2. Room temperature solute permeabilities and hydraulic conductivities, and their associated activation energies for C57BL/6 mouse embryonic stem cells with respect to 4 cryoprotective agents (CPA).

	Hydraulic conductivity μm/min/atm	Solute permeability μm/min
Dimethyl sulfoxide	0.41 ± 0.03 ^a	4.59 ± 0.41 ^c
Activation energy	14.29 ^b	15.47 ^d
r^2	0.9847	0.9119
Ethylene glycol	0.48 ± 0.06 ^a	4.17 ± 0.24 ^c
Activation energy	15.35 ^b	13.19 ^d
r^2	0.9680	0.8293
Propylene glycol	0.42 ± 0.03 ^a	6.58 ± 0.38
Activation energy	14.12 ^b	14.08 ^d
r^2	0.9829	0.8943
Glycerol	0.14 ± 0.01	1.05 ± 0.07
Activation energy	-	-
r^2	-	-

Due to the relatively low room temperature values for hydraulic conductivity and solute permeability, glycerol was deemed an unsuitable CPA for equilibrium freezing, and measurements at additional temperatures were not conducted. All CPA were at 1.0 M concentration. Hydraulic conductivity and solute permeability values are expressed as mean ± SEM. Superscripts indicate no significant difference among values of each term within the same column.

Table 2.3. Predicted optimal freezing rates for the C57BL/6 mouse embryonic stem cell line.

1.0 M CPA	Rate (°C/min)	Plunge Temperature (°C)
Dimethyl sulfoxide	4.1	-33
Ethylene glycol	1.4	-41
Propylene glycol	1.2	-41

Room temperature L_p^{CPA} values did not differ significantly for Me₂SO, EG, or PG; however L_p^{GLY} was significantly lower than L_p^{CPA} for Me₂SO, EG, and PG ($p<0.05$). Room temperature values for P_{PG} were significantly higher than for P_{EG} , P_{Me_2SO} , and P_{GLY} . P_{GLY} values were significantly lower than P_{EG} and P_{Me_2SO} values ($p<0.05$). Due to these markedly lower room temperature values for L_p^{GLY} and P_{GLY} , GLY was deemed an unsuitable CPA for equilibrium freezing, and measurements at additional temperatures were not conducted. There was no significant difference in E_a values of Me₂SO, EG, and PG for either L_p^{CPA} or P_{CPA} .

Theoretical simulations

A two-step freezing protocol was determined to be optimal for the C57BL/6 mESC line, whereby cells are slowly cooled in a controlled-rate freezer to a temperature (“plunge temperature”) at which they would be rapidly transferred to liquid nitrogen (LN₂). Predicted optimal freezing rates and plunge temperatures, which together in theory create conditions favoring intracellular vitrification, are listed in Table 2.3. The predicted optimal freezing rates were determined to be 4.1°C/minute for Me₂SO, 1.4°C/minute for EG, and 1.2°C/minute for PG, with plunge temperatures of -33°C, -41°C, and -41°C, respectively. PG was chosen as the most effective CPA for empirical validations, and compared against Me₂SO, the CPA of standard protocols.

Empirical validation of predicted optima

Percent PTR in standard conditions did not differ significantly when using cryostraws ($34.2 \pm 6.0\%$) or cryovials ($31.9 \pm 1.6\%$) ($p < 0.05$).

In concurrent studies comparing predicted optimal cooling rates and plunging temperatures, there was no significant effect of seeding (data not shown). Percent post-thaw recovery under standard freezing conditions (Me_2SO , cooling rate of $1^\circ\text{C}/\text{minute}$, and plunge temperature of -80°C) was $31.8 \pm 4.5\%$. Percent post-thaw recovery using Me_2SO at the predicted optimal cooling rate of $4^\circ\text{C}/\text{minute}$ was $39.0 \pm 4.9\%$ using predicted optimal plunge temperature, and $44.8 \pm 6.1\%$ using low plunge temperature. Percent post-thaw recovery using PG at the predicted optimal cooling rate of $1^\circ\text{C}/\text{minute}$ was $48.4 \pm 5.2\%$ at low plunge temperature. These results did not differ significantly. Percent post-thaw recovery using PG at the predicted optimal cooling rate of $1^\circ\text{C}/\text{minute}$ and predicted optimal plunge temperature of -41°C was $63.9 \pm 6.3\%$, a 2-fold, significant increase as compared to standard freezing conditions ($p < 0.05$).

Discussion

Me_2SO has been used for decades to decrease solute effects during cryopreservation of cells [40][41][42]. The Me_2SO slow freezing protocol, involving a cooling rate of $1^\circ\text{C}/\text{minute}$ and plunging into LN_2 at -80°C , has been applied to a variety of cell types with variable results, indicating that modification of this protocol may be beneficial in many circumstances. For example, cryopreservation of human ESCs using

this protocol has been found to diminish *Oct-4* expression [43], and studies of cord blood CD34⁺ cells have suggested that PG is a more appropriate CPA than Me₂SO [13]. Potential variation in response to any cryopreservation protocol can largely be attributed to wide-ranging differences in fundamental cryobiological parameters specific to individual cell types and species [44][45].

Three short technical reports have been published that relate to mouse embryonic stem cell cryopreservation [46][47][48]. These discuss small-scale, 96-well plate protocols for the freezing of mESC transgenic clones. To our knowledge, there have been no rigorous, cell-line specific, published studies on the optimization of cryopreservation protocols for mESCs that would be applicable to mESC banking and culture needs. This study demonstrates that it is possible to dramatically increase post-thaw recovery of mESCs using a fundamental approach to predict optimal equilibrium freezing conditions and CPA. The resulting new protocol greatly increases mESC cryopreservation efficiency, maximizing the use of frozen aliquots within the laboratory as well as in transport and exchange of mESCs between researchers.

Our fundamentally derived approach required the determination of optimum CPA, CPA concentration, equilibrium cooling rate, warming rate, and plunging temperatures. The optimum CPA was considered to be PG for two reasons. First, its high P_{CPA} values at room temperature, as compared to Me₂SO and EG, would enable the most rapid addition and removal of CPA at room temperature with minimal damage to the cell membrane [49]. Secondly, PG is a more stable glass former, *i.e.* vitrifies more easily, than either Me₂SO or EG [50][51], therefore devitrification resulting in intracellular ice formation (IIF) during either cooling or warming is less likely in the

presence of PG as compared to Me₂SO or EG. For empirical validation of predicted optima, the effectiveness of PG as a CPA was compared against the CPA used in standard freezing protocols, Me₂SO, using cryo-straws vs. vials as vessels. There was no significant difference ($p<0.05$) in percent PTR when standard conditions were utilized with either cryo-straws or vials.

Computer simulations of cell response during cooling and warming were conducted by applying mathematical equations describing mass transfer (water, solutes) across cell membranes [52]. A key assumption of this model is that cells respond as “ideal osmometers,” meaning the equilibrium cell volume is linearly related to the reciprocal of the extracellular osmolality. This is described using the Boyle Van’t Hoff equation and a single parameter, V_b [53][54]. C57BL/6 mESCs behaved as linear osmometers over the range of 200-2800 mOsm, indicating that cell volume is not regulated through an active process in the hypo- or hyperosmotic range studied. V_b was determined to be 49.8% of isosmotic cell volume. This value is comparable to the V_b of human spermatozoa (50% of isosmotic cell volume) [55] and human red blood cells (43% of isosmotic cell volume) [56], and is notably higher than the range of V_b measured for other stem cells, including human umbilical cord blood CD34+ cells (27% and 32% of their respective isosmotic cell volumes) [13][57], and human bone marrow-derived hematopoietic progenitor cells (20.5% of isosmotic cell volume) [58].

Osmotic tolerance limits were established based on the retention of membrane integrity in 80% of the cell population following exposure to anisosmotic solutions using NaCl as the impermeable solute. These 80% limits were established for C57BL/6 mESCs to be between approximately 139 and 1075 mOsm. Therefore, 1.0 M CPA,

added drop-wise [59], would maintain the cell within its osmotic tolerance limits, and from a practical standpoint, this concentration was comparable to the standard freezing protocol which employs 10% Me₂SO (1.3 M) and 50% FBS in cell culture medium. Cell injury has been found to vary at similar anisosmotic exposures depending on whether ionic or nonionic solutes are used to induce anisosmolality. For example, hypertonic injury to human spermatozoa has been found to be greater with ionic NaCl solutions than with nonionic sucrose solutions [60], and other studies have shown that in concentrated ionic solutions, cellular membranes can become increasingly permeable to these ions over time [61][62][63]. While this effect is not universal [64], it is possible that the use of NaCl in our osmotic tolerance experiments had an effect independent of osmolality that was not discernible with the present experiments.

Computer simulations using P_{CPA} , L_p^{CPA} , and V_b predicted an optimal cooling rate of 1.2°C/minute for 1.0 M PG and 4.1°C/minute for 1.0 M Me₂SO, indicating that the standard cooling rate of 1°C/minute is inadequate for Me₂SO when applied to this cell line. Use of the predicted optimal cooling rate of 1°C/minute and a plunge temperature of -41°C for 1.0 M PG significantly improved percent PTR of viable C57BL/6 mESCs. The PTR we achieved under these conditions was $63.9 \pm 6.3\%$, a significant 2-fold improvement over standard freezing conditions. Interestingly, but not unexpectedly, percent PTR did not increase significantly when the optimal cooling rate was continued below the predicted optimal plunge temperature to a lower plunge temperature (a standard condition) of -80°C. Continued dehydration beyond -41°C would further minimize intracellular ice formation by favoring vitrification; however, this dehydration would lead to damaging solute effects with deleterious effects on post-thaw recovery.

This effect of dehydration beyond the predicted optimal plunge temperature may also be applied to cells frozen in 1.0 M Me₂SO, frozen at the predicted optimal cooling rate, but plunged into LN₂ at -80°C.

The predicted optimal cooling rate for Me₂SO failed to improve percent PTR even when paired with the optimal plunge temperature. For Me₂SO, there may be a broad range of protocols that would produce similar PTR if a predicted optimal lies in this range [18]. Reduced PTR may also be due to the damaging effects of IIF during either or both cooling and warming. Total solute concentration (>40% volume), the glass-forming capacity of the CPA, and the interaction between cooling and warming rates influence the likelihood of IIF and whether or not a vitrified solution will become crystallized [65][66]. It is possible that the criterion of 40% CPA by weight is an inadequate concentration for vitrification in the presence of Me₂SO; however, investigation of this concept is beyond the scope of this study. Another potential source of cell injury could be that the devitrification of extra- or intracellular glass that formed during the plunge into LN₂ occurs during warming if rates are too slow. Previous studies of two-step, interrupted slow freezing of eight-cell mouse embryos have demonstrated the warming rate dependence of survival [67][68]. While cell dehydration occurred during the initial slow freezing step, the cells still contained freezable water at -40°C. Due to the high viscosity of the intracellular environment in the presence of CPA, the solution vitrified to form a metastable glass. However, with slow warming, the glass devitrified with subsequent recrystallization, damaging the embryos. It is possible that the warming rate of approximately 700°C/minute, although predicted by computer simulation to be within a range that would have negative effects on cell survival, was actually inadequate for the

prevention of ice recrystallization during the warming process. As stated previously, Me₂SO tends to have less stable glass-forming properties than PG [50], which would increase the likelihood of this effect.

The improved cryopreservation protocol for the C57BL/6 mESC line utilizes 1.0 M PG, a cooling rate of 1°C/minute, warming rate of approximately 700°C/minute and a plunge temperature of -41°C (Figure 2.5) and will greatly facilitate banking, transport and post-thaw reconstitution of cultures. Our hypothesis-based, fundamental cryobiological approach resulted in a two-fold increase in PTR of membrane-intact mESC as compared to the standard freezing protocol, as measured by propidium iodide exclusion. The methods to improve cryopreservation protocols outlined in this study will speed analysis of future mouse ESC lines, which is especially important for current mESC lines that have poor PTR, and for future, perhaps rare mESC lines involved in projects such as the “Knock-Out Mouse Project”. Finally, defining methods to improve cryopreservation in mESC protocols gives clues as to how to improve cryopreservation of human ESC lines.

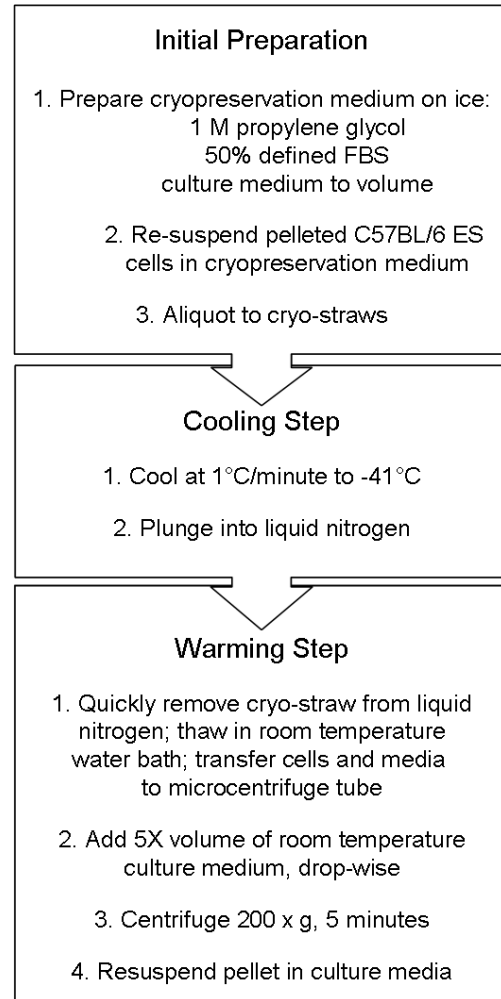


Figure 2.5. Improved freezing protocol for C57BL/6 mouse embryonic stem cells. FBS, fetal bovine serum.

References

1. Bedell, M.A., N.A. Jenkins, and N.G. Copeland, *Mouse models of human disease. Part I: techniques and resources for genetic analysis in mice*. Genes Dev, 1997. **11**(1): p. 1-10.
2. Bedell, M.A., et al., *Mouse models of human disease. Part II: recent progress and future directions*. Genes Dev, 1997. **11**(1): p. 11-43.
3. Austin, C.P., et al., *The knockout mouse project*. Nat Genet, 2004. **36**(9): p. 921-4.
4. Auwerx, J., et al., *The European dimension for the mouse genome mutagenesis program*. Nat Genet, 2004. **36**(9): p. 925-7.
5. Munroe, R.J., et al., *Mouse mutants from chemically mutagenized embryonic stem cells*. Nat Genet, 2000. **24**(3): p. 318-21.
6. *Touching base*. Nat Genet, 2006. **38**(10): p. 1107.
7. Critser, J.K. and L.E. Mobraaten, *Cryopreservation of murine spermatozoa*. IJAR J, 2000. **41**(4): p. 197-206.
8. Pegg, D.E. and M.P. Diaper, *Freezing versus vitrification: Basic principles*, in *Cryopreservation and Low Temperature Biology in Blood Transfusion*, C.T. Smit Sibinga, P.C. Das, and H.T. Meryman, Editors. 1990, Kluwer Academic Publishers: Dordrecht. p. 55-69.
9. Fahy, G.M., et al., *Vitrification as an approach to cryopreservation*. Cryobiology, 1984. **21**(4): p. 407-26.
10. Katkov, I.I., et al., *Low- and high-temperature vitrification as a new approach to biostabilization of reproductive and progenitor cells*. International Journal of Refrigeration, 2006. **29**: p. 346-357.
11. Isachenko, E., et al., *Vitrification of mammalian spermatozoa in the absence of cryoprotectants: from past practical difficulties to present success*. Reprod Biomed Online, 2003. **6**(2): p. 191-200.
12. Yavin, S. and A. Arav, *Measurement of essential physical properties of vitrification solutions*. Theriogenology, 2007. **67**(1): p. 81-9.

13. Woods, E.J., et al., *Osmometric and permeability characteristics of human placental/umbilical cord blood CD34+ cells and their application to cryopreservation*. J Hematother Stem Cell Res, 2000. **9**(2): p. 161-73.
14. Mazur, P., *Kinetics Of Water Loss From Cells At Subzero Temperatures And The Likelihood Of Intracellular Freezing*. J Gen Physiol, 1963. **47**: p. 347-69.
15. Liu, J., J.A. Christian, and J.K. Critser, *Canine RBC osmotic tolerance and membrane permeability*. Cryobiology, 2002. **44**(3): p. 258-68.
16. Devireddy, R.V., et al., *Subzero water permeability parameters of mouse spermatozoa in the presence of extracellular ice and cryoprotective agents*. Biol Reprod, 1999. **61**(3): p. 764-75.
17. Agca, Y., et al., *Chimpanzee (Pan troglodytes) spermatozoa osmotic tolerance and cryoprotectant permeability characteristics*. J Androl, 2005. **26**(4): p. 470-7.
18. Woods, E.J., et al., *A theoretically optimized method for cord blood stem cell cryopreservation*. J Hematother Stem Cell Res, 2003. **12**(3): p. 341-50.
19. Fujikawa, S., *The effect of various cooling rates on the membrane ultrastructure of frozen human erythrocytes and its relation to the extent of haemolysis after thawing*. J Cell Sci, 1981. **49**: p. 369-82.
20. Mazur, P., *Freezing of living cells: mechanisms and implications*. Am J Physiol, 1984. **247**(3 Pt 1): p. C125-42.
21. Nobel, P.S., *The Boyle-Van't Hoff relation*. Journal of Theoretical Biology, 1969. **23**(3): p. 375-9.
22. Mazur, P., W.F. Rall, and S.P. Leibo, *Kinetics of water loss and the likelihood of intracellular freezing in mouse ova. Influence of the method of calculating the temperature dependence of water permeability*. Cell Biophys, 1984. **6**(3): p. 197-213.
23. Jacobs, M.H., *The simultaneous measurement of cell permeability to water and to dissolved substances*. Journal of Cellular and Comparative Physiology, 1933. **2**(4): p. 427-444.
24. Mazur, P., S.P. Leibo, and E.H. Chu, *A two-factor hypothesis of freezing injury. Evidence from Chinese hamster tissue-culture cells*. Exp Cell Res, 1972. **71**(2): p. 345-55.

25. Doetschman, T., *Gene Targeting in Embryonic Stem Cells: I. History and Methodology*, in *Transgenic Animal Technology: A Laboratory Handbook, Second Edition*, C.A. Pinkert, Editor. 2002, Academic Press: San Diego.
26. Gordeeva, O.F., et al., [*Expression of regulatory genes Oct-4, Pax-6, Prox-1, Ptx-2 at the initial stages of differentiation of embryonic stem cells in vitro*]. Ontogenез, 2003. **34**(3): p. 174-82.
27. *Preparation of ES Cells for Injection*, in *Manipulating the Mouse Embryo: A Laboratory Manual*, A. Nagy, et al., Editors. 2003, Cold Spring Harbor Laboratory Press: Cold Spring Harbor, New York. p. 469.
28. Schenke-Layland, K., et al., *Collagen IV induces trophoectoderm differentiation of mouse embryonic stem cells*. Stem Cells, 2007. **25**(6): p. 1529-38.
29. McGann, L.E., A.R. Turner, and J.M. Turc, *Microcomputer interface for rapid measurements of average volume using an electronic particle counter*. Med Biol Eng Comput, 1982. **20**(1): p. 117-20.
30. Benson, J.D., et al., *Mercury free operation of the Coulter counter MultiSizer II sampling stand*. Cryobiology, 2005. **51**(3): p. 344-7.
31. Benson, C.T., et al., *Determination of the osmotic characteristics of hamster pancreatic islets and isolated pancreatic islet cells*. Cell Transplant, 1993. **2**(6): p. 461-5.
32. Fedorow, C., et al., *Osmotic and cryoprotectant permeation characteristics of islet cells isolated from the newborn pig pancreas*. Cell Transplant, 2001. **10**(7): p. 651-9.
33. Phelps, M.J., et al., *Effects of Percoll separation, cryoprotective agents, and temperature on plasma membrane permeability characteristics of murine spermatozoa and their relevance to cryopreservation*. Biol Reprod, 1999. **61**(4): p. 1031-41.
34. Ebertz, S.L. and L.E. McGann, *Cryoprotectant permeability parameters for cells used in a bioengineered human corneal equivalent and applications for cryopreservation*. Cryobiology, 2004. **49**(2): p. 169-80.
35. Katkov, II, *A two-parameter model of cell membrane permeability for multisolute systems*. Cryobiology, 2000. **40**(1): p. 64-83.
36. Gilmore, J.A., et al., *Determination of plasma membrane characteristics of boar spermatozoa and their relevance to cryopreservation*. Biol Reprod, 1998. **58**(1): p. 28-36.

37. Songsasen, N. and S.P. Leibo, *Cryopreservation of mouse spermatozoa. I. Effect of seeding on fertilizing ability of cryopreserved spermatozoa*. Cryobiology, 1997. **35**(3): p. 240-54.
38. Petersen, A., et al., *A new approach for freezing of aqueous solutions under active control of the nucleation temperature*. Cryobiology, 2006. **53**(2): p. 248-57.
39. Zolman, J.F., *Biostatistics: Experimental Design and Statistical Inference*. 1993, New York: Oxford University Press, Inc. 343.
40. Pegg, D.E., *Red cell volume in glycerol/sodium chloride/water mixtures*. Cryobiology, 1984. **21**(2): p. 234-9.
41. Lovelock, J.E. and M.W. Bishop, *Prevention of freezing damage to living cells by dimethyl sulphoxide*. Nature, 1959. **183**(4672): p. 1394-5.
42. Fuller, B.J., *Cryoprotectants: the essential antifreezes to protect life in the frozen state*. Cryo Letters, 2004. **25**(6): p. 375-88.
43. Katkov, II, et al., *Cryopreservation by slow cooling with DMSO diminished production of Oct-4 pluripotency marker in human embryonic stem cells*. Cryobiology, 2006. **53**(2): p. 194-205.
44. Gao, D., P. Mazur, and J.K. Critser, *Fundamental Cryobiology of Mammalian Sperm*, in *Reproductive Tissue Banking: Scientific Principles*, A.M. Karow and J.K. Critser, Editors. 1997, Academic Press: San Diego. p. 263-328.
45. Woods, E.J., et al., *Fundamental cryobiology of reproductive cells and tissues*. Cryobiology, 2004. **48**(2): p. 146-56.
46. Ure, J.M., S. Fiering, and A.G. Smith, *A rapid and efficient method for freezing and recovering clones of embryonic stem cells*. Trends Genet, 1992. **8**(1): p. 6.
47. Chan, S.Y. and M.J. Evans, *In situ freezing of embryonic stem cells in multiwell plates*. Trends Genet, 1991. **7**(3): p. 76.
48. Udy, G.B. and M.J. Evans, *Microplate DNA preparation, PCR screening and cell freezing for gene targeting in embryonic stem cells*. Biotechniques, 1994. **17**(5): p. 887-94.
49. Gilmore, J.A., et al., *Osmotic properties of boar spermatozoa and their relevance to cryopreservation*. J Reprod Fertil, 1996. **107**(1): p. 87-95.
50. Baudot, A., L. Alger, and P. Boutron, *Glass-forming tendency in the system water-dimethyl sulfoxide*. Cryobiology, 2000. **40**(2): p. 151-8.

51. Baudot, A. and V. Odagescu, *Thermal properties of ethylene glycol aqueous solutions*. Cryobiology, 2004. **48**(3): p. 283-94.
52. Kedem, O. and A. Katchalsky, *Thermodynamic analysis of the permeability of biological membranes to non-electrolytes*. 1958. Biochim Biophys Acta, 1989. **1000**: p. 413-30.
53. Meryman, H.T., *Freezing injury and its prevention in living cells*. Annu Rev Biophys Bioeng, 1974. **3**(0): p. 341-63.
54. Mazur, P. and U. Schneider, *Osmotic responses of preimplantation mouse and bovine embryos and their cryobiological implications*. Cell Biophys, 1986. **8**(4): p. 259-85.
55. Gilmore, J.A., et al., *Effect of cryoprotectant solutes on water permeability of human spermatozoa*. Biol Reprod, 1995. **53**(5): p. 985-95.
56. Solomon, A.K., M.R. Toon, and J.A. Dix, *Osmotic properties of human red cells*. J Membr Biol, 1986. **91**(3): p. 259-73.
57. Hunt, C.J., S.E. Armitage, and D.E. Pegg, *Cryopreservation of umbilical cord blood: I. Osmotically inactive volume, hydraulic conductivity and permeability of CD34(+) cells to dimethyl sulphoxide*. Cryobiology, 2003. **46**(1): p. 61-75.
58. Gao, D.Y., et al., *Fundamental cryobiology of human hematopoietic progenitor cells. I: Osmotic characteristics and volume distribution*. Cryobiology, 1998. **36**(1): p. 40-8.
59. Gilmore, J.A., et al., *Determination of optimal cryoprotectants and procedures for their addition and removal from human spermatozoa*. Hum Reprod, 1997. **12**(1): p. 112-8.
60. Gao, D.Y., et al., *Hyperosmotic tolerance of human spermatozoa: separate effects of glycerol, sodium chloride, and sucrose on spermolysis*. Biol Reprod, 1993. **49**(1): p. 112-23.
61. Lovelock, J.E., *The haemolysis of human red blood-cells by freezing and thawing*. Biochim Biophys Acta, 1953. **10**(3): p. 414-26.
62. Chan, H.C. and D.J. Nelson, *Chloride-dependent cation conductance activated during cellular shrinkage*. Science, 1992. **257**(5070): p. 669-71.
63. Weinstein, A.M. and J.L. Stephenson, *Electrolyte transport across a simple epithelium. Steady-state and transient analysis*. Biophys J, 1979. **27**(2): p. 165-86.

64. Woods, E.J., et al., *Osmotic characteristics of isolated human and canine pancreatic islets*. Cryobiology, 1997. **35**(2): p. 106-13.
65. Liu, J., et al., *Cryobiology of rat embryos II: A theoretical model for the development of interrupted slow freezing procedures*. Biol Reprod, 2000. **63**(5): p. 1303-12.
66. Shaw, J.M., et al., *Vitrification properties of solutions of ethylene glycol in saline containing PVP, Ficoll, or dextran*. Cryobiology, 1997. **35**(3): p. 219-29.
67. Rall, W. and C. Polge, *Effect of warming rate on mouse embryos frozen and thawed in glycerol*. J Reprod Fertil., 1984. **70**(1): p. 285-92.
68. Rall, W.F., D.S. Reid, and C. Polge, *Analysis of slow-warming injury of mouse embryos by cryomicroscopical and physiochemical methods*. Cryobiology, 1984. **21**(1): p. 106-21.

CHAPTER 3

COMPARATIVE FUNDAMENTAL CRYOBIOLOGY OF MULTIPLE MOUSE EMBRYONIC STEM CELL LINES AND THE IMPLICATIONS FOR EMBRYONIC STEM CELL CRYOPRESERVATION PROTOCOLS

Introduction

Coordinated projects, such as the Knockout Mouse Project (KOMP)[1], Canada's North American Conditional Mouse Mutagenesis Program (NorCOMM, <http://norcomm.phenogenomics.ca>), and the European Conditional Mouse Mutagenesis Program (EUCOMM, <http://www.eucomm.org>)[2], will create thousands of mutant mouse embryonic stem cell (mESC) lines as a step towards producing thousands of genetically modified mice for biomedical research. They will also create the logistical problem of animal storage and maintenance. Storage and maintenance of live animal lines when not actively under research are highly impractical [3], but cryo-banking of mouse lines as embryonic stem cells (ESC) is cost-effective, and the restoration of mESCs into live, reproductively viable mice is routine. The efficiency of this process is

greatly enabled when cryopreservation and thawing methods produce healthy, rapidly dividing, germ-line competent cells.

Percent post-thaw recovery (PTR) following cell cryopreservation has been demonstrated to vary widely across and within species, and ESCs are no exception. Human and non-human primate ESCs are notoriously difficult to cryopreserve and there have been numerous studies designed to improve PTR using variations of non-equilibrium and equilibrium-cooling methods [4-14]. Mouse ESC cryopreservation, on the other hand, has generally been regarded as successful [15] and relatively few reports have been published that center around post-thaw recovery following cryopreservation [16-19]. However, it is difficult to compare estimates of mESC recovery between reports such as those of Ure *et al.* [16] and Udy *et al.* [18], which count recovery of colonies as opposed to individual cells, and reports such as that by Miszta-Lane *et al.* and Kashuba Benson *et al.* [20], where the percent of single cells are reported. Additionally, the report by Miszta-Lane *et al.* [19] centers on the 129R1 mESC line, which is one cell line that cryopreserves satisfactorily. Anecdotal reports (personal communication, D. Nielsen, Stem Cell Technologies technical support, 2004; personal communication, Xin Yu, University of California-Davis, 2004) and a recent publication from Kashuba Benson *et al.* [20] concerning the C57BL/6 cell line show PTR of mESCs to be widely variable across cell lines.

A fundamental approach to improving cryopreservation methods is based on Mazur's Two Factor Hypothesis [21], in which the ideal freezing protocol is one that optimally balances two key damaging forces of intracellular ice formation and solute effects. Systematic analysis of key cryobiological parameters of a cell enables the

description of the total cell response to water and solute (in particular, cryoprotective agents (CPAs)) movement across the cell membrane and the temperature dependence of this process. These parameters include osmotic tolerance limits (OTL), osmotically inactive cell volume (V_b), hydraulic conductivity (L_p), and CPA permeability of the cell membrane (P_{CPA}). Activation energy (E_a) is described for L_p and P_{CPA} . Quantification of these parameters will enable computer modeling to estimate optimal cooling and warming rates as well as optimal plunge temperatures that keep intra- and extra-cellular temperatures within 2 degrees of each other to avoid supercooling and resulting ice formation [21], and also cool quickly enough to avoid damaging solute effects.

We previously designed a method to improve post-thaw recovery for a C57BL/6 mESC line by which ESC lines could be systematically analyzed in order to derive optimal cooling and warming rates as well as plunge temperatures [20]. In the present study, we analyzed and compared four mESC lines of different genetic backgrounds (BALB/c, CBA, FVB, and 129R1) in order to determine fundamental cryobiological factors that are responsible for the observed wide variation in PTR. With these data, we can determine protocols individualized to each cell line that optimize PTR or gain clues as to whether a “one-size fits all” protocol could be designed to optimize PTR in all mESC lines or in groups of mESC lines with common characteristics.

Table 3.1. Definition of major symbols and terms

Symbol or abbreviation	Description	Units	Value
e, i	Superscripts: e, external; i, internal	None	None
s, n, w	Subscripts: s, solute; n, non-permeating; w, water	None	None
L_p^{CPA}	Hydraulic conductivity in the presence of cryoprotectant	$\mu\text{m min}^{-1} \text{ atm}^{-1}$	Parameter
P_{CPA}	Solute permeability	$\mu\text{m min}^{-1}$	Parameter
E_a	Activation energy	kcal mol^{-1}	Parameter
T	Temperature	K	295
A	Cell surface area	μm^2	Parameter
V	Cell volume	μm^3	Variable
V_b	Osmotically inactive cell volume	μm^3	Parameter
$V_w(t)$	Intracellular water volume at time t	μm^3	Variable
$n_s^i(t)$	Moles of internal permeating solute at time t	Moles	Variable
t	Time	Seconds	Variable
M_{iso}	Osmolality of initial (isotonic) intracellular salts	$\text{Osm kg}^{-1} \text{ H}_2\text{O}$	0.290
M_n^e	Osmolality of extracellular salts	$\text{Osm kg}^{-1} \text{ H}_2\text{O}$	0.290
n_n^i	Osmoles of intracellular salts	Osm	Variable
M	Molality	$\text{mol kg}^{-1} \text{ H}_2\text{O}$	Variable
\bar{V}	Partial molal volume of solute	L mole^{-1}	Variable
R	The universal gas constant	$\text{kcal mole}^{-1} \text{ K}^{-1}$	1.987×10^{-3}

Materials & Methods

Embryonic stem cells

The following mESC lines were acquired at early passage: BALB/c (Thromb-X Group, Chemicon International, Temecula, CA, now part of Millipore, Billerica, MA), CBA (Thromb-X Group), FVB/N (Thromb-X Group), and 129R1 (A. Nagy, Mount Sinai Hospital, Toronto, Canada). Mouse ESC cultures were negative for all pathogens (IMPACT I test, Research Animal Diagnostic Laboratory, Columbia, Missouri; www.radil.missouri.edu/info/index.asp).

Cell culture and standard cryopreservation method

Embryonic stem cells were cultured on primary mouse embryonic fibroblast cells (PMEF) (Millipore, Billerica, MA) at 37°C and 5% CO₂. Culture media for the 129R1 mESC line and BALB/c mESC line (R1/C culture medium) contained 15% Defined FBS (Hyclone, Logan, UT), 0.1mM non-essential amino acids (GIBCO/ Invitrogen, Carlsbad, CA), 1.0 mM sodium pyruvate (GIBCO), 100 µM beta-mercaptoethanol (Sigma Aldrich, St. Louis, MO), 50 IU/mL penicillin (GIBCO), 50 µg/mL streptomycin (GIBCO), and 1000 U ESGRO/mL (Millipore) in high glucose DMEM (Millipore). CBA and FVB mESCs were cultured in RESGRO culture medium (Millipore). Embryonic stem cells were passaged and/or collected every 2 days or at approximately 80% confluence.

For the standard equilibrium cooling method, cells were resuspended in freezing medium (1.3 M (10%) Me₂SO (Sigma Aldrich), 50% defined fetal bovine serum (Hyclone), and 40% culture medium) in 1mL aliquots in cryovials (Nalgene Nunc International, Rochester, NY). Cryovials were transferred to a commercially available freezing kit (Nalgene), refrigerated at -80°C overnight (a process which cools at a rate of approximately 1°C/minute), and subsequently transferred to liquid nitrogen (LN₂).

Embryonic stem cells were used within 10 passages from the original, and were of normal karyotype at highest passage. Cell counts were performed using a hemacytometer and Trypan blue stain (Sigma Aldrich) for membrane integrity for all standard culture.

Separation of mESCs from feeders by differential sedimentation

For all experiments, mESCs were separated from the feeder cells using a differential sedimentation technique previously described by Doetschman [22]. The separation of PMEF from mESCs is routine, and there are many variations of the basic method exploiting the difference in the rate at which fibroblast feeder cells and mESCs settle and adhere to culture dishes [23][24][25]. Briefly, trypsinized ESC cultures containing PMEF were centrifuged, resuspended in 10 mL of culture medium, and plated on the original 100mm cell culture dish for 30 minutes at 37°C. Following incubation, the cell suspension was transferred to a second culture dish for one-hour incubation at 37°C in order to remove remaining fibroblast feeders. Following the second incubation,

the cell suspension was removed, and these collected ESCs were counted, centrifuged, and resuspended in either DPBS or culture medium for experimentation.

Percent post-thaw recovery by cell line

For all cell lines, mESCs in culture were trypsinized into single cell suspensions, feeder cells were removed, and mESCs were resuspended at 1×10^6 cells/mL in standard freezing medium containing prepared R1/C culture medium (described under Cell Culture and Cryopreservation Methods). Membrane integrity prior to cryopreservation was assessed by flow cytometry analysis (FACScan, BD Biosciences, San Jose, CA) of propidium iodide staining of suspended cells in 1X PBS. Immediately post-thaw, ESCs were diluted, drop-wise, by 5 volumes of culture media, centrifuged, resuspended in 1X PBS, stained with propidium iodide, and analyzed by flow cytometry for membrane integrity. Percent post-thaw recovery was expressed with consideration for both total cell count and percent membrane intact cells before and after cryopreservation:

$$\text{PTR} = \frac{\text{total post - thaw membrane intact cells}}{\text{total pre - freeze membrane intact cells}}(100)$$

Electronic particle counter

Using the method previously described by Kashuba Benson *et al.* [20], a modified [26] electronic particle counter (EPC) (Coulter Counter model ZM, Beckman Coulter, Inc., Fullerton, CA) was used for all cellular volumetric measurements with volume

calibration using standard nominal 10 μm polystyrene latex particles (Beckman Coulter, Inc., Fullerton, CA) at 0, 6, 12, and 22°C. Raw volumetric data were exported into Mathematica (Wolfram Research Inc., Champaign, Illinois) computing package for processing and analysis.

Determination of osmotic tolerance limits

Osmotic tolerance limits were defined by the maintenance of plasma membrane integrity, as indicated by propidium iodide exclusion in 80% of the ESC population following exposure to anisosmotic conditions using sodium chloride as the impermeable solute, in the manner previously described by Kashuba Benson *et al.* [20]. Briefly, solutions of varying osmolality were prepared using Dulbecco's Phosphate Buffered Saline (DPBS) that was adjusted to the appropriate osmolality by the addition of either double distilled water or sodium chloride (Sigma Aldrich). The solutions were adjusted to pH 7.1 using sodium hydroxide or hydrochloric acid as necessary. The osmolality of each solution was verified using a vapor pressure osmometer (Wescor, Logan, UT). On three separate days for each ESC line, ESCs were trypsinized and separated from fibroblast feeders. Equal numbers of cells were then exposed to solutions of 37, 75, 150, 600, 1200, 2400 and 4800 mOsm ($n=3$ for each solution) for 10 minutes at room temperature. Cells were abruptly returned to isosmotic by the abrupt addition of appropriate volumes of hyperosmotic solution in the case of hypoosmotic conditions, and hypoosmotic solution in the case of hyperosmotic conditions. Cells were then centrifuged for five minutes at 200g and resuspended in isosmotic solution. Cells

exposed to anisosmotic conditions were compared to controls in which the same quantities of cells were exposed to isosmotic conditions (285 mOsm) following the same protocol. Plasma membrane integrity was assessed by flow cytometry analysis (FACScan, Becton Dickinson, San Jose, CA) of propidium iodide exclusion.

Measurement of cell osmotic response

Embryonic stem cell volumetric response to variable osmolality was measured at 22°C using an EPC, as previously described [20][27][28][29][30][31]. Mean cell volume response was measured in real time following abrupt exposure to 206, 285, 600, 900, 1350, and 2880 mOsm solutions prepared from 10X PBS (Sigma) and Milli-Q water and adjusted to pH 7.1 with hydrochloric acid. The osmolality of the solutions was verified using a vapor pressure osmometer (Wescor). Data were averaged over 100 ms intervals prior to analysis. Three replicates were performed for each experimental condition. For a representative plot of the output, please refer to Figure 2.1A [20]. Equilibrated cell volumes were normalized to their respective isotonic values, and plotted against the reciprocal of normalized osmolality in accordance with the Boyle Van't Hoff relationship [32]. Linear regression was performed using Mathematica to fit the Boyle Van't Hoff equation to the data. This equation is defined by:

$$V = V_{w,iso} M_{iso} / M + V_b,$$

where V is cell volume at osmolality M , $V_{w,iso}$ is isotonic cell water volume, M_{iso} is isotonic osmolality, and V_b is the osmotically inactive cell volume. V_b was determined by

performing a linear regression of volume as a function of the reciprocal of osmolality and extrapolating to infinite osmolality (i.e. $1/M=0$).

Determination of permeability parameters

As previously described by Kashuba Benson *et al.* [20], volume changes over time were measured by an EPC following abrupt addition of cells to 1.0 M CPA in 1X PBS. Volumetric changes were measured in the presence of 1.0 M Me₂SO, 1.0 M EG, and 1.0 M PG at 0, 6, 12, 22, and 34°C. For a representative plot of the experimental output, please refer to Figure 2.1B [20]. Measurements of cells in the presence of 1.0 M GLY were determined at 22 °C. Three replicates were performed for each treatment on 3 different days.

Data were fit to the following two-parameter mass transport model [33] to determine membrane permeability coefficients for cryoprotective agents (P_{CPA}) and hydraulic conductivity in the presence of cryoprotectants (L_p^{CPA}) at all temperatures:

$$\frac{dV_w}{dt} = -L_p A R T \left(M_s^e + M_n^e - \frac{n_s^i + n_n^i}{V_w} \right),$$

$$\frac{dn_s^i}{dt} = P_s A \left(M_s^e - \frac{n_s^i}{V_w} \right).$$

Here, superscripts e and i indicate extra- and intracellular quantities, respectively, subscripts s and n indicate permeating and non-permeating quantities, respectively, and A is the volume independent spherical surface area at V_{iso} . Finally, we assume the relationship $n^i = V_w M^i$ where V_w is the intracellular water volume.

The Arrhenius relationship^{c,f}[34] was used to determine the activation energies, E_a , for the parameters L_p^{CPA} and P_{CPA} by plotting the permeability value (L_p^{CPA} or P_{CPA}) at any absolute temperature T as $R \ln(P(T))$ versus $1/T$:

$$P(T) = P_0 \exp\left[\frac{E_a}{R}\left(\frac{1}{T_0} - \frac{1}{T}\right)\right],$$

where P_0 is the value at some reference temperature T_0 , R is the gas constant and E_a is the activation energy for the process, expressed in kcal/mol and determined by the slope of the linear regression.

Statistical analysis

For all comparisons, standard analysis of variance (ANOVA) was performed with the SAS General Linear Models program (SAS Institute, Inc., Cary, NC) using an alpha value of $p<0.05$. In situations where a plot of the residuals of a data set was not normally distributed, data were normalized using either natural logarithm or square root transformation. Based on the results of the ANOVA for V_b and lower OTL values, Fisher's least significant difference tests were conducted to evaluate significant differences between mESC lines ($p<0.05$). All values are presented as mean \pm SEM, unless stated otherwise.

Results

Percent post-thaw recovery varied by cell line under standard conditions

Percent post-thaw recovery of mESC lines varied significantly across cell lines ($p<0.05$) under standard freezing conditions. Percent post-thaw recovery was $32.5 \pm 4.0\%$ (average \pm SEM) for the BALB/c line, $17.2 \pm 1.6\%$ for the CBA line, $10.0 \pm 2.7\%$ for the FVB line, and $24.4 \pm 1.1\%$ for the 129R1 line (Figure 3.1). Values were significantly different between the BALB/c, CBA, and FVB lines and between the FVB and 129R1 mESC lines ($p<0.05$).

Osmotically inactive cell volume

Mouse ESCs from all lines behaved as ideal osmometers over a range of 200 mOsm to 2800 mOsm. Extrapolation of the regression line to infinite osmolality gave a V_b of $43.2 \pm 2.4\%$ of isosmotic cell volume for the BALB/c line, $39.1 \pm 3.3\%$ for the CBA line, $52.6 \pm 2.4\%$ for the FVB line, and $52.0 \pm 4.5\%$ for the 129R1 line. There was a significant main effect of genetic background on V_b ($p<0.05$), with V_b of the CBA mESC line significantly lower than that of the FVB or R1 mESC line ($p<0.05$). The previously published V_b value for the C57BL/6 mESC line [20] is listed for comparative purposes with values for the cell lines in this study in Table 3.2.

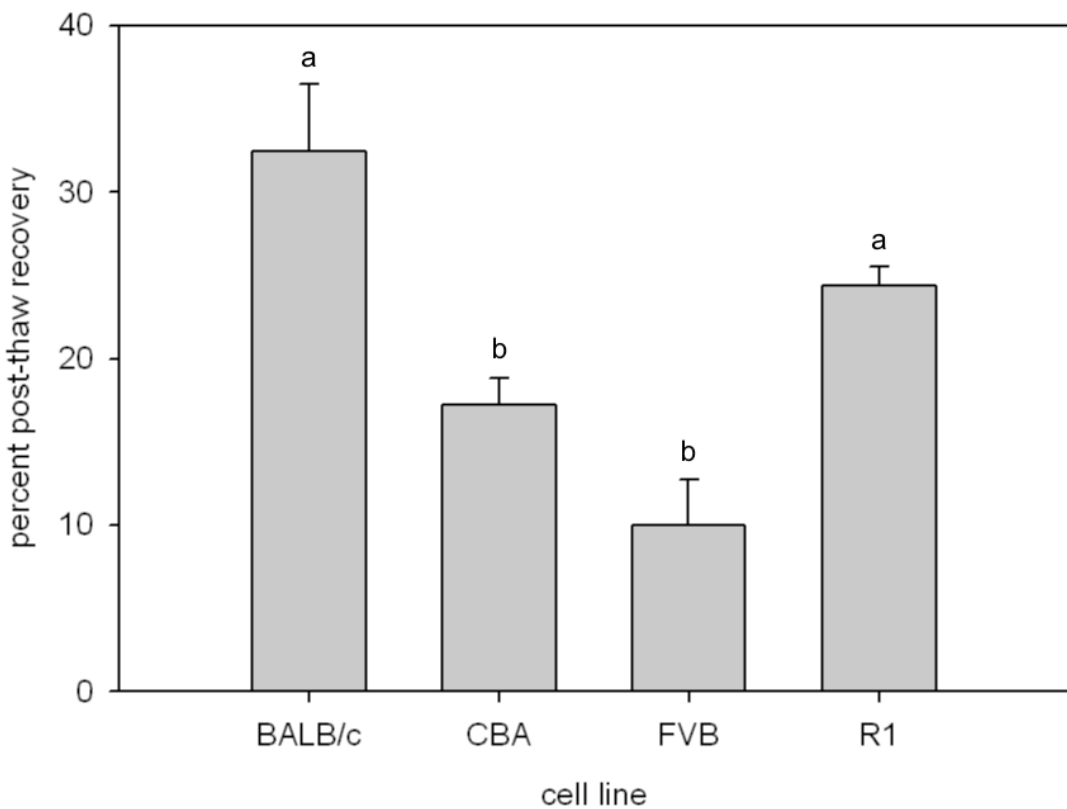


Figure 3.1. Percent post-thaw recoveries of membrane-intact BALB/c, CBA, FVB, and 129R1 (R1) mouse embryonic stem cells frozen in cryovials in standard freezing conditions (10^6 cells/mL, 1°C/minute cooling rate, 1.0 M Me₂SO, -80°C plunge temperature). Percent post-thaw recovery is expressed as mean \pm SEM. Different superscripts indicate significantly different means ($p < 0.05$).

Table 3.2. Osmotically inactive cell volume (V_b) of four mouse embryonic stem cell lines.

Cell line	V_b (% of isosmotic)
C57BL/6 [20]	49.7 ± 1.3
BALB/c	43.2 ± 2.4 ^a
CBA	39.1 ± 3.3 ^{a,b}
FVB	52.6 ± 2.4 ^{a,c}
R1	52.0 ± 4.5 ^{a,c}

V_b is expressed as mean percent of isosmotic cell volume ± SEM. V_b listed for the C57BL/6 line was previously published [20] and is listed for comparative purposes, therefore C57BL/6 values were not included in statistical analyses. Different superscripts indicate statistically significant differences ($p<0.05$).

Osmotic tolerance

The effects of anisosmotic conditions on mESC membrane integrity, as determined by propidium iodide (PI) exclusion, are shown along with previously published 80% osmotic tolerance limits for the C57BL/6 mESC line [20] for illustrative purposes, in Figure 3.2. Extrapolation from the regression line between data points indicated that 80% of the mESC population retained membrane integrity between 142 ± 5 mOsm (average ± SEM) and 816 ± 40 mOsm (1.6 and 0.6 x V_{iso} , BALB/c), 153 ± 5 mOsm and 784 ± 10 mOsm (1.6 and 0.6 x V_{iso} , CBA), 163 ± 5 mOsm and 671 ± 80 mOsm (1.4 and 0.7 x V_{iso} , FVB), and 143 ± 5 mOsm and 1003 ± 141 mOsm (1.5 and 0.7 x V_{iso} , 129R1). There was a significant main effect of genetic background on the lower OTL ($p<0.05$), in which the lower OTL of the FVB cell line was significantly higher ($p<0.05$) than that of the R1 or BALB/c mESC line. Genetic background was not a significant main effect for upper OTL, however the upper OTL of the 129R1 cell line was

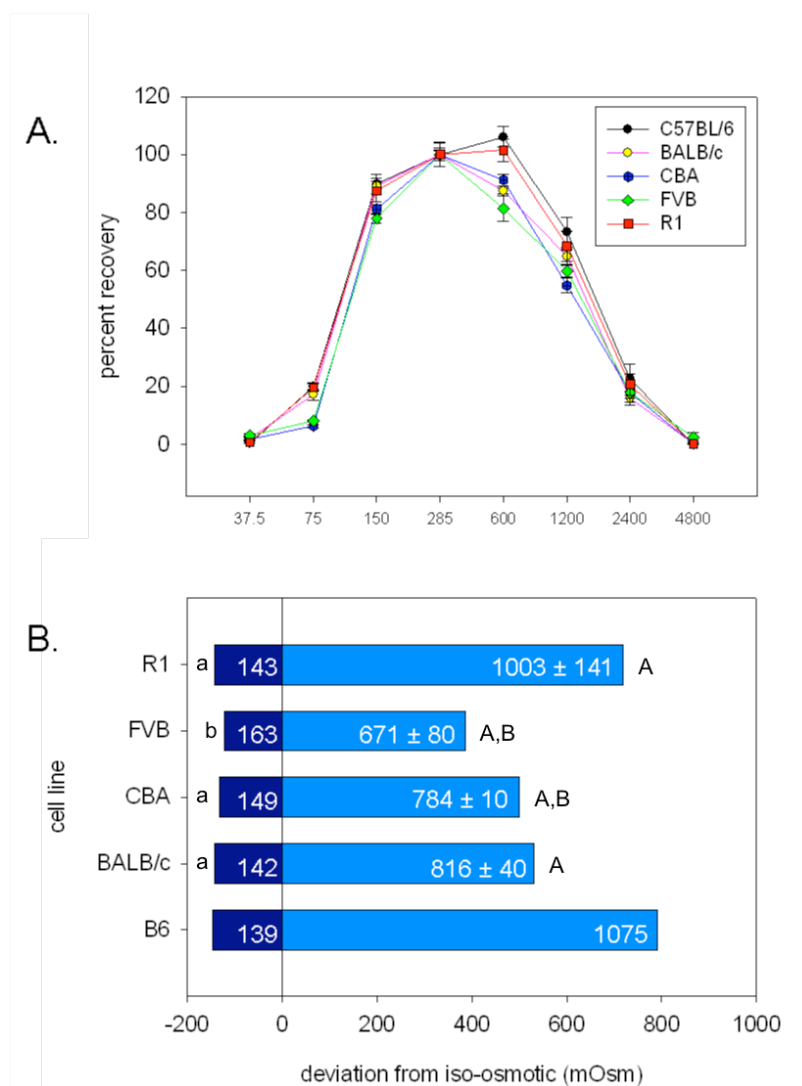


Figure 3.2. Osmotic tolerance limits (OTL) of five mouse embryonic stem cell (mESC) lines as determined by plasma membrane integrity. Previously published data for the C57BL/6 mESC line [20] are included for comparative purposes but were not included in statistical analyses. Equal quantities of mESCs were exposed to solutions of 38, 75, 150, 600, 1200, 2400, and 4800 mOsm for 10 minutes at room temperature, and compared with controls exposed to isosmotic solution (285 mOsm) in the same manner. Plasma membrane integrity was assessed by flow cytometry analysis of propidium iodide exclusion. A. Inverted U-shaped osmotic tolerance curves of BALB/c, C57BL/6 (B6), CBA, FVB, and 129R1 (R1) mESC lines. B. OTL, defined as the range of osmolalities in which 80% of cells maintained plasma membrane integrity, for each of 5 different mESC lines (n=3). “0” represents isosmotic (285 mOsm). Distance from isosmotic is in terms of mOsm. Inset numbers indicate the extrapolated mean osmolalities (through linear regression) \pm SEM at which 80% of mESCs retained membrane integrity. SEM for all lower OTL was \pm 5mOsm. Different lower case superscripts indicate statistically significant differences in lower OTL ($p<0.05$). Different upper case superscripts indicate statistically significant differences in upper OTL ($p<0.05$).

significantly higher than the upper OTL of the FVB cell line ($p<0.05$). Genetic background was not a main effect for the range of OTL; however the range of OTL for the 129R1 line was significantly greater than that of the FVB line ($p<0.05$).

Permeability parameters

Changes in mESC volume in the presence of 1.0 M CPA, measured over time by electronic particle counter (EPC) at 0, 6, 12, 22, and 34°C, were fitted to compute L_p^{CPA} and P_{CPA} . Room temperature (RT) values of L_p^{CPA} , P_{CPA} , and their associated activation energies (E_a^{Lp} and E_a^{Pcpa}) are shown in Table 3.3. For all cell lines, L_p^{GLY} and $P_{\text{CPA}}^{\text{GLY}}$ values were significantly lower ($p<0.05$) than either L_p or P_{CPA} values in the presence of Me₂SO, PG, or EG. Based upon this finding, GLY was deemed inappropriate for equilibrium freezing of these mESC lines and E_a values were not assessed.

a. Hydraulic conductivity at room temperature

There was a significant main effect of genetic background and CPA, as well as a significant interaction between genetic background and CPA on L_p values at room temperature (22°C) ($p<0.05$). Overall, L_p^{CPA} values differed significantly between all cell lines ($p<0.05$). Highest to lowest L_p values were: 129R1, FVB, CBA, and BALB/c. In a comparison of overall values for CPAs, L_p^{GLY} was significantly lower than $L_p^{\text{Me}2\text{SO}}$, L_p^{PG} , or L_p^{EG} ($p<0.05$). Overall, $L_p^{\text{Me}2\text{SO}}$ values were significantly higher than L_p^{PG} and L_p^{EG} .

values at room temperature, and there was no significant difference between L_p^{PG} and L_p^{EG} values ($p<0.05$). Please refer to Table 3.3 for a list of L_p^{CPA} values.

There were differences among cell lines in L_p^{CPA} values at 22°C. Values for $L_p^{Me_2SO}$ did not differ significantly between the CBA and BALB/c lines or between the FVB and 129R1 mESC lines. However, these values were significantly lower ($p<0.05$) for the CBA and BALB/c cell lines relative to the FVB and 129R1 mESC lines. Room temperature L_p^{EG} values of the 129R1 mESC line were significantly higher ($p<0.05$) than those of the BALB/c and CBA mESC lines. Values of L_p^{PG} were significantly higher ($p<0.05$) for the 129R1 mESC line relative to the BALB/c and CBA mESC lines. Among all L_p^{GLY} values, those for the BALB/c line were significantly lower ($p<0.05$) than those of the CBA, FVB, and 129R1 mESC lines; however there was no significant difference between CBA, FVB, and 129R1 mESC lines.

The effect of CPA on L_p values was analyzed within each cell line. Within the BALB/c, FVB, and 129R1 lines, L_p^{GLY} was significantly lower than L_p for all other CPAs ($p<0.05$). However, within the CBA line, L_p^{GLY} was significantly lower than $L_p^{Me_2SO}$ and L_p^{PG} . However, there was no significant difference between L_p^{GLY} and L_p^{EG} ($p<0.05$). There was no significant difference between L_p of Me₂SO, PG, and EG within the BALB/c, CBA, or 129R1 mESC lines. However, for the FVB line, $L_p^{Me_2SO}$ was significantly higher than L_p in the presence of EG, PG, or GLY.

b. Temperature dependence of hydraulic conductivity

There was a main effect of cell line on E_a^{LP} . In a comparison of cell lines, overall E_a^{LP} values for the 129R1 line were significantly higher than those of the CBA and FVB lines ($p<0.05$). While the overall effect of the combination of cell line and CPA was not significant, E_a^{LP} in the presence of Me₂SO was significantly higher for the 129R1 line than for that of the CBA line ($p<0.05$). Please refer to Table 3.3 for a list of E_a^{LP} values.

c. Solute permeability at room temperature

There was a significant main effect of cell line and CPA, as well as a significant interaction between genetic background and CPA on P_{CPA} ($p<0.05$). There were significant overall differences ($p<0.05$) in P_{CPA} values between all cell lines with the exception of between the CBA and BALB/c mESC lines. The order from lowest to highest P_{CPA} values was: 129R1, FVB, (CBA or BALB/c). As stated previously, P_{GLY} was significantly lower than P_{Me2SO} , P_{EG} , or P_{PG} . Overall, P_{PG} was significantly higher than P_{Me2SO} ($p<0.05$); however there was no significant difference between P_{EG} and either P_{Me2SO} or P_{PG} .

Within each CPA group, there were differences among cell lines for P_{CPA} values. Room temperature P_{Me2SO} and P_{PG} values did not significantly differ between the FVB and 129R1 cell lines or between the CBA and BALB/c cell lines; however P_{Me2SO} values for the FVB and 129R1 mESC lines were significantly lower ($p<0.05$) than those of the BALB/c and CBA lines. Room temperature P_{EG} values did not differ significantly

between the FVB and 129R1 cell lines. However, there were significant differences with other cell lines comparisons. Highest to lowest P_{EG} by cell line was: BALB/c, CBA, (FVB or 129R1) ($p<0.05$). There were no significant differences in P_{GLY} values between cell lines.

The effect of CPA on P_{CPA} values was analyzed within each cell line. For all cell lines, P_{GLY} was significantly lower ($p<0.05$) than P_{Me_2SO} , P_{EG} , and P_{PG} . Within the CBA, 129R1, and FVB cell lines, there was no significant difference between P_{Me_2SO} , P_{EG} , and P_{PG} . Within the BALB/c cell line, P_{DMSO} was significantly lower than P_{EG} ($p<0.05$). Please refer to Table 3.3 for a list of P_{CPA} values.

d. Temperature dependence of solute permeability

There was a significant main effect of genetic background as well as CPA on E_a^{Pcpa} , with values for the BALB/c line significantly lower ($p<0.05$) than those of the FVB and CBA lines. E_a^{Pcpa} values were significantly higher ($p<0.05$) in the presence of PG than in the presence of Me₂SO or EG. The BALB/c E_a^{Pcpa} in the presence of EG was significantly lower ($p<0.05$) than that of the CBA line in the presence of PG. Please refer to Table 3.3 for a list of E_a^{Pcpa} values.

Table 3.3. Room temperature hydraulic conductivity (L_p), cryoprotectant permeability (P_{CPA}), and their associated activation energies (E_a) for five mouse embryonic stem cell (mESC) lines in the presence of 1.0 M cryoprotective agent (CPA).

Cell Line	Dimethyl sulfoxide ^a		Ethylene glycol ^b		1,2-propanediol ^c		L_p
	L_p	$E_a^{L_p}$	L_p	$E_a^{L_p}$	L_p	$E_a^{L_p}$	
C57BL/6*	0.41 ± 0.03	14.29	0.48 ± 0.06	15.35	0.42 ± 0.03	14.12	0.14 ± 0.01
BALB/c	0.15 ± 0.01	12.33 ± 0.60	0.15 ± 0.01	12.94 ± 0.49	0.18 ± 0.01	13.80 ± 0.52	0.05 ± 0.01
CBA	0.21 ± 0.01	10.82 ± 1.61	0.15 ± 0.01	13.01 ± 1.09	0.19 ± 0.01	11.51 ± 0.45	0.09 ± 0.01
FVB	0.39 ± 0.04	12.29 ± 1.42	0.24 ± 0.03	13.01 ± 1.09	0.22 ± 0.04	10.09 ± 1.34	0.10 ± 0.01
R1	0.53 ± 0.12	16.82 ± 1.98	0.35 ± 0.02	14.52 ± 0.50	0.33 ± 0.04	12.94 ± 1.03	0.10 ± 0.01
	P_{CPA}	$E_a^{P_{CPA}}$	P_{CPA}	$E_a^{P_{CPA}}$	P_{CPA}	$E_a^{P_{CPA}}$	P_{CPA}
C57BL/6*	4.59 ± 0.41	15.47	4.17 ± 0.24	13.19	6.58 ± 0.38	14.08	1.05 ± 0.07
BALB/c	8.62 ± 0.53	13.44 ± 0.81	11.74 ± 0.84	13.04 ± 0.21	10.51 ± 0.67	15.15 ± 1.11	1.99 ± 0.25
CBA	9.10 ± 0.60	17.35 ± 2.37	8.41 ± 0.28	16.75 ± 1.16	9.40 ± 0.61	19.79 ± 0.46	2.32 ± 0.28
FVB	4.53 ± 0.37	16.94 ± 1.47	5.32 ± 0.50	14.95 ± 0.66	6.92 ± 0.64	19.00 ± 1.99	1.33 ± 0.37
R1	4.00 ± 0.48	13.80 ± 1.78	3.92 ± 0.23	15.85 ± 0.63	5.24 ± 0.27	18.17 ± 0.70	0.99 ± 0.07

Due to the relatively low room temperature values for L_p and P_{CPA} , GLY was deemed inappropriate for equilibrium freezing and E_a was not assessed. L_p values are expressed as mean ± SEM $\mu\text{m}\cdot\text{min}^{-1}\cdot\text{atm}^{-1}$; P_{CPA} is expressed as mean ± SEM $\mu\text{m}\cdot\text{min}^{-1}$; E_a is expressed as mean ± SEM $\text{kcal}\cdot\text{mol}^{-1}$. Superscripts indicate significant difference in L_p and P_{CPA} values, $p < 0.05$, between overall CPA groups. For additional statistical comparisons, please refer to the “Results” section text. *Values for C57BL/6 mESC line are previously published values [20] listed for ease of comparison but were not included in statistical analyses.

Discussion

Post-thaw recovery following cryopreservation has been demonstrated to vary widely across cell types as well as among and within species. These differences can be attributed to wide-ranging differences in fundamental cryobiological parameters specific to individual cell types and species [35][36]. This variability even extends to individuals, a good example being bull spermatozoa, where not only is there variability from individual to individual, but also from sample to sample from the same individual [37]. Embryonic stem cells have demonstrated tremendous variability in post-thaw recovery from species to species. Embryonic stem cell post-thaw recovery using 1 M Me₂SO, a cooling rate of 1°C/minute, and plunge temperature of -80°C can range from 0.1 to 1% in human ESCs [38][39], from 0.4 to 5% in non-human primate ESCs [38](personal communication, Shoukhrat Mitalipov, Oregon National Primate Research Center, 2004), and anywhere from 10% to 90 percent with mESCs [19][20] (personal communication, Deanna Nielsen, Stem Cell Technologies technical support, 2004; personal communication, Xin Yu, University of California-Davis, 2004). With the exception of the 2007 report of an 88% post-thaw recovery rate in the 129R1 mESC line by Miszta-Lane *et al.* [19], and a 31.9% post-thaw recovery rate in a C57BL/6 mESC line by Kashuba Benson *et al.* [20], reports of variability in post-thaw recovery of mESCs have been largely anecdotal or confined to laboratory observation. This study examined the post-thaw recoveries of four mESC lines from differing genetic backgrounds and describes the fundamental cryobiological cell parameters that would contribute to such differences. Defining such parameters allows us to predict cell volume excursions during

the addition and removal of CPAs and estimate the degree of dehydration cells undergo during cooling [40], and accordingly develop cryopreservation protocols that maximize post-thaw recovery by minimize damaging intracellular ice formation and solute effects.

As expected, with the standard cryopreservation protocol (1 M Me₂SO, 1°C/minute cooling rate to -80°C, plunge into liquid nitrogen, then warming in a 37°C water bath), the percent post-thaw recoveries of membrane-intact cells of BALB/c, CBA, FVB, and 129R1 mESC lines were shown to vary significantly by cell line, with a range of 10.0 to 32.5% recovery (Figure 3.1). Interestingly, the post-thaw recovery of 129R1 mESCs of $24.4 \pm 1.2\%$ was dramatically different from the 88% recovery rate reported by Miszta-Lane *et al.* [19] under similar conditions. Our definition of post-thaw recovery may have been stricter, resulting in lower percentages, as we considered only the single-cell population during FACScan analysis and excluded cell clusters. Importantly, our method accounted for cell lysis during cryopreservation and warming by considering the total number of cells, membrane-intact and not, both prior to and following cryopreservation.

Osmotic tolerance ranges differed significantly at the lower limits, and there were some differences at upper osmotic tolerance range in the absence of an overall cell line effect. However, with the broad range of osmotic tolerance limits displayed by all cell lines in this study (Figure 3.2), these differences were not great enough to warrant changing the standard freezing media CPA concentration of 10%, or roughly 1 M, for any individual line as the addition of 1 M CPA, especially drop-wise [41], should not have a damaging osmotic effect. In fact, osmotic tolerance limits such as these would possibly

enable even higher concentrations of CPAs to be used in vitrification protocols if necessary, as long as the CPAs were added in stepwise fashion. In general, all cell lines displayed a relatively wide range of osmotic tolerance, expressed as factors of V_{iso} , ranging from lower volume limits of $0.6\text{-}0.7 \times V_{iso}$ to upper limits of $1.4\text{-}1.6 \times V_{iso}$. These ranges are consistent with previous findings with the C57BL/6 mESC line ($0.6\text{-}1.5 \times V_{iso}$)[20] and are also comparable to limits of other cell types such as canine pancreatic islets ($0.6\text{-}1.52 \times V_{iso}$)[42], human spermatozoa ($0.75\text{-}1.02 \times V_{iso}$)[43], human umbilical cord blood CD34+ cells ($0.6\text{-}1.52 \times V_{iso}$)[44], and human granulocytes ($0.7\text{-}1.68 \times V_{iso}$)[45].

Recently, Katkov [46] published an analysis of parameter estimation in the cryobiological literature, stating that it may be incorrect to assume that the temperature dependence of the solute permeability parameter P_{CPA} follows the Arrhenius relationship (with activation energy E_a^{Pcpa}). Katkov's argument is that in fact, P_{CPA} is actually a lumped parameter $P_{CPA} = \omega RT$, where ω is the "solute mobility" term which should have an Arrhenius-like dependence on temperature (with activation energy E_a^ω). It is unclear if this assertion is true for the two parameter model used in our paper, as the solute mobility term was introduced in the model developed by Kedem and Katchalsky [47], but nevertheless our study was instigated before this argument was made and therefore optimal freezing protocols were produced with predictions of subzero P_{CPA} made with E_a^{Pcpa} . Because the solute permeability data were fit (with a high correlation coefficient) with the assumption that P_{CPA} has an Arrhenius temperature dependence, the error induced by using this model is minimized at temperatures near the range in which measurements were made. Much below these temperatures, say less than -10 deg C, P_{CPA}

is small enough so that the effects of error in parameter values are greatly reduced, and the effects on optimal cooling rates are effectively zero.

The combination of the significant effects of cell line on V_b , permeability parameters, and E_a strongly suggests that optimal cooling rates will vary with cell line and that a “one-size fits all” protocol will not suffice. Additionally, significant overall effects of CPA on permeability parameters and E_a^{Pcpa} suggest that optimal cooling rates will also vary by CPA. As was previously determined with the C57BL/6 mESC line [20], GLY was determined to be unsuitable for equilibrium cooling for all mESC lines studied due to its markedly lower room temperature values of L_p and P_{CPA} . Future studies will include theoretical simulations to predict optimal cooling rates for cryopreservation methods involving Me₂SO, EG, and PG. Experimental validation of the predicted optimal cooling rates as well as predicted optimal plunge temperatures will be performed with Me₂SO and PG. 1,2-propanediol will be preferentially studied due to its more stable glass forming properties relative to EG and Me₂SO [48][49] and due to overall P_{PF} being significantly higher than P_{Me_2SO} at room temperature across the four mESC lines studied (Chapter 2), which would enable the most rapid addition and removal of CPA at room temperature with minimal damage to the cell membrane [50][20]. Predicted optimal cooling rates of Me₂SO will be explored for comparative purposes, as it is the CPA used in standard cryopreservation protocols.

References

1. Austin, C.P., et al., *The knockout mouse project*. Nat Genet, 2004. **36**(9): p. 921-4.
2. Auwerx, J., et al., *The European dimension for the mouse genome mutagenesis program*. Nat Genet, 2004. **36**(9): p. 925-7.
3. Critser, J.K. and L.E. Mobraaten, *Cryopreservation of murine spermatozoa*. IJAR J, 2000. **41**(4): p. 197-206.
4. Heng, B.C., et al., *Kinetics of cell death of frozen-thawed human embryonic stem cell colonies is reversibly slowed down by exposure to low temperature*. Zygote, 2006. **14**(4): p. 341-8.
5. Heng, B.C., et al., *Loss of viability during freeze-thaw of intact and adherent human embryonic stem cells with conventional slow-cooling protocols is predominantly due to apoptosis rather than cellular necrosis*. J Biomed Sci, 2006. **13**(3): p. 433-45.
6. Reubinoff, B.E., et al., *Effective cryopreservation of human embryonic stem cells by the open pulled straw vitrification method*. Hum Reprod, 2001. **16**(10): p. 2187-94.
7. Ji, L., J.J. de Pablo, and S.P. Palecek, *Cryopreservation of adherent human embryonic stem cells*. Biotechnol Bioeng, 2004. **88**(3): p. 299-312.
8. Ha, S.Y., et al., *Cryopreservation of human embryonic stem cells without the use of a programmable freezer*. Hum Reprod, 2005. **20**(7): p. 1779-85.
9. Ware, C.B., A.M. Nelson, and C.A. Blau, *Controlled-rate freezing of human ES cells*. Biotechniques, 2005. **38**(6): p. 879-80, 882-3.
10. Baran, S.W. and C.B. Ware, *Cryopreservation of rhesus macaque embryonic stem cells*. Stem Cells Dev, 2007. **16**(2): p. 339-44.
11. Kim, S.J., et al., *Effects of type IV collagen and laminin on the cryopreservation of human embryonic stem cells*. Stem Cells, 2004. **22**(6): p. 950-61.
12. Wu, C.F., et al., *Improved cryopreservation of human embryonic stem cells with trehalose*. Reprod Biomed Online, 2005. **11**(6): p. 733-9.
13. Richards, M., et al., *An efficient and safe xeno-free cryopreservation method for the storage of human embryonic stem cells*. Stem Cells, 2004. **22**(5): p. 779-89.

14. Zhou, C.Q., et al., *Cryopreservation of human embryonic stem cells by vitrification*. Chin Med J (Engl), 2004. **117**(7): p. 1050-5.
15. Heng, B.C., et al., *The cryopreservation of human embryonic stem cells*. Biotechnol Appl Biochem, 2004.
16. Ure, J.M., S. Fiering, and A.G. Smith, *A rapid and efficient method for freezing and recovering clones of embryonic stem cells*. Trends Genet, 1992. **8**(1): p. 6.
17. Chan, S.Y. and M.J. Evans, *In situ freezing of embryonic stem cells in multiwell plates*. Trends Genet, 1991. **7**(3): p. 76.
18. Udy, G.B. and M.J. Evans, *Microplate DNA preparation, PCR screening and cell freezing for gene targeting in embryonic stem cells*. Biotechniques, 1994. **17**(5): p. 887-94.
19. Miszta-Lane, H., et al., *Effect of slow freezing versus vitrification on the recovery of mouse embryonic stem cells*. Cell preservation technology, 2007. **5**(1): p. 16-24.
20. Kashuba Benson, C.M., J.D. Benson, and J.K. Critser, *An improved cryopreservation method for a mouse embryonic stem cell line*. Cryobiology, 2008. **56**(2): p. 120-30.
21. Mazur, P., S.P. Leibo, and E.H. Chu, *A two-factor hypothesis of freezing injury. Evidence from Chinese hamster tissue-culture cells*. Exp Cell Res, 1972. **71**(2): p. 345-55.
22. Doetschman, T., *Gene Targeting in Embryonic Stem Cells: I. History and Methodology*, in *Transgenic Animal Technology: A Laboratory Handbook, Second Edition*, C.A. Pinkert, Editor. 2002, Academic Press: San Diego.
23. Gordeeva, O.F., et al., [*Expression of regulatory genes Oct-4, Pax-6, Prox-1, Ptx-2 at the initial stages of differentiation of embryonic stem cells in vitro*]. Ontogenез, 2003. **34**(3): p. 174-82.
24. *Preparation of ES Cells for Injection*, in *Manipulating the Mouse Embryo: A Laboratory Manual*, A. Nagy, et al., Editors. 2003, Cold Spring Harbor Laboratory Press: Cold Spring Harbor, New York. p. 469.
25. Schenke-Layland, K., et al., *Collagen IV induces trophoectoderm differentiation of mouse embryonic stem cells*. Stem Cells, 2007. **25**(6): p. 1529-38.

26. Benson, J.D., et al., *Mercury free operation of the Coulter counter MultiSizer II sampling stand*. Cryobiology, 2005. **51**(3): p. 344-7.
27. McGann, L.E., A.R. Turner, and J.M. Turc, *Microcomputer interface for rapid measurements of average volume using an electronic particle counter*. Med Biol Eng Comput, 1982. **20**(1): p. 117-20.
28. Benson, C.T., et al., *Determination of the osmotic characteristics of hamster pancreatic islets and isolated pancreatic islet cells*. Cell Transplant, 1993. **2**(6): p. 461-5.
29. Fedorow, C., et al., *Osmotic and cryoprotectant permeation characteristics of islet cells isolated from the newborn pig pancreas*. Cell Transplant, 2001. **10**(7): p. 651-9.
30. Phelps, M.J., et al., *Effects of Percoll separation, cryoprotective agents, and temperature on plasma membrane permeability characteristics of murine spermatozoa and their relevance to cryopreservation*. Biol Reprod, 1999. **61**(4): p. 1031-41.
31. Ebertz, S.L. and L.E. McGann, *Cryoprotectant permeability parameters for cells used in a bioengineered human corneal equivalent and applications for cryopreservation*. Cryobiology, 2004. **49**(2): p. 169-80.
32. Nobel, P.S., *The Boyle-Van't Hoff relation*. Journal of Theoretical Biology, 1969. **23**(3): p. 375-9.
33. Katkov, II, *A two-parameter model of cell membrane permeability for multisolute systems*. Cryobiology, 2000. **40**(1): p. 64-83.
34. Mazur, P., *Kinetics Of Water Loss From Cells At Subzero Temperatures And The Likelihood Of Intracellular Freezing*. J Gen Physiol, 1963. **47**: p. 347-69.
35. Gao, D., P. Mazur, and J.K. Critser, *Fundamental Cryobiology of Mammalian Sperm*, in *Reproductive Tissue Banking: Scientific Principles*, A.M. Karow and J.K. Critser, Editors. 1997, Academic Press: San Diego. p. 263-328.
36. Woods, E.J., et al., *Fundamental cryobiology of reproductive cells and tissues*. Cryobiology, 2004. **48**(2): p. 146-56.
37. Chaveiro, A., et al., *Significant variability among bulls in the sperm membrane permeability for water and glycerol: possible implications for semen freezing protocols for individual males*. Cryobiology, 2006. **53**(3): p. 349-59.

38. Fujioka, T., et al., *A simple and efficient cryopreservation method for primate embryonic stem cells*. Int J Dev Biol, 2004. **48**(10): p. 1149-54.
39. *Introduction to Human Embryonic Stem Cell Culture Methods*. 2003 [cited; Available from: <http://www.wicell.org/forresearchers/index.jsp?catid=12&subcatid=20>.
40. Agca, Y., et al., *Membrane permeability characteristics of metaphase II mouse oocytes at various temperatures in the presence of Me₂SO*. Cryobiology, 1998. **36**(4): p. 287-300.
41. Gilmore, J.A., et al., *Determination of optimal cryoprotectants and procedures for their addition and removal from human spermatozoa*. Hum Reprod, 1997. **12**(1): p. 112-8.
42. Zieger, M.A., et al., *Osmotic tolerance limits of canine pancreatic islets*. Cell Transplant, 1999. **8**(3): p. 277-84.
43. Gao, D.Y., et al., *Prevention of osmotic injury to human spermatozoa during addition and removal of glycerol*. Hum Reprod, 1995. **10**(5): p. 1109-22.
44. Woods, E.J., et al., *Osmometric and permeability characteristics of human placental/umbilical cord blood CD34+ cells and their application to cryopreservation*. J Hematother Stem Cell Res, 2000. **9**(2): p. 161-73.
45. Armitage, W.J. and P. Mazur, *Osmotic tolerance of human granulocytes*. Am J Physiol, 1984. **247**(5 Pt 1): p. C373-81.
46. Katkov, II, *Challenge from the simple: some caveats in linearization of the Boyle-van't Hoff and Arrhenius plots*. Cryobiology, 2008. **57**(2): p. 142-9.
47. Kedem, O. and A. Katchalsky, *Thermodynamic analysis of the permeability of biological membranes to non-electrolytes*. 1958. Biochim Biophys Acta, 1989. **1000**: p. 413-30.
48. Baudot, A., L. Alger, and P. Boutron, *Glass-forming tendency in the system water-dimethyl sulfoxide*. Cryobiology, 2000. **40**(2): p. 151-8.
49. Baudot, A. and V. Odagescu, *Thermal properties of ethylene glycol aqueous solutions*. Cryobiology, 2004. **48**(3): p. 283-94.
50. Gilmore, J.A., et al., *Osmotic properties of boar spermatozoa and their relevance to cryopreservation*. J Reprod Fertil, 1996. **107**(1): p. 87-95.

CHAPTER 4

OPTIMIZED MOUSE EMBRYONIC STEM CELL CRYOPRESERVATION PROTOCOLS: A COMPARISON OF PREDICTED OPTIMAL COOLING RATES AND PLUNGE TEMPERATURES ACROSS FOUR MOUSE EMBRYONIC STEM CELL LINES AND EMPIRICAL VALIDATION OF PREDICTED OPTIMA

Introduction

Mouse embryonic stem cells (mESCs) have been developed from numerous genetic backgrounds and have contributed to a virtual explosion in the number of existing genetically engineered mouse (GEM) models available for human biomedical research [1][2]. Thousands of additional mutant mESC lines will be created through coordinated efforts to systematically knock out all mouse genes via projects such as the Knockout Mouse Project (KOMP)[3], the North American Conditional Mouse Mutagenesis Program (NorCOMM, <http://norcomm.phenogenomics.ca>), and the European Conditional Mouse Mutagenesis Program (EUCOMM, <http://www.eucomm.org>). Storage of valuable genetic material in the form of mESCs is cost-effective and requires

minimal space; however, reported variation of 10 to 90% post-thaw recovery (PTR), depending on the cell line (please refer to Chapter 2) [4][5][6], raises concerns regarding both the efficacy and reliability of its approach.

Fundamental cryobiological parameters describe osmotically driven transport across cell membranes and are key to hypothesis-driven predictions of successful outcomes from cryopreservation protocols [7]. They can be used to calculate osmotically driven volume excursions during the addition and removal of cryoprotectants (CPAs) and during the cooling and thawing process [8][9][10][11]. Using these parameters, optimal cooling rates and plunge temperatures can be predicted with the aim of cooling cell suspensions as rapidly as possible without causing a large difference between the intracellular freezing point and the intracellular temperature; warming rates tend to be optimal when they mimic their corresponding cooling rates [12].

We previously described a method to systematically analyze the fundamental cryobiological parameters of a C57BL/6 mESC line. We conducted theoretical simulations utilizing Mazur's two factor hypothesis [13] to predict optimal cooling rates and plunge temperatures (target temperatures for the rapid plunging of cells into liquid nitrogen for the intent of vitrifying the remaining water that are calculated based on vitrification-favoring concentrations of CPA) for this cell line, and performed experimental validations of our predictions. Using the same systematic approach and analysis, the fundamental cryobiological parameters of four additional mESC lines (BALB/c, CBA, FVB, and 129R1) were characterized in order to test the hypothesis that mESCs from different genetic backgrounds would be significantly different, and

therefore the optimal cryopreservation protocols for mESCs from different genetic backgrounds would be different.

Materials & Methods

Embryonic stem cells

The following mESC lines were acquired at passage 11 to 12: BALB/c (Thromb-X Group, Chemicon International, Temecula, CA, now part of Millipore, Billerica, MA), CBA (Thromb-X Group), FVB/N (Thromb-X Group), and 129R1 (A. Nagy, Mount Sinai Hospital, Toronto, Canada). Mouse ESC cultures were negative for all pathogens (IMPACT I test, Research Animal Diagnostic Laboratory, Columbia, Missouri; www.radil.missouri.edu/info/index.asp).

Cell culture and standard cryopreservation method

Mouse ESCs were cultured on primary mouse embryonic fibroblast cells (PMEF) (Millipore, Billerica, MA) at 37°C and 5% CO₂. Culture media for the 129R1 mESC line and BALB/c cell line contained 15% Defined FBS (Hyclone, Logan, UT), 0.1mM non-essential amino acids (GIBCO/ Invitrogen, Carlsbad, CA), 1.0 mM sodium pyruvate (GIBCO), 100 µM beta-mercaptoethanol (Sigma Aldrich, St. Louis, MO), 50 IU/mL penicillin (GIBCO), 50 µ g/mL streptomycin (GIBCO), and 1000 U ESGRO/mL

(Millipore) in high glucose DMEM (Millipore). CBA and FVB mESCs were cultured in RESGRO culture medium (Millipore). Embryonic stem cells were passaged and/or collected every 2 days or at approximately 80% confluence.

For the standard slow cooling method, cells were resuspended in freezing medium (1.3 M (10%) Me₂SO (Sigma Aldrich), 50% defined fetal bovine serum (Hyclone), and 40% culture medium) in 1mL aliquots in cryovials (Nalgene Nunc International, Rochester, NY). Cryovials were transferred to a commercially available freezing kit (Nalgene), refrigerated at -80°C overnight (a process which cools at a rate of 1°C/minute), and subsequently transferred to liquid nitrogen (LN₂).

Embryonic stem cells were used within 10 passages from the original, and were of normal karyotype at highest passage. Cell counts were performed using a hemacytometer and Trypan blue stain (Sigma Aldrich) for membrane integrity for all standard culture.

Separation of mESCs from feeders by differential sedimentation

For all experiments, feeder cells were separated from mESCs by differential sedimentation, a technique previously described by Doetschman [14]. There are many variations of this method [15][16][17], which exploits the difference in the rate at which fibroblast feeder cells and mESCs settle and adhere to culture dishes. Briefly, trypsinized mESC cultures containing PMEF were centrifuged, resuspended in 10 mL of culture medium, and plated on the original 100mm cell culture dish. After 30 minutes at 37°C, the cell suspension was transferred to a second culture dish for one-hour incubation at

37°C. Following the second incubation, the cell suspension was removed, and these collected mESCs were counted, centrifuged, and resuspended in either DPBS or culture medium for experimentation.

Theoretical simulations

We used the method previously described by Kashuba Benson *et al.* [4] to conduct theoretical stimulations in order to determine optimal CPA addition and removal protocols of a 1.0 M solution of dimethyl sulfoxide (Me₂SO), 1,2-propanediol (PG), or ethylene glycol (EG) for BALB/c, CBA, FVB, and 129R1 mESCs using fundamental cryobiological parameters delineated in Chapter 3. As previously described, a protocol was defined to be optimal if it minimized the number of addition and dilution steps while maintaining mESCs within the defined range of osmotic tolerance. The overall goal was to minimize cell volume excursion and cryoprotectant exposure time at ambient temperatures. A computer model was used for these procedures. Experimental conditions included osmotic tolerance limits, initial intracellular concentration, and temperature. The program automatically optimized addition and removal steps and provided the appropriate concentration of diluent.

Theoretical optimization of cryopreservation protocols was performed, based on Mazur's two factor hypothesis [13], as previously described for the C57BL/6 cell line [4]. According to Mazur's two factor hypothesis, sub-optimal cooling rates cause damage due to unnecessarily prolonged exposure to the high concentrations of solutes that occur at low temperatures, and super-optimal cooling rates cause damage due to insufficient

cellular dehydration that leads to deleterious intracellular ice formation. The optimal cooling rate is that which minimizes cooling exposure time while maintaining at most two degrees of supercooling [13]. In effect, cells should be cooled as quickly as possible without causing the intracellular concentration to be such that the freezing point is more than two degrees above the cellular environment. This optimization is achieved by pairing solute-solvent flux models with the appropriate ternary phase diagram (NaCl-CPA-Water) to determine to what degree supercooling would occur [4].

We utilize a two-step freezing protocol, where cells are cooled at a controlled rate to a “plunge temperature”, at which point they are immersed in liquid nitrogen, the goal being to minimize intracellular ice formation and promote vitrification [4]. Computer simulations based on the above model estimated the temperature at which the combination of cooling rate and initial CPA concentration would result in an intracellular CPA concentration of 40% by weight, and this was deemed the optimal plunge temperature. Computer simulations of freezing for all cell lines and CPAs were performed iteratively until optimal cooling rates were determined, as previously described [4]. For an illustrative curve of determination of optimal cooling rates, please refer to Figure 1, previously published for the C57BL/6 mESC line [4].

As with the C57BL/6 mESC line [4], the two parameter mathematical model described above was used to simulate warming [18]. The subsequent volume excursion upon equilibration was compared with predicted osmotic tolerance limits. Warming rates up to $1 \times 10^4^\circ\text{C}/\text{min}$ were simulated to verify that damage due to volume changes would not occur, and the optimal warming rate was considered to be that which was fast enough to prevent devitrification, yet not “too fast” such that after warming, the influx of water

would cause the cell to exceed osmotic tolerance limits. A typical method for warming is to place a straw in room temperature or 37°C water and it remains only to verify that cell volume excursions are within the osmotic tolerance limits. For an illustrative curve of optimal warming rates, please refer back to Figure 2.2 [4].

Empirical validation of predicted optima

Empirical validation of predicted freezing rates was conducted with 1.0 M PG and 1.0 M Me₂SO. Each mESC line was cultured in standard conditions to 80% confluence, separated from fibroblast feeders, and resuspended in freezing medium at a concentration of 1 x 10⁶ cells/mL. Propylene glycol freezing medium consisted of 1.0 M PG (Sigma), suspended in 129R1/BALB/c culture medium and 50% v/v defined fetal bovine serum (FBS) (Hyclone). Dimethyl sulfoxide freezing medium consisted of 1.0 M Me₂SO (Sigma), suspended in 129R1/BALB/c culture medium and 50% v/v FBS. Cells were cooled in sealed 250 µL cryostraws (IMV International, Maple Grove, MN) in a Planer Kryo 10 Series III programmable freezer (TS Scientific).

A 4 x 4 factorial design was used to compare protocols using combinations of PG vs. Me₂SO, predicted optimal vs. suboptimal cooling rates, seeding vs. no seeding, and predicted optimal plunge temperatures vs. the standard -80°C. Please refer to Table 4.1 for cell line- and CPA-specific predicted optimal cooling rates and plunge temperatures. Standard conditions were considered 1 M Me₂SO, 1°C/minute, and a plunge temperature of -80°C.

Non-optimal rates were defined as the predicted optimal rate for the opposite CPA when the predicted optimal cooling rate was 1°C/minute for at least one CPA. In the case of the FVB cell line, where neither Me₂SO nor PG had predicted optimal cooling rates of 1°C/minute, predicted optimals of 3.8°C/minute (Me₂SO) and 3.3°C/minute (PG) were compared to non-optimal rates of 1°C/minute (*i.e.* the standard cooling rate).

Initial studies comparing the effects of seeding (which is defined as the induced nucleation of intracellular ice crystals, theorized to increase the uniformity of sample cooling [19][20], and was achieved by application of a LN₂-cooled forceps to the freezing vessel until visible ice crystals form) *vs.* not seeding revealed no significant difference (data not shown); therefore, these comparisons were not included in additional studies.

As previously described for the C57BL/6 mESC line [4], theoretical simulations predicted that warming rates between 10 and 1 x 10⁴°C/minute would have negligible effects on cell survival. Cryostraws were thawed in a room temperature water bath (22 ± 1°C), resulting in a measured warming rate of approximately 700°C/minute (data not shown). Embryonic stem cells were thawed, diluted drop-wise by 5 volumes of culture media, centrifuged, resuspended in 1x PBS, stained with propidium iodide, and passed through a FACScan flow cytometer (BD Biosciences, San Jose, CA) for analysis of percent post-thaw recovery (PTR).

Statistical analysis

Data were analyzed using standard analysis of variance (ANOVA) performed using the SAS General Linear Models program (SAS Institute, Inc., Cary, NC) with an

alpha value of $p < 0.05$. In situations where a plot of the residuals of a data set was not normally distributed, data were normalized using either natural logarithm or square root transformation. Post-thaw recoveries were compared to standard cryopreservation conditions for each mESC line using Tukey's test. All values are given as mean \pm SEM, unless stated otherwise.

Results

Theoretical simulations

We utilized a two-step freezing protocol for the BALB/c, CBA, FVB, and 129R1 mESC lines. By this method, cells are slowly cooled in a controlled-rate freezer to an appropriate plunge temperature, at which point they are rapidly transferred to liquid nitrogen. Predicted optimal cooling rates and plunge temperatures for the four mESC lines included in this study are listed in Table 4.1.

Table 4.1. Predicted optimal cooling rates for the BALB/c, CBA, FVB, 129R1, and previously published C57BL/6 [4] mouse embryonic stem cell lines for three cryoprotectants.

Cell Line	EG	PG	Me ₂ SO
BALB/c	1.1 (-41)	1.0 (-41)	6.5 (-32)
C57BL/6	1.4 (-41)	1.2 (-41)	4.1 (-33)
CBA	1.1 (-41)	1.1 (-41)	5.0 (-32)
FVB	1.9 (-41)	3.3 (-40)	3.8 (-33)
129R1	1.6 (-41)	3.0 (-41)	1.3 (-33)

Predicted optimal plunge temperatures are listed in brackets adjacent to cooling rates. Cooling rates are in °C/minute; plunge temperatures are listed in °C. EG, ethylene glycol; PG, 1,2-propanediol; Me₂SO, dimethyl sulfoxide.

Empirical validation of predicted optima

It is important to note that predicted optimal plunge temperatures are only optimal for predicted optimal cooling rates, however in order to define them from the standard plunge temperature of -80°C, we refer to them as “predicted optimal” plunge temperatures in the presentation and discussion of our results.

a. Overview of significant main effects for all four mESC lines

For all cell lines, PTR varied significantly by day as well as by CPA, where the use of 1 M PG resulted in significantly higher PTR than with 1 M Me₂SO ($p<0.05$). There was a significant main effect of plunge temperature for all cell lines, in which PTR was significantly higher using the standard plunge temperature of -80°C than with using predicted optimal plunge temperatures ($p<0.05$). With the exception of the CBA mESC line, the predicted optimal cooling rates significantly improved PTR ($p<0.05$).

For the CBA and 129R1 mESC lines, there was a significant interaction of cooling rate and plunge temperature ($p<0.05$). For the CBA mESC line, the predicted optimal cooling rate combined with the predicted optimal plunge temperature resulted in significantly lower PTR than with all other combinations of cooling rates and plunge temperatures ($p<0.05$). For the 129R1 mESC line, the combination of suboptimal cooling rate combined with the standard plunge temperature resulted in higher PTR than with other combinations of cooling rates and plunge temperatures ($p<0.05$).

Finally, there was a significant interaction between CPA, cooling rate, and plunge temperature ($p<0.05$) for all mESC lines, the results of which will be presented per individual mESC line.

Table 4.2. Experimental cryopreservation protocols that resulted in improved percent post-thaw recovery (PTR) of BALB/c mouse embryonic stem cells as compared to the standard cryopreservation method.

Protocol	CPA (1 M)	CR (°C/minute)	PT (°C)	PTR (%)	Fold Improvement
Standard	Me ₂ SO	1.0 (SO)	-80 (SO)	24.0 ± 3.9 ^a	-
1	Me ₂ SO	6.5 (PO)	-80 (SO)	43.8 ± 4.9 ^b	1.8
2	PG	1.0 (PO)	-80 (SO)	48.7 ± 7.1 ^b	2.0
3	PG	1.0 (PO)	-41 (PO)	42.6 ± 4.9 ^b	1.8

CPA, cryoprotectant; CR, cooling rate; PT, plunge temperature; SO, suboptimal value; PO, predicted optimal value. While predicted optimal plunge temperatures are only optimal for predicted optimal cooling rates, they are indicated to be “predicted optimal” in order to easily define them from the standard plunge temperature. Different superscripts indicate significantly different values ($p<0.05$).

Table 4.3. Experimental cryopreservation protocols that resulted in improved percent post-thaw recovery (PTR) of CBA mouse embryonic stem cells as compared to the standard cryopreservation method.

Protocol	CPA (1 M)	CR (°C/minute)	PT (°C)	PTR (%)	Fold Improvement
Standard	Me ₂ SO	1.0 (SO)	-80 (SO)	12.2 ± 0.7 ^a	-
1	Me ₂ SO	5.0 (PO)	-80 (SO)	20.9 ± 1.6 ^b	1.7
2	PG	5.0 (SO)	-80 (SO)	23.3 ± 3.9 ^b	1.9
3	PG	5.0 (SO)	-41 (PO)	20.3 ± 2.4 ^b	1.7

CPA, cryoprotectant; CR, cooling rate; PT, plunge temperature; SO, suboptimal value; PO, predicted optimal value. While predicted optimal plunge temperatures are only optimal for predicted optimal cooling rates, they are indicated to be “predicted optimal” in order to easily define them from the standard plunge temperature. Different superscripts indicate significantly different values ($p<0.05$).

Table 4.4. Experimental cryopreservation protocols that resulted in improved percent post-thaw recovery (PTR) of FVB mouse embryonic stem cells as compared to the standard cryopreservation method.

Protocol	CPA (1 M)	CR (°C/minute)	PT (°C)	PTR (%)	Fold Improvement
Standard	Me ₂ SO	1.0 (SO)	-80 (SO)	3.6 ± 0.5 ^a	-
1	Me ₂ SO	5.0 (PO)	-33 (PO)	25.2 ± 4.0 ^b	7.0
2	Me ₂ SO	5.0 (PO)	-80 (SO)	20.7 ± 2.9 ^c	5.8
3	PG	1.0 (PO)	-41 (PO)	16.7 ± 3.8 ^c	4.6
4	PG	1.0 (PO)	-80 (SO)	15.8 ± 3.2 ^c	4.4
5	PG	5.0 (SO)	-41 (PO)	6.7 ± 1.2 ^d	1.9

CPA, cryoprotectant; CR, cooling rate; PT, plunge temperature; SO, suboptimal value; PO, predicted optimal value. While predicted optimal plunge temperatures are only optimal for predicted optimal cooling rates, they are indicated to be “predicted optimal” in order to easily define them from the standard plunge temperature. Different superscripts indicate significantly different values ($p<0.05$).

Table 4.5. Experimental cryopreservation protocols that resulted in improved percent post-thaw recovery (PTR) of 129R1 mouse embryonic stem cells as compared to the standard cryopreservation method.

Protocol	CPA (1 M)	CR (°C/minute)	PT (°C)	PTR (%)	Fold Improvement
Standard	Me ₂ SO	1.0 (PO)	-80 (SO)	28.4 ± 1.3 ^a	-
1	Me ₂ SO	1.0 (PO)	-33 (PO)	43.0 ± 2.3 ^b	1.5
2	PG	1.0 (SO)	-41 (PO)	59.4 ± 2.6 ^b	2.1
3	PG	1.0 (SO)	-80 (SO)	40.8 ± 2.7 ^b	1.4

CPA, cryoprotectant; CR, cooling rate; PT, plunge temperature; SO, suboptimal value; PO, predicted optimal value. While predicted optimal plunge temperatures are only optimal for predicted optimal cooling rates, they are indicated to be “predicted optimal” in order to easily define them from the standard plunge temperature. Different superscripts indicate significantly different values ($p<0.05$).

b. Empirical validation of predicted optima for the BALB/c mESC line

The standard cryopreservation method yielded a PTR of $24.0 \pm 3.9\%$ with the BALB/c mESC line.

Three experimental protocols utilizing predicted optimal cooling rates for both Me₂SO and PG resulted in significantly improved PTR by 1.8 to 2 fold; these protocols are listed with their associated PTR in Table 4.2. The predicted optimal plunge temperature was utilized in one of these protocols; the remaining two protocols that improved PTR utilized standard plunge temperatures.

Predicted optimal cooling rates did not significantly decrease PTR for any cell line except for the BALB/c mESC line, in which one experimental protocol involving 1 M Me₂SO and combining the predicted optimal cooling rate and predicted optimal plunge temperature significantly decreased PTR to $9.8 \pm 3.0\%$ ($p<0.05$).

c. Empirical validation of predicted optima for the CBA mESC line

The standard cryopreservation method yielded a PTR of $12.2 \pm 0.7\%$ for the CBA mESC line.

The predicted optimal cooling rate for 1 M Me₂SO combined with standard plunge temperature significantly improved PTR of CBA mESC by 1.7 fold. The use of the predicted optimal plunge temperature with the predicted optimal cooling rate for 1 M Me₂SO resulted in a PTR that was not significantly different from that of the standard method, but was significantly lower than in the same conditions using the standard plunge temperature ($p<0.05$).

The suboptimal cooling rate for 1 M PG combined with either the standard plunge temperature or the predicted optimal plunge temperature significantly improved PTR 1.9 and 1.7 fold, respectively ($p<0.05$). Predicted optimal cooling rates for 1 M PG did not significantly improve PTR. Please refer to Table 4.3 for a summary of protocols that improved PTR of the CBA mESC line.

d. Empirical validation of predicted optima for the FVB mESC line

The standard cryopreservation method yielded a PTR of $3.6 \pm 0.5\%$ for the FVB mESC line.

Predicted optimal cooling rates for both Me₂SO and PG resulted in significantly improved PTR using both predicted optimal and standard plunge temperatures. The best

PTR ($p<0.05$) was obtained using Me₂SO, the predicted optimal cooling rate, and predicted optimal plunge temperature.

The suboptimal cooling rate for 1 M PG, in combination with the predicted optimal plunge temperature resulted in a 1.9 fold improvement in PTR as compared to the standard method; however, the improvement in PTR using this method was significantly lower than the 4.4 to 7 fold improvement gained using the predicted optimal cooling rates. Please refer to Table 4.4 for a summary of protocols that improved PTR of the FVB mESC line.

e. Empirical validation of predicted optima for the 129R1 mESC line

The standard cryopreservation method yielded a PTR of $28.4 \pm 1.3\%$ ($p<0.05$) for the 129R1 mESC line.

The standard cooling rate of 1°C/minute was also the predicted optimal cooling rate for Me₂SO, and the use of the predicted optimal plunge temperature with this cooling rate significantly improved PTR by 1.5 fold over the standard method.

Predicted optimal cooling rates for PG did not significantly improve PTR for the 129R1 mESC line, however the suboptimal cooling rates for PG combined with the predicted optimal and standard plunge temperatures significantly improved PTR by 1.4 and 2.1 fold, respectively. Please refer to Table 4.5 for a summary of protocols that improved PTR of the 129R1 mESC line.

Discussion

The purpose of this study was to apply fundamental cryobiological principles to predict optimal CPA, cooling rates and plunge temperatures in order to generate mESC cryopreservation protocols that yield improved PTR. Percent post-thaw recovery of mESCs has been demonstrated to vary considerably between cell lines (please refer to Chapter 2) [4][5]. Improved PTR, especially via universally applicable cryopreservation protocols, would facilitate banking, maintenance, and inter-laboratory exchange of mESC lines.

Theoretical simulations

Predicted optimal cooling rates ranged from 1.3 to 6.5°C/minute for 1 M Me₂SO, 1.0 to 3.0°C/minute for PG, and 1.1 to 1.9°C/minute for EG. The relatively narrow range of predicted optimal cooling rates for EG, combined with the uniformly predicted optimal plunge temperature of -41°C, suggests that a single optimal cryopreservation protocol could potentially be applied to all mESC lines using this CPA. However, to confine our experiments to a manageable level, and to be able to compare our results with those obtained for the C57BL/6 mESC line, we chose two CPAs for experimental validation. PG was selected for its more stable glass-forming properties as compared to EG and Me₂SO [21][22] and due to overall P_{PF} being significantly higher than P_{Me_2SO} at room temperature across the four mESC lines studied (Chapter 2), which would enable the

most rapid addition and removal of CPA at room temperature with minimal damage to the cell membrane [23][4]. Dimethyl sulfoxide was chosen for comparative purposes as it is the CPA used in standard cryopreservation protocols.

Empirical validation of predicted optima

a. Main effects of CPA, cooling rate, and plunge temperature

The empirical validation experiment was a $2 \times 2 \times 2 \times 2$ factorial design. In the absence of a main effect of seeding, the complex interaction between CPA, cooling rate, and plunge temperature was a significant effect ($p < 0.05$) over the eight treatment groups for each mESC line. As demonstrated in Table 4.1, the predicted optimal cooling rate was different for each CPA. At the same time, the predicted optimal plunge temperature was different for each predicted optimal cooling rate. The factorial design of the empirical validation experiment created a situation in which non-predicted optimal cooling rates were lower than predicted optimal cooling rates in some cases, and higher than predicted optimal cooling rates in other cases. When paired with the non-optimal cooling rate, the plunge temperature would no longer be optimal. With cooling rates higher than optimal, the plunge temperature would be too high, too little intracellular dehydration will occur, and damaging intracellular ice formation would be a problem. With lower than optimal cooling rates, the plunge temperature would be too low, excessive intracellular dehydration would be allowed to occur for a lengthier period, and cells would endure damaging solute effects [13]. A fundamental question in cryobiology

is whether intracellular ice formation and solute effects are equally damaging to cells [24]. Depending on which effect is more critical for mESC survival during cryopreservation and warming, bias could be introduced into the experiment in which rates that were “too high” might fare worse than rates that were “too low”. With lower-than-optimal rates, the cell would have the chance to dehydrate before reaching the plunge temperature, and intracellular ice formation would be less likely to occur; if the cell is sensitive to solute effects, PTR might still be suboptimal, but if the cell is not sensitive to solute effects, PTR might actually improve when compared to a predicted optimal rate that is too high.

In examining the main effect of CPA, cooling rate, and plunge temperature, most cell lines followed the same trends. For CPA, which was significant for all lines, protocols utilizing 1 M PG consistently yielded higher overall PTR than those with 1 M Me₂SO. One explanation might be that PG is a more stable glass former than Me₂SO or EG [21][22], thus devitrification during either cooling or warming, resulting in damaging ice crystal formation, is less likely in the presence of PG as opposed to Me₂SO. Cooling rate was a main effect for the FVB, BALB/c, and 129R1 mESC lines, but not for the CBA line. With the CBA mESC line, only one protocol involving a predicted optimal cooling rate, in this case for 1 M Me₂SO, yielded improved PTR. For the remaining three mESC lines, predicted optimal cooling rates, as expected, yielded higher PTR overall than non-optimal cooling rates.

The main effect of plunge temperature, a significant main effect for all mESC lines in this study, was contrary to our expectations in that for all lines, a plunge temperature of -80°C yielded overall better PTR than our predicted optimal plunge

temperatures. However, as we discussed previously, plunge temperatures are only “optimal” for their predicted optimal cooling rates, and low temperature plunges would be more appropriate than higher plunge temperatures for cooling rates that were higher than predicted optimal cooling rates. Combined with potential underestimations of E_a due to extrapolations of suprazero E_a measurements to subzero temperatures which would lead to calculations of optimal plunge temperatures that were too high, the standard -80°C plunge temperature may have been advantageous. The significance of the main effect of plunge temperature, however, emphasizes the importance of pairing cooling rates and plunge temperature and the negative effects that occur when plunge temperature is inappropriate. Thus, for example, while cooling rate was not a significant main effect for the CBA strain, the interaction between cooling rate and plunge temperature was significant.

b. Interactions between CPA, cooling rate, and plunge temperature

(i) Situations in which the combined predicted optimal plunge temperature and higher-than-optimal cooling rate improved PTR

There were two instances where a predicted optimal plunge temperature was paired with a higher cooling rate and post-thaw recovery was actually improved as compared to PTR under standard conditions. With the FVB cell line, this situation (1 M PG, a suboptimal cooling rate of 5°C/minute, and plunge temperature of -41°C) resulted in PTR that was 1.9 fold greater (at $6.7 \pm 1.2\%$) than PTR under standard conditions (3.6

\pm 0.5%) (Table 4.4). However, these results were well below the 4.4- to 7-fold improvement in recovery using the predicted optimal cooling rates with or without predicted optimal plunge temperatures. A more interesting example with the CBA cell line using 1 M PG, a five-fold higher-than-optimal cooling rate of 5°C/minute, and plunge temperature of -41°C yielded a 1.7-fold improvement in PTR which was not significantly different from improvements in PTR achieved with the predicted optimal cooling rates for 1 M DMSO or with 1 M PG, the same suboptimal 5°C/minute cooling rate, and a plunge temperature of -80°C (Table 4.3), suggesting that despite the increased cooling rate, cellular dehydration was adequate enough to preclude intracellular ice formation.

(ii) Cases in which PTR under predicted optimal cooling rates was significantly decreased by predicted optimal plunge temperatures

There were also cases in which predicted optimal plunge temperatures combined with optimal cooling rates resulted in lower PTR than when optimal cooling rates were paired with -80°C plunge temperature. For the BALB/c mESC line, predicted optimal cooling rates yielded higher PTR than non-optimal cooling rates (Table 4.2). However, in the presence of 1 M Me₂SO, the predicted optimal plunge temperature combined with the predicted optimal cooling rate resulted in decreased PTR as compared to both PTR under the same conditions with a plunge temperature of -80°C, and PTR using the standard method. For the CBA mESC line, the predicted optimal cooling rate for 1 M

Me_2SO resulted in significantly improved PTR when paired with a plunge temperature of -80°C; however, when paired with the predicted optimal plunge temperature, the conditions resulted in a PTR that was significantly lower than with a -80°C plunge temperature and not significantly different from PTR under the standard protocol. Both examples suggest that there was inadequate cellular dehydration using the predicted optimal plunge temperature of -32°C, which resulted in damaging intracellular ice formation during either the subsequent cooling or warming phase.

(iii) Cases where suboptimal cooling rates increased PTR

For both the CBA and 129R1 mESC lines, there was a significant interaction of cooling rate and plunge temperature, and both results were unexpected. For the CBA mESC line, the combination of predicted optimal cooling rate and predicted optimal plunge temperature significantly lowered PTR. For the 129R1 mESC line, suboptimal cooling rates combined with the standard plunge temperature significantly improved PTR. These effects originated from the greatly successful outcome of PTR using suboptimal cooling rates for PG.

With the CBA and 129R1 mESC lines, PTR using predicted optimal cooling rates for 1 M PG did not improve PTR, but suboptimal cooling rates for the same CPA did, in fact, increase PTR. In the case of the CBA mESC line, non-optimal cooling rates were five-fold higher than predicted optimal rates, suggesting that our predicted optimal rates were too low. In the case of the 129R1 mESC line, non-optimal cooling rates were three-

fold lower than predicted optimal rates, suggesting that our predicted optimal rates were too high.

(iv) Sources of error in the prediction of optimal cooling rates and plunge temperatures

The three situations listed above can perhaps be explained by constraints of current fundamental cryobiological models, including potential error in extrapolating suprazero E_a to subzero temperatures, questionable model appropriateness at high solute concentrations, and warming rate interactions. Here and in other studies, the assumption is made that suprazero measurements of permeability parameters, including E_a , can be extrapolated to subzero temperatures, but this may not be accurate. Hydrogen bonding interactions between water and lipid molecules, and the lipid dynamics required to allow water passage across a cell membrane generally result in high E_a^{Lp} [25]. Nonlinearities in the Arrhenius relationship involving L_p may arise from heterogeneity in water transport properties, and temperature-dependent changes in the fluidity of the lipid membrane [25], and thus it is beneficial to measure E_a over as broad a temperature range as possible. However, it is technically difficult to conduct subzero measurements of cryobiological parameters due to the distortion and obscuring of cells by extracellular ice [26]. A recent report by Kleinhans and Mazur [26] utilized an interrupted, rapid cooling method to compare subzero E_a to values obtained above 0°C. Their best-fit value obtained below 0°C was determined to be 50% higher than the suprazero value, indicating that the suprazero to subzero assumption may not be correct [26]. Inaccurate reflections of subzero permeability parameters by suprazero extrapolations may have led to error in the

calculation of predicted optimal cooling rates and plunge temperatures that in turn resulted in little or no improvement of PTR in certain circumstances. While our measurements were conducted over a very broad temperatures ranging from 0°C to 37°C, subzero measurements were not conducted. It may be beneficial to allow cells to cool for an additional number of degrees beyond the predicted optimal plunge temperature in order to compensate for inaccuracies of suprazero measurements of E_a .

Additional error may occur when one is applying assumptions made under physiological conditions, *i.e.* relatively dilute solutions, to make predictions for how cells will behave under non-physiologic, nondilute conditions that cells undergo during cryopreservation. Elmoazzen *et al.* [7] recently described a new nondilute solute transport model that does not make the previous dilute solution or near-equilibrium assumptions and suggested that previous models may have an unexpected and undesirable concentration dependence of permeability, implying that applications of measurements in one setting may not be appropriate in very different settings. This potential inaccuracy introduced into our model by assumed concentration independence may have contributed to unexpected results encountered in our experiments.

Finally, our results may have been affected by warming rate interactions. The effects of a particular warming rate are strongly dependent on the cooling rate. If cooling rates are high, there is insufficient cellular dehydration and a higher probability of intracellular ice formation. In this case, rapid warming may favor high survival as it tends to inhibit devitrification and the recrystallization of intracellular ice, because small crystal formation is favored by high cooling rates, small crystals have high surface energies which encourages their growth, and slow warming would provide more time for

crystal growth upon warming [27]. Warming rate has more unpredictable effects on slowly cooled cells (*i.e.* cells that are cooled slowly enough to allow sufficient dehydration, thus avoiding intracellular ice formation); in this circumstance, warming rate can have no effect (as with human myeloid stem cells frozen slowly in Me₂SO [28]), slow warming may be more damaging than rapid warming (for example, eight-cell mouse embryos cooled slowly in glycerol [29]), or rapid warming may be more damaging than slow (as with eight-cell mouse embryos cooled in Me₂SO[29])[27]. Our warming rate of approximately 700°C/minute was predicted by computer simulations to be within a range that would have negligible effects on cell survival; however, this rate may well have influenced cell survival based on whether calculated optimal cooling rates were true, as well as based on how effectively our predicted optimal plunge temperatures provided conditions favoring vitrification at plunge temperatures. As it is difficult to predict warming rate interactions for mESCs, or to know if there is variation between cell lines, it would be beneficial for future studies to include a study on warming rate interactions in multiple cell lines for all CPAs.

From examining PTR results of interactions between CPA, cooling rate, and plunge temperature, predicted optimal cooling rates for 1 M Me₂SO seemed in general to be more successful than predicted optimal cooling rates for 1 M PG in generating at least moderate improvement in PTR. In all four mESC lines, the predicted optimal cooling rates for Me₂SO resulted in improved PTR as compared to standard protocols. However, improved PTR occurred in only two out of four mESC lines using predicted optimal cooling rates for 1 M PG. When examining PTR using 1 M PG in all mESC lines, including the previously published C57BL/6 mESC line [4], the PTRs of four out of five

mESC lines (BALB/c, C57BL/6, FVB, and 129R1) were significantly improved ($p<0.05$) simply by changing from 1 M Me₂SO to 1 M PG. A cooling rate of 1°C/minute was predicted to be optimal in three out of the five mESC lines.

Improvements in PTR were most dramatic for the FVB mESC line, where the predicted optimal cooling rate combined with the predicted optimal plunge temperature for 1 M Me₂SO resulted in a 7-fold improvement in PTR. The very low PTR achieved with the standard freezing protocol for the FVB mESC line made any significant increase in PTR sound impressive when expressed in fold recovery. In general, the PTR of the CBA and FVB mESC lines, which, out of the four mESC lines, yield the lowest PTR under standard conditions, was raised to more practical levels (at best, $23.3 \pm 3.9\%$ and $25.2 \pm 4.0\%$ vs. $12.2 \pm 0.7\%$ and $3.6 \pm 0.5\%$, respectively), but the highest PTR was approximately less than half that of the highest PTR for the BALB/c and 129R1 mESC lines. For the BALB/c and 129R1 mESC lines, the greatest improvement in PTR was approximately 2-fold, raising PTR from $24.0 \pm 3.9\%$ and $28.4 \pm 1.3\%$ to, at best, $48.7 \pm 7.1\%$ and $59.4 \pm 2.6\%$, respectively.

Summary

We predicted optimal cooling rates and plunge temperatures in the presence of 1 M Me₂SO and 1 M PG using fundamental cryobiological parameters, including OTL, V_b , L_p , P_{CPA} , and their associated E_a , for the BALB/c, CBA, FVB, and 129R1 mESC lines. The results of our studies as well as the previous C57BL/6 mESC study by Kashuba

Benson *et al.* [4] suggest that a protocol utilizing 1 M PG, a cooling rate of 1°C/minute, and plunge temperature of -41°C will yield improved PTR relative to standard methods for most mESC lines. This protocol can be easily applied in a laboratory setting (Figure 4.1). For the FVB line in particular, the improvement in PTR was considerable under these conditions. From these observations, it seems probable that this optimized protocol can be applied to all mESC lines to generate improved PTR relative to the current standard method. The exception in our studies was with the CBA mESC line, for which we recommend a cooling rate of 5°C/minute in the presence of either 1 M Me₂SO or 1 M PG, and a predicted optimal plunge temperature of -80°C. There are enough differences between mESC lines and enough mESC lines in existence such that exceptions to this universal protocol will occur, and these exceptional lines can be approached on a case-by-case basis using the systemic fundamental cryobiological approach to improving PTR that was originally described for the C57BL/6 mESC line [4].

Future studies addressing potential sources of error, including the examination of warming rate interactions, subzero *vs.* suprazero measurements of E_a , and exploration of alternative models appropriate for high solute concentrations could result in further improvements to mESC protocols. Considering that mESC lines have been characterized and banked while utilizing cryopreservation methods solely utilizing Me₂SO, it would be advisable to study the effects of PG and additional prospective CPAs on mESC gene expression, growth characteristics, and germ-line transmission. Future studies should also include the empirical validation of cooling rates and predicted plunge temperatures for EG in comparison to the standard method, as predicted optima for this CPA seem to be very similar for all mESC lines studied to date.

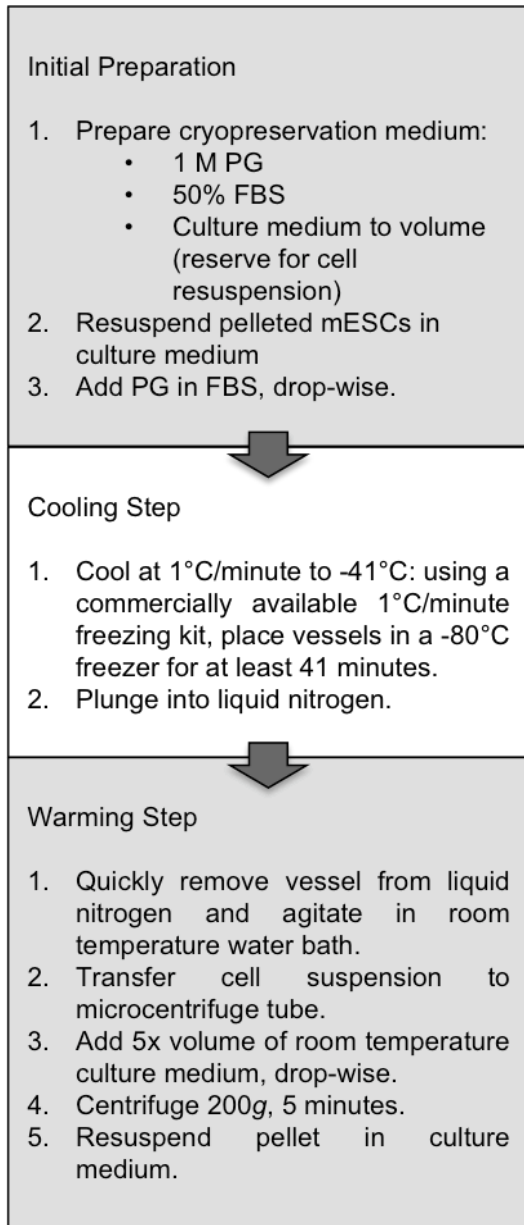


Figure 4.1. A new standard protocol for mouse embryonic stem cells (mESCs). PG, propylene glycol. FBS, fetal bovine serum.

References

1. Bedell, M.A., N.A. Jenkins, and N.G. Copeland, *Mouse models of human disease. Part I: techniques and resources for genetic analysis in mice*. Genes Dev, 1997. **11**(1): p. 1-10.
2. Bedell, M.A., et al., *Mouse models of human disease. Part II: recent progress and future directions*. Genes Dev, 1997. **11**(1): p. 11-43.
3. Austin, C.P., et al., *The knockout mouse project*. Nat Genet, 2004. **36**(9): p. 921-4.
4. Kashuba Benson, C.M., J.D. Benson, and J.K. Critser, *An improved cryopreservation method for a mouse embryonic stem cell line*. Cryobiology, 2008. **56**(2): p. 120-30.
5. Miszta-Lane, H., et al., *Effect of slow freezing versus vitrification on the recovery of mouse embryonic stem cells*. Cell preservation technology, 2007. **5**(1): p. 16-24.
6. Chan, S.Y. and M.J. Evans, *In situ freezing of embryonic stem cells in multiwell plates*. Trends Genet, 1991. **7**(3): p. 76.
7. Elmoazzen, H.Y., J.A. Elliott, and L.E. McGann, *Osmotic transport across cell membranes in nondilute solutions: a new nondilute solute transport equation*. Biophys J, 2009. **96**(7): p. 2559-71.
8. Gao, D.Y., et al., *Prevention of osmotic injury to human spermatozoa during addition and removal of glycerol*. Hum Reprod, 1995. **10**(5): p. 1109-22.
9. Gilmore, J.A., et al., *Determination of optimal cryoprotectants and procedures for their addition and removal from human spermatozoa*. Hum Reprod, 1997. **12**(1): p. 112-8.
10. Mazur, P., *Kinetics Of Water Loss From Cells At Subzero Temperatures And The Likelihood Of Intracellular Freezing*. J Gen Physiol, 1963. **47**: p. 347-69.
11. Liu, J., et al., *Cryobiology of rat embryos II: A theoretical model for the development of interrupted slow freezing procedures*. Biol Reprod, 2000. **63**(5): p. 1303-12.
12. Mazur, P., *Freezing of living cells: mechanisms and implications*. Am J Physiol, 1984. **247**(3 Pt 1): p. C125-42.

13. Mazur, P., S.P. Leibo, and E.H. Chu, *A two-factor hypothesis of freezing injury. Evidence from Chinese hamster tissue-culture cells*. Exp Cell Res, 1972. **71**(2): p. 345-55.
14. Doetschman, T., *Gene Targeting in Embryonic Stem Cells: I. History and Methodology*, in *Transgenic Animal Technology: A Laboratory Handbook, Second Edition*, C.A. Pinkert, Editor. 2002, Academic Press: San Diego.
15. Gordeeva, O.F., et al., [*Expression of regulatory genes Oct-4, Pax-6, Prox-1, Ptx-2 at the initial stages of differentiation of embryonic stem cells in vitro*]. Ontogenet, 2003. **34**(3): p. 174-82.
16. *Preparation of ES Cells for Injection*, in *Manipulating the Mouse Embryo: A Laboratory Manual*, A. Nagy, et al., Editors. 2003, Cold Spring Harbor Laboratory Press: Cold Spring Harbor, New York. p. 469.
17. Schenke-Layland, K., et al., *Collagen IV induces trophoectoderm differentiation of mouse embryonic stem cells*. Stem Cells, 2007. **25**(6): p. 1529-38.
18. Katkov, II, *A two-parameter model of cell membrane permeability for multisolute systems*. Cryobiology, 2000. **40**(1): p. 64-83.
19. Songsasen, N. and S.P. Leibo, *Cryopreservation of mouse spermatozoa. I. Effect of seeding on fertilizing ability of cryopreserved spermatozoa*. Cryobiology, 1997. **35**(3): p. 240-54.
20. Petersen, A., et al., *A new approach for freezing of aqueous solutions under active control of the nucleation temperature*. Cryobiology, 2006. **53**(2): p. 248-57.
21. Baudot, A., L. Alger, and P. Boutron, *Glass-forming tendency in the system water-dimethyl sulfoxide*. Cryobiology, 2000. **40**(2): p. 151-8.
22. Baudot, A. and V. Odagescu, *Thermal properties of ethylene glycol aqueous solutions*. Cryobiology, 2004. **48**(3): p. 283-94.
23. Gilmore, J.A., et al., *Osmotic properties of boar spermatozoa and their relevance to cryopreservation*. J Reprod Fertil, 1996. **107**(1): p. 87-95.
24. Pegg, D.E. and M.P. Diaper, *On the mechanism of injury to slowly frozen erythrocytes*. Biophys J, 1988. **54**(3): p. 471-88.
25. Verkman, A.S., *Water permeability measurement in living cells and complex tissues*. J Membr Biol, 2000. **173**(2): p. 73-87.

26. Kleinhans, F.W. and P. Mazur, *Determination of the water permeability (L_p) of mouse oocytes at -25 degrees C and its activation energy at subzero temperatures.* Cryobiology, 2009. **58**(2): p. 215-24.
27. Mazur, P., *Principles of Cryobiology*, in *Life in the Frozen State*, B.J. Fuller, N. Lane, and E.E. Benson, Editors. 2004, CRC Press LLC: New York. p. 3-65.
28. Wells, J.R., A. Sullivan, and M.J. Cline, *A technique for the separation and cryopreservation of myeloid stem cells from human bone marrow.* Cryobiology, 1979. **16**(3): p. 201-10.
29. Rall, W. and C. Polge, *Effect of warming rate on mouse embryos frozen and thawed in glycerol.* J Reprod Fertil., 1984. **70**(1): p. 285-92.

CHAPTER 5

THE INFLUENCE OF TEMPERATURE, CRYOPROTECTIVE AGENTS, AND LATRUNCULIN ON FUNDAMENTAL CRYOBIOLOGICAL PARAMETERS AND THEIR IMPLICATIONS TO IMPROVING CRYOPRESERVATION METHODS

Introduction

In studies outlined in the previous chapters, all evaluations of membrane permeability parameters and osmotic response of mouse embryonic stem cells (mESCs) were conducted at 0°C or higher. A common criticism of the utilization of measured fundamental cryobiological parameters to improve cryopreservation protocols is that the parameters are usually measured at supra-zero temperatures and may not accurately reflect subzero cell responses [1][2][3]. Heterogeneity in water transport properties and temperature-dependent changes in the fluidity of the lipid membrane may lead to nonlinearities in the Arrhenius relationship (temperature dependence or activation energy, E_a) involving hydraulic conductivity (L_p) [4], and thus it is beneficial to determine E_a over a temperature range that is as broad as possible. Problematically, it is often technically difficult to conduct subzero measurements of cryobiological parameters using visual methods due to the distortion and obscuring of cells by extracellular ice [1].

To address this concern and investigate these phenomena, preliminary experiments were conducted using light microscopy techniques to measure these osmotic

characteristics of the C57BL/6 mouse embryonic stem cell (mESC) line at sub-zero temperatures. However, the measured osmotically inactive cell volume (V_b), in the absence of CPA, using this method at these temperatures was markedly lower than the 49.7% (of isosmotic cell volume, V_{iso}) [5] extrapolated from room temperature experiments (Figure 5.1). This discrepancy raised concerns about the assumption of the temperature independence of V_b . In addition to being estimated from room temperature osmotic responses, V_b is also usually estimated in the absence of CPA, with the assumption that V_b is independent of extracellular media. Because other osmotic characteristics such as water permeability change significantly in the presence of CPA, we also investigated this assumption.

The difference in observed *vs.* extrapolated V_b could be due to inaccuracies of measurement of cells in the presence of extracellular ice, where distortion of the spherical cell is assumed to be commonplace [1] and may lead to inaccuracies in estimating both cell volume and surface area, which in turn introduce error in the calculation of subzero permeability parameters (see Figure 5.2 for an illustration of error of measurement with deviation from a spherical shape). Organized disruption of the cytoskeleton, especially through reversible methods such as Latrunculin A (LATA), would potentially allow spherical shrinkage of cells and thus greater accuracy in measurement at subzero temperatures. The latrunculins are highly specific, cell-permeant macrolides isolated from the Red Sea sponge, *Latrunculia magnifica*, that depolymerize F-actin microfilaments by one-to-one binding with G-actin in a reversible manner [6][7]. Interestingly, incubation and subsequent cryopreservation in the presence of LATA has been found to increase the post-thaw recovery of cryopreserved mouse oocytes, possibly

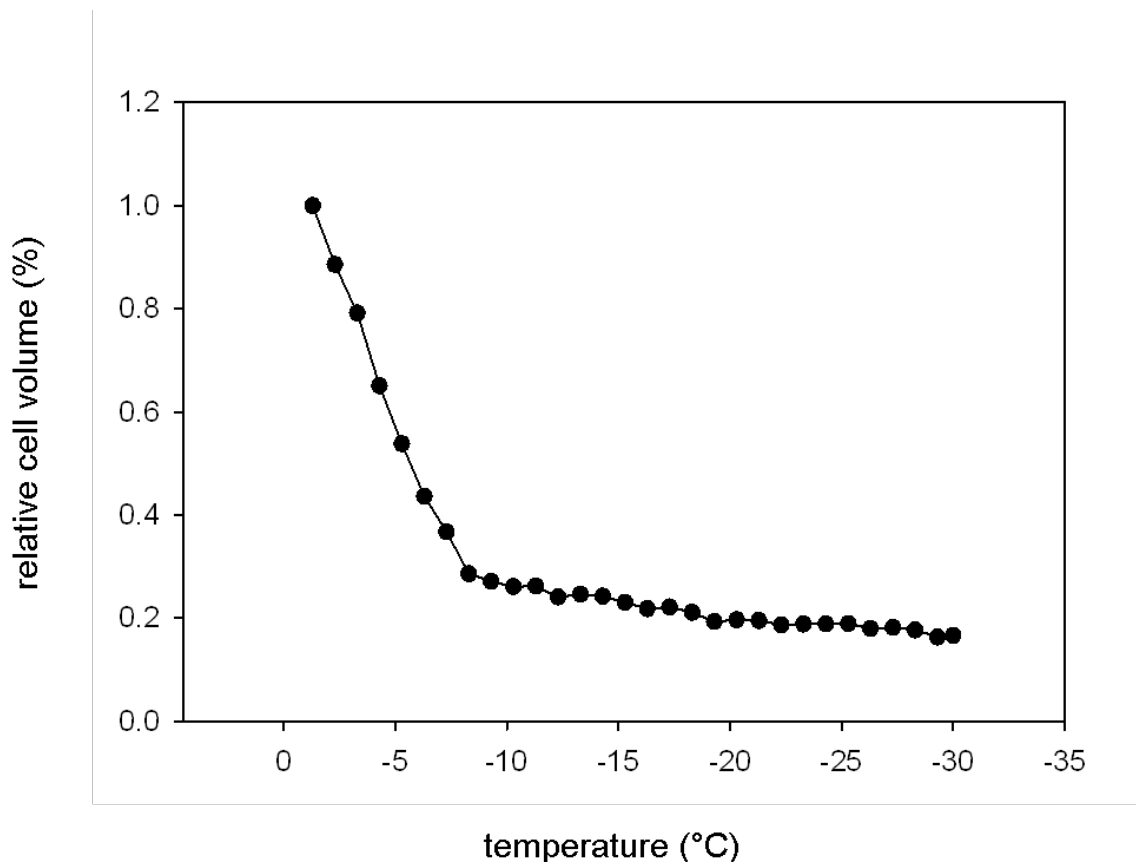
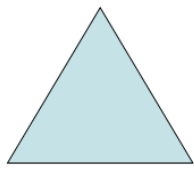
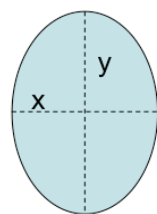


Figure 5.1. Observed minimal cell volume during preliminary subzero permeability experiments was 17% of isotonic cell volume at -1°C, a value much lower than the previously extrapolated V_b of 49.7% (of isotonic cell volume) [5] estimated at room temperature.



Equilateral Triangle
Error = 5.6%



Square
Error = - 4.2%

Ellipse
 $n=x/y$ or y/x
Error < 10%, if $0.8 < n < 1.2$
Error < 5%, if $0.9 < n < 1.1$

Figure 5.2. When estimating spherical volumes, the magnitude of error changes according to the true shape of the measured area.

through the maintenance of viscoelastic properties of the oocyte by the prevention of irreversible cryopreservation-induced actin damage, the enhanced ability of cells to repair cell membrane rents upon disassembly of their actin cytoskeleton, and/or the prevention of mechanical stress from differential responses of the cytoskeleton, cell membrane, and other cytoskeleton-associated organelles to the cryopreservation process [8]. We determined it was necessary to test the potential effects of LATA-induced F-actin depolymerization on the dynamics of the cell membrane that contribute to permeability parameters and osmotic response and are unique to each cell type.

In this study, we examined the interaction of LATA-induced F-actin depolymerization, temperature, and dimethyl sulfoxide (Me_2SO) on V_b , L_p , and mESC plasma membrane permeability to CPA (P_{CPA}) in order to identify sources of error in measurement of V_b , to evaluate the potential usefulness of LATA in sub-zero permeability experiments, and to determine whether accuracy in the prediction of optimal cooling rates and plunge temperatures could be influenced or aided by alternative approaches.

Materials & Methods

Embryonic stem cells

The C57BL/6 mESC line was acquired at passage 11 from Specialty Media Group (Chemicon International, Temecula, California, now part of Millipore, Billerica, Massachusetts). C57BL/6 mESC cultures were negative for all pathogens (IMPACT I

test, Research Animal Diagnostic Laboratory, Columbia, Missouri;
www.radil.missouri.edu)

Cell culture and cryopreservation method

Mouse ESCs were cultured on primary mouse embryonic fibroblast cells (PMEF) (Millipore) at 37°C and 5% CO₂. Culture media contained 15% defined fetal bovine serum (FBS) (Hyclone, Logan, UT), 0.1 mM non-essential amino acids (GIBCO/Invitrogen, Carlsbad, CA), 1.0 mM sodium pyruvate (GIBCO), 100 µM β-mercaptoethanol (Sigma-Aldrich, St. Louis, MO), and 1000 U ESGRO/mL (Millipore) in high glucose DMEM (Millipore). Mouse ESCs were passaged and/or collected every 2 days or at approximately 80% confluence.

For cryopreservation, cells were resuspended in freezing medium (1.3 M (10% v/v) dimethyl sulfoxide (Me₂SO, Sigma-Aldrich), 50% defined FBS, and 40% culture medium) in 1 mL aliquots in cryovials (Nalgene Nunc International, Rochester, NY). Cryovials were transferred to a commercially available 1°C/minute freezing kit (Nalgene), refrigerated at -80°C overnight, and subsequently transferred to liquid nitrogen.

At the conclusion of all experiments, passage 18 (the highest passage) cells were karyotyped (Chih-Lin Hsieh, Arcadia, CA), and five out of twenty cells were found to have Trisomy 8. This is commonly found in mESC karyotypes [9][10].

Separation of mESCs from feeders

For all experiments, ESCs were separated from feeder cells using a differential sedimentation technique previously described by Doetschman [11]. There are many variations of this basic method [12][13][14], which exploits the different settling and adherence rates of PMEF and mESCs to culture dishes. Briefly, trypsinized mESC suspensions containing PMEF were centrifuged, resuspended in culture medium, and incubated in the original cell culture dish for 30 minutes at 37°C. The suspension was then transferred to a second culture dish and incubated for 1 hour at 37°C. Following the second incubation, the cell suspension was removed and mESCs were counted, centrifuged, and resuspended in either DPBS or culture medium for experimentation. In our hands, the Doetschman sedimentation method resulted in the removal of greater than 99% of contaminating feeder cells from the cell suspension (data not shown).

Determining the effective concentration of Latrunculin A

Mouse ESCs were cultured to 80% confluence on glass cover slips, then incubated at 37°C for one hour in culture medium containing 0, 0.1, 0.2, 0.5, 1, 2, or 3 µg/mL of LATA (Invitrogen). Cells were then washed twice with pre-warmed PBS, fixed in 3.7% formaldehyde solution, and stained for F-actin with Alexa Fluor 488 Phalloidin (Invitrogen) according to the package insert protocol for formaldehyde-fixed adherent cells grown on coverslips (Phallotoxins package insert, Invitrogen). Fluorescence was observed using conventional fluorescent microscopy (Zeiss Axiophot,

Zeiss Axiopath Systems, Carl Zeiss MicroImaging, Inc., Thornwood, New York). Three replicates of each treatment were performed on each of three days.

Determining levels of toxicity of Latrunculin A

In order to determine whether LATA had dose-dependent damaging effects that could reduce cell count or impair cell membrane integrity, mESCs were cultured to 80% confluence, trypsinized into single cell suspension, filtered through a 40 µm cell strainer (Becton Dickinson Labware, Becton Dickinson and Company, Franklin Lakes, NJ), and equal numbers of mESCs in single cell suspension were incubated for one hour at 37°C in culture medium containing 0, 0.1, 0.2, 0.5, 1, 2, or 3 µg/mL of LATA. Following incubation, suspensions were collected and centrifuged. Pellets were then resuspended in 1x PBS, stained with propidium iodide, and passed through a FACScan flow cytometer (BD Biosciences, San Jose, CA) for analysis of cell number and membrane integrity. Percent membrane integrity was defined as the percent of single cells excluding propidium iodide normalized to that of the control population (0 µg/mL LATA). Cell count per sample over a 10 second time period was also analyzed for each sample.

The effects of Latrunculin A on post-thaw recovery of mESCs

Empirical cryobiological studies were conducted to determine whether LATA would improve percent post-thaw recovery of mESC. Mouse ESCs, cultured in standard conditions, were separated from fibroblast feeders and incubated for one hour at 37°C in

the presence or absence of LATA at concentrations of 0, 0.2, 0.5, 1.0, and 2.0 $\mu\text{g/mL}$ of LATA. Mouse ESCs were then centrifuged and the pellet resuspended at a concentration of 1×10^6 cells/mL of freezing medium containing the same concentration of LATA in the absence of Me_2SO . Additionally, cells incubated without LATA were cryopreserved in the presence of 10% (1.3 M) Me_2SO , and cells incubated with 1.0 $\mu\text{g/mL}$ of LATA were also cryopreserved in the presence of 1.0 $\mu\text{g/mL}$ LATA and 10% Me_2SO . Suspensions were transferred to cryovials and placed in a commercially available 1°C/minute Nalgene freezing kit, refrigerated at -80°C overnight, and then transferred to liquid nitrogen. Samples were thawed in a 37°C water bath, diluted drop-wise by 5 volumes of culture media, centrifuged, resuspended in 1x PBS, stained with propidium iodide for membrane integrity, and passed through a FACScan flow cytometer (BD Biosciences, San Jose, CA) for analysis of post-thaw recovery of membrane intact single cells as a percentage of pre-cryopreservation levels.

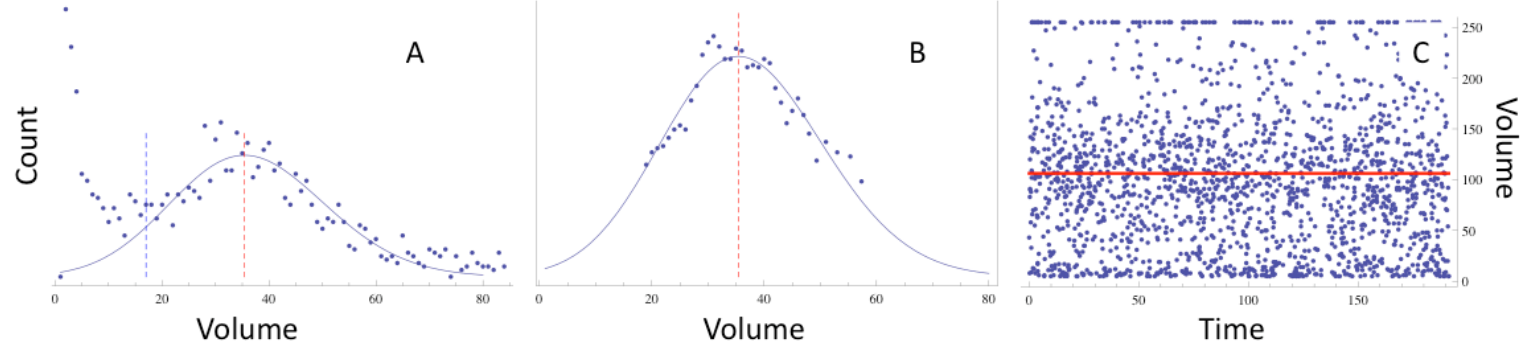
Electronic Particle Counter

A modified electronic particle counter (EPC) (Coulter Counter model AM, Beckman Coulter, Inc., Fullerton, CA), fixed to operate without a mercury-filled manometer as per Benson *et al.* [15], was used for all cellular volumetric measurements. The machine was equipped with a standard 50 μm aperture tube and computer interface [16], and raw data was exported into the Mathematica (Wolfram Research Inc., Champaign, IL) computing package for processing and analysis. Volume was calibrated using standard nominal 10 μm polystyrene latex particles (Beckman Coulter, Inc.,

Fullerton, CA) at all temperatures and osmolalities. The relationship between conductivity and latex bead volume was assumed to be the same as that between conductivity and ESC volume.

The effect of CPA, temperature, and Latrunculin A on cell osmotic response

Mouse ESCs were incubated for one hour at 37°C in the presence (LATA cells) or absence (control cells) of 0.5 µg/mL (1 µM) LATA, centrifuged, and resuspended in 1x PBS with or without 1 µM LATA, respectively. Embryonic stem cell volumetric response to variable osmotic stresses of each group of treated cells was measured at 22 ± 1°C and -3 ± 1°C using an EPC as previously described [16][17][18][19][20][5]. Mean cell volume response of LATA-treated and control cells was measured in real time following abrupt exposure to 290, 450, 600, 900, and 1200 mOsm solutions in the presence or absence of 1.5 M Me₂SO (cells were pre-equilibrated in 1.5 M Me₂SO at room temperature for 5 minutes prior to their exposure to anisosmotic solutions, then equilibrated for a minimum of 5 minutes in salt solutions). Solutions were prepared from 1x PBS with NaCl added to increase osmolality; solutions were adjusted to pH 7.1 as necessary with hydrochloric acid. A vapor pressure osmometer (Westcor, Logan, UT) was used to verify the osmolality of the solutions. Data were averaged over 100 ms intervals prior to analysis, and three replicates were performed for each experimental condition. Volume histograms were analyzed with a custom mathematical algorithm and fit to a normal distribution function (Figure 5.3), similar to the method used by Armitage and Juss [21]. Equilibrated cell volumes were normalized to their respective isotonic



117

Figure 5.3. Typical output plots of the method used to find population mean volumes in “noisy” data with the Coulter counter. A, histogram of the raw data (C) with the resulting fit (solid line). A mathematical algorithm searched for a cut-off value (dashed blue line) for the noise at lower volumes. Data below this volume were discarded. In order to reduce population tail bias, count (y-axis) values below this point were also discarded, leaving the symmetrical population in B. These data were fit to a normal distribution function, and the mean value was kept. The resulting fit is shown in A and B, where the mean value is shown as a dashed red line, and in C, where the mean value is shown as a solid red line.

values and then plotted against the reciprocal of normalized osmolality in accordance with the Boyle Van't Hoff relationship [22]. The Boyle Van't Hoff equation was fit to the data using linear regression calculated using Mathematica. This equation is defined by

$$V = V_{w,iso} M_{iso} / M + V_b,$$

where V is cell volume at osmolality M , $V_{w, iso}$ is isotonic cell water volume, M_{iso} is isotonic osmolality, and V_b is the osmotically inactive cell volume. V_b was determined by performing a linear regression of volume as a function of the reciprocal of osmolality and extrapolating to infinite osmolality (i.e. $1/M = 0$), as previously described [5].

The equation for V_b in the presence of a permeating CPA is derived as follows. The total cell volume V_{total} is the sum of water volume, solute volume and osmotically inactive volume:

$$V_{total} := V_w + \bar{V}_s s + V_b,$$

where \bar{V}_s is the partial molar volume of the permeating solute. The molality of the solute in the cell is given by $M_s = s/V_w$, thus:

$$V_{total} = V_w + \bar{V}_s M_s V_w + V_b = (1 + \bar{V}_s M_s) V_w + V_b.$$

Finally, the Boyle Van't Hoff relationship is $\pi^{iso} V_w^{iso} = \pi V_w$, where π is the osmolality and the superscript *iso* indicates values at isosmolality. In solving for V_w and substituting this relationship into the above equation, we get

$$V_{total} = (1 + \bar{V}_s M_s) \frac{\pi^{iso}}{\pi} V_w^{iso} + V_b.$$

If we take the limit as π approaches infinity, we see that in theory,

$$\lim_{\pi \rightarrow \infty} V_{total} = \lim_{\pi \rightarrow \infty} (1 + \bar{V}_s M_s) \frac{\pi^{iso}}{\pi} V_w^{iso} + V_b = V_b.$$

Therefore, the presence of CPA should not affect the V_b .

Extrapolated V_b values were adjusted for relative V_{iso} ; *i.e.* V_b was multiplied by the ratio of the V_b of the corresponding treatment to the V_b of control cells (0 μ M LATA, 0 M Me₂SO, 22°C) and listed for comparative purposes beside unadjusted values (Table 5.2).

The effect of Latrunculin A on permeability parameters at supra- and sub-zero temperatures

In order to explore the effects of LATA on permeability parameters measured at 22°C and -3°C, mESC were incubated for one hour at 37°C in the presence (LATA cells) or absence (control cells) of 0.5 μ g/mL (1 μ M) LATA, centrifuged, and resuspended in 1x PBS with or without 1 μ M LATA, respectively. For both groups, volume changes over time following abrupt addition of cells to 1.5 M Me₂SO in 1x PBS were measured using an EPC at 22°C and -3°C. Three replicates were performed for each treatment on three different days.

Data were analyzed using the method previously described by Kashuba Benson *et al.* [5]. Briefly, data from LATA-treated and control groups at both temperatures were fit to the following two parameter mass transport model [23] to determine hydraulic conductivity (L_p) and membrane permeability to cryoprotective agents (P_{CPA}):

$$\frac{dV_w}{dt} = -L_p ART \left(M_s^e + M_n^e - \frac{n_s^i + n_n^i}{V_w} \right),$$

$$\frac{dn_s^i}{dt} = P_s A \left(M_s^e - \frac{n_s^i}{V_w} \right).$$

In these equations, superscripts e and i indicate extra- and intracellular quantities, respectively, subscripts s and n indicate permeating and non-permeating quantities, respectively, and A is the volume independent spherical surface area at V_{iso} . The relationship $n^i = V_w M^i$, where V_w is the intracellular water volume, is an assumption of the model. Values of V_{iso} and V_b were matched according to LATA treatment or non-treatment, and had been calculated in LATA-treated or untreated cells at room temperature in the absence of CPA (Table 5.3).

Statistical analysis

Data were analyzed using standard analysis of variance (ANOVA), which was performed with the SAS General Linear Models program (SAS Institute, Inc., Cary, NC) using an alpha value of $p < 0.05$. In cases where a plot of the residuals of a data set was not normally distributed, data were normalized using either natural logarithm or square root transformation. All values are presented as mean \pm SEM, unless stated otherwise.

Results

Determining the effective concentration of Latrunculin A

As determined by fluorescence microscopy evaluation of Alexa Fluor 488 Phalloidin-stained mESC colonies, a concentration of 0.5 µg/mL (1 µM) was determined to be the effective minimal concentration for complete depolymerization of the actin cytoskeleton (Figure 5.4g, h). With increasing concentrations of LATA, there was decreased green fluorescence (indicating F-actin depolymerization), increased rounding of cells and separation of cells from the colonies, and decreased colony size and frequency. At 0.5 µg/mL LATA, colonies were readily observed on the cover slips, however actin staining had decreased substantially relative to the control and to 0.2 µg/mL LATA treated colonies. While colonies were still readily observed by conventional light microscopy, with fluorescence microscopy, organized fluorescent cell structures were no longer observable as actin filaments disappeared and were reduced to multiple green pinpoint foci. At concentrations greater than 0.5 µg/mL, the frequency of colonies on the slides decreased from moderate frequency per high-powered field, to small (<50 µ diameter), rare partial colonies (1 µg/mL and 2 µg/mL LATA, Figure 5.4i-l) or no colonies (3 µg/mL LATA, Figure 5.4m, n).

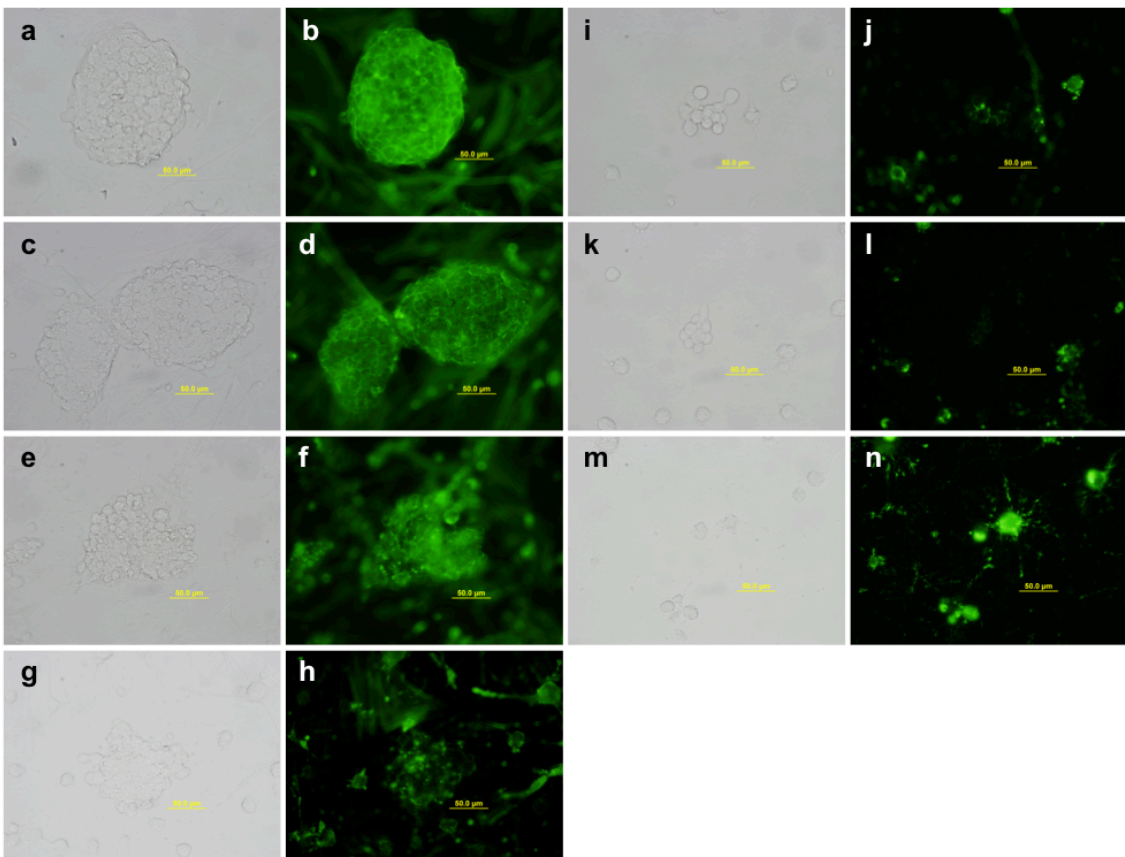


Figure 5.4. A minimal concentration of 0.5 $\mu\text{g}/\text{mL}$ (1 μM) Latrunculin A (LATA) was determined to be adequate for depolymerization of the actin cytoskeleton of C57BL/6 mouse embryonic stem cells (mESCs). Mouse ESCs cultured on glass coverslips were incubated in culture medium for one hour at 37°C in the presence of the following concentrations of LATA: 0 $\mu\text{g}/\text{mL}$ (a, b), 0.1 $\mu\text{g}/\text{mL}$ (c, d), 0.2 $\mu\text{g}/\text{mL}$ (e, f), 0.5 $\mu\text{g}/\text{mL}$ (g, h), 1.0 $\mu\text{g}/\text{mL}$ (i, j), 2.0 $\mu\text{g}/\text{mL}$ (k, l), and 3.0 $\mu\text{g}/\text{mL}$ (m, n). Slides were fixed in 3.7% formaldehyde, stained for F-actin with Alexa Fluor 488 Phalloidin (green color), and observed under fluorescence microscopy. Panels with the grey background are representative colonies under conventional light microscopy; panels with a black background are representative of the corresponding colonies under fluorescence microscopy. While colonies were still readily observed by conventional light microscopy at concentrations of 0.5 $\mu\text{g}/\text{mL}$ LATA, under fluorescence microscopy, organized fluorescent cell structures were no longer observable as actin filaments disappeared and were reduced to multiple green pinpoint foci.

Latrunculin A has minimal toxicity at levels of 3 µg/mL

Latrunculin A concentrations of 0.1 and 0.2 µg/mL had no significant effect on percent membrane integrity of the single cell mESC population, but at concentrations of 0.5, 1.0, 2.0, and 3.0 µg/mL, there was a significant increase in percent membrane integrity to 106 ± 1% at all concentrations ($p<0.05$) (Figure 5.5a). There was a significant increase in cell counts, normalized to control cell counts, at 0.2, 0.5, 1.0, 2.0, and 3.0 µg/mL LATA ($p<0.05$) (127 ± 7%, 141 ± 8%, 143 ± 9%, 155 ± 9%, and 146 ± 9%, respectively) (Figure 5.5b), and a corresponding significant decrease ($p<0.05$) in the percent of counts in the upper right quadrant, representing clusters of two or more cells, of the FACScan dot plots at all concentrations of LATA (Figures 5.5c and 5.5d). Percent cell counts relative to control values for Quadrant III were 71 ± 3%, 59.5 ± 3%, 58 ± 3%, 61 ± 3%, 64 ± 3%, and 65 ± 3% for 0.1, 0.2, 0.5, 1.0, 2.0, and 3.0 µg/mL LATA concentrations, respectively. At the effective concentration of 1.0 µM LATA, percent membrane integrity was 106 ± 1% relative to the untreated control, and cell counts were 141 ± 7.5% that of control treatments (refer to Discussion for detailed explanation).

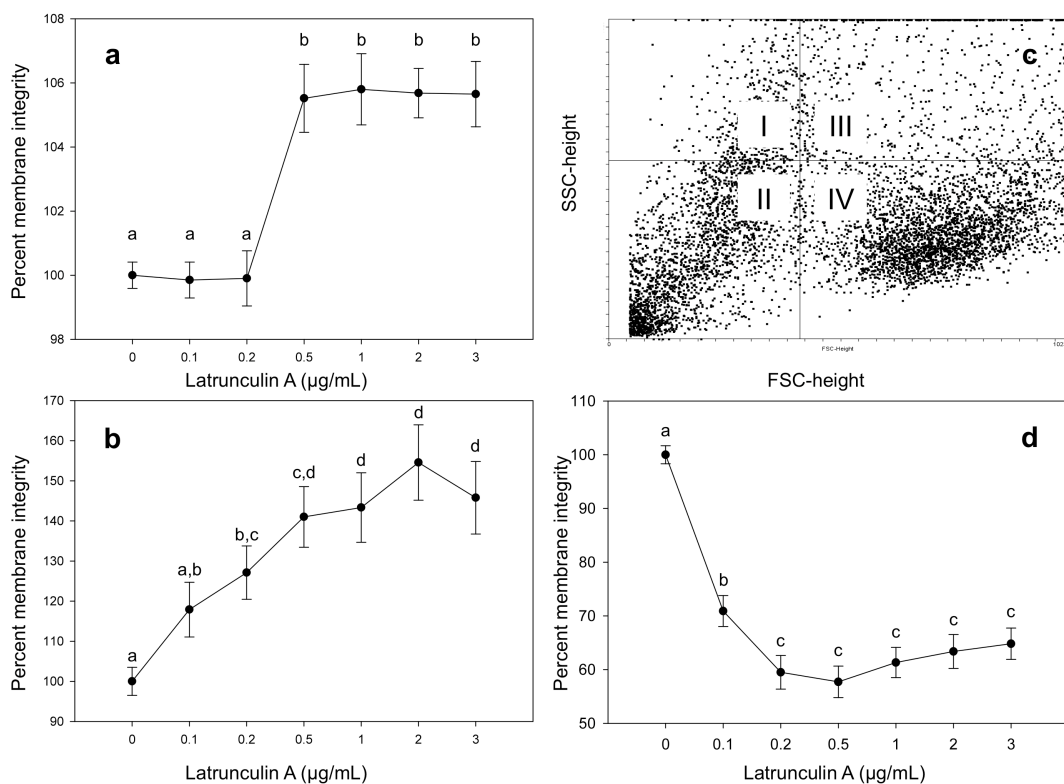


Figure 5.5. The effect of Latrunculin A (LATA) on cell count and membrane integrity of C57BL/6 mouse embryonic stem cells (mESCs). Equal numbers of mESCs in single cell suspension were incubated for one hour in the presence of 0, 0.1, 0.2, 0.5, 1.0, 2.0, and 3.0 $\mu\text{g}/\text{mL}$ of LATA. After one hour, cells were quantified and analyzed by flow cytometry for propidium iodide exclusion. **a)** Percent membrane integrity, normalized to control conditions (0 $\mu\text{g}/\text{mL}$ LATA), in response to varying concentrations of LATA. Percent membrane integrity was significantly higher at LATA concentrations of 0.5, 2.0, and 3.0 $\mu\text{g}/\text{mL}$ ($p<0.05$). **b)** Cell counts over a 10 second period, expressed as percent relative to control conditions (0 $\mu\text{g}/\text{mL}$ LATA), after incubation in the presence of different concentrations of LATA. Cell counts were significantly increased at LATA levels of 0.2 $\mu\text{g}/\text{mL}$ or higher ($p<0.05$). **c)** Representative flow cytometry dot plot of mouse embryonic stem cells showing forward scatter (x-axis) and side scatter (y-axis). Quadrant IV depicts the population of mostly membrane-intact, single mESCs. Quadrant III depicts mostly clusters of two or more, mostly membrane-intact, mESCs. **d)** Quadrant III cell counts over a 10 second period, expressed as percent relative to control (0 $\mu\text{g}/\text{mL}$ LATA), in the presence of different concentrations of LATA. Cell counts were significantly decreased at LATA levels of 0.1 $\mu\text{g}/\text{mL}$ or higher ($p<0.05$), likely due to dissociation of cell clusters into single cells, resulting in increased counts of membrane-intact, single mESCs. Different superscripts indicate statistically different values ($p<0.05$) for each panel.

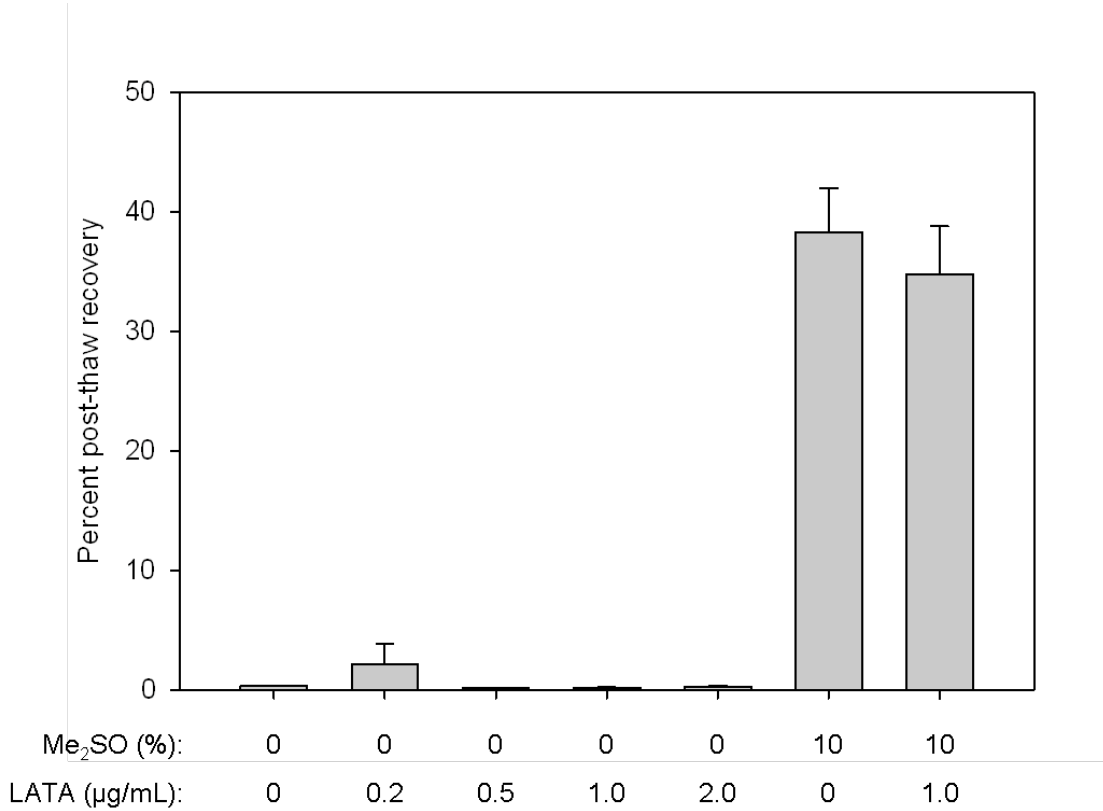


Figure 5.6. The presence or absence of LATA had no significant effect on the post-thaw recovery of mESCs in the presence or absence of 10% Me₂SO. Mouse ESCs were separated from feeders and cultured for one hour in the present or absence of different concentrations of LATA, and subsequently cryopreserved with the same concentration of LATA in the presence or absence of 10% dimethyl sulfoxide (Me₂SO) as indicated above. Percent post-thaw recovery in the presence of 10% Me₂SO was significantly higher ($p<0.05$) than that in the absence of Me₂SO, but there was no significant difference in percent post-thaw recovery of LATA-treated cells in the presence of 10% Me₂SO (v/v).

The effects of Latrunculin A on post-thaw recovery of mESCs

The presence or absence of LATA had no significant effect on the post-thaw recovery of mESCs in the presence or absence of 10% Me₂SO. In the absence of Me₂SO and LATA, percent post-thaw recovery was 0.3 ± 0.04%, a value not significantly different from percent post-thaw recovery in the absence of Me₂SO and presence of 0.2, 0.5, 1.0, or 2.0 µg/mL LATA, where percent post-thaw recovery was 2.1 ± 1.8%, 0.2 ± 0.02%, 0.2 ± 0.04%, and 0.3 ± 0.06%, respectively (Figure 5.6). Percent post-thaw recovery was 38.3 ± 3.7% in the presence of 10% Me₂SO and absence of LATA, which was significantly different ($p<0.05$) from percent post-thaw recovery of mESCs in the absence of Me₂SO, but did not differ significantly from the post-thaw recovery of 34.8 ± 4.0% of cells cryopreserved in the presence of 10% Me₂SO and 1µg/mL LATA (Figure 5.6).

The effect of CPA, temperature, and Latrunculin A on mESC osmotic response

a. V_{iso} is decreased at -3°C, with LATA treatment, or in the presence of Me₂SO

There were main effects of temperature, CPA and treatment with 1 µM LATA, and on V_{iso} ($p<0.05$). Isosmotic cell volume decreased in the presence of 1.5 M Me₂SO, with LATA treatment, or at low temperatures. The largest V_{iso} (644 ± 16 µm³) was measured in control cells (no LATA treatment) at 22°C in the absence of CPA. With

either LATA treatment or in the presence of Me₂SO at 22°C, V_{iso} was significantly decreased ($p<0.05$) ($576 \pm 23 \mu\text{m}^3$ and $572 \pm 18 \mu\text{m}^3$, respectively). With both LATA treatment and the presence of Me₂SO at 22°C, V_{iso} further decreased significantly ($p<0.05$) to $513 \pm 21 \mu\text{m}^3$. This value was not significantly different from V_{iso} of control cells at -3°C in the presence of Me₂SO ($469 \pm 9 \mu\text{m}^3$). Isosmotic cell volume was lowest in control cells in the presence of Me₂SO at -3°C ($363 \pm 7 \mu\text{m}^3$). Please refer to Table 5.1 for a summary of V_{iso} corresponding to different treatments.

Table 5.1. Isosmotic cell volumes (V_{iso}) of 0 and 1.0 μM Latrunculin A (LATA)-treated mouse embryonic stem cells in the presence or absence of 1.5 M dimethyl sulfoxide (Me₂SO) at 22°C and -3°C.

Temperature	1.5 M Me ₂ SO	1 μM LATA	$V_{\text{iso}} (\mu\text{m}^3)$
22°C	-	-	$644 \pm 16^{\text{a}}$
22°C	-	+	$576 \pm 23^{\text{b}}$
22°C	+	-	$572 \pm 18^{\text{b}}$
22°C	+	+	$513 \pm 21^{\text{c}}$
-3°C	+	-	$469 \pm 9^{\text{c}}$
-3°C	+	+	$363 \pm 7^{\text{d}}$

Isosmotic cell volume is expressed as mean ± SEM (μm^3). Different superscripts indicate significantly different values ($p<0.05$). N.B.: volumes displayed are not adjusted for the presence of Me₂SO, which would account for $\leq 1.5\%$ of cell volume even with V_b values as low as 30% (of isosmotic volume).

b. At room temperature, LATA treatment significantly lowers adjusted V_b

The effects of LATA, temperature, and CPA on V_b are shown in Table 5.2. There was a significant main effect of CPA, where V_b in the presence of 1.5 M Me₂SO was significantly higher ($p<0.05$), and a significant main effect of temperature, where V_b was significantly higher at -3°C ($p<0.05$). There was also a significant interaction between temperature, CPA, and treatment with 1 μM LATA on V_b ($p<0.05$). The V_b of control cells in the presence of 1.5 M Me₂SO at -3°C was significantly higher than the V_b of all

additional treatments ($p<0.05$) except for that of LATA-treated cells in the presence of 1.5 M Me_2SO measured at 22°C (Table 5.2).

When these values were adjusted for relative V_{iso} , CPA and temperature were no longer significant main effects, however there was a significant main effect of treatment with LATA and a significant interaction between temperature and LATA ($p<0.05$). Overall, the adjusted V_b of LATA-treated cells was significantly lower than the V_b of control cells. However, an analysis of the interaction of LATA and temperature revealed that at 22°C, LATA-treated cells had significantly greater V_b than control cells, while at -3°C, LATA-treated cells had significantly lower V_b than control cells ($p<0.05$). The V_b of control cells in the presence of 1.5 M Me_2SO at -3°C was significantly higher than the V_b of control cells (0 μM LATA, 0 Me_2SO , 22°C) and of LATA-treated cells in the presence of 1.5 M Me_2SO at -3°C ($p<0.05$) (Table 5.2).

Table 5.2. Osmotically inactive cell volume (V_b) of 0 and 1.0 μM Latrunculin A (LATA)-treated mouse embryonic stem cells in the presence or absence of 1.5 M dimethyl sulfoxide (Me_2SO) at 22°C and -3°C.

Temperature	1.5 M Me_2SO	1 μM LATA	$V_b \pm \text{SEM} (\%)$	Adjusted $V_b \pm \text{SEM} (\%)$
22°C	-	-	38.7 ± 1.6 ^a	38.7 ± 1.6 ^a
22°C	-	+	47.4 ± 4.8 ^a	42.4 ± 4.3 ^{a,b}
22°C	+	-	50.1 ± 2.8 ^a	46.9 ± 2.4 ^{a,b}
22°C	+	+	60.3 ± 6.1 ^{a,b}	48.0 ± 4.9 ^{a,b}
-3°C	+	-	83.8 ± 8.6 ^b	61.0 ± 6.2 ^b
-3°C	+	+	54.1 ± 13.2 ^a	30.5 ± 7.5 ^a

V_b is expressed as mean percent of isosmotic cell volume (V_{iso}) ± SEM. The far right column lists V_b after adjusting values for the ratio of treatment-specific V_{iso} to that of the control V_{iso} (0 M Me_2SO , 0 μM LATA, 22°C). Superscripts indicate statistically significant differences of values within each column ($p<0.05$).

The effect of CPA, temperature, and Latrunculin A on permeability parameters

a. Treatment of cells with LATA significantly affects L_p

In comparisons of L_p of 1 μM LATA-treated and untreated control cells at 22°C and -3°C, there was a significant main effect of LATA treatment, in which treatment with LATA resulted in significantly lower L_p values ($p<0.05$). There was also a significant main effect of the interaction of LATA treatment and temperature ($p<0.05$). At 22°C, L_p of LATA-treated cells was significantly lower than that of control cells ($p<0.05$). At -3°C there was no significant difference between L_p values. Please refer to Table 5.3 for a list of L_p values at 22°C and -3°C.

Table 5.3. The effect of treatment with 1 μM Latrunculin A (LATA) on the hydraulic conductivity (L_p) and permeability of cryoprotectant (P_{CPA}) of C57BL/6 mouse embryonic stem cells at 22°C and -3°C.

T (°C)	1 μM LATA	V_{iso} (μm^3)	V_b (%)	L_p ($\mu\text{m}/\text{min}/\text{atm}$)	P_{CPA} ($\mu\text{m}/\text{min}$)
22	-	644	38.7	$0.29 \pm 0.01^{\text{a}}$	2.81 ± 0.27
22	+	576	47.4	$0.20 \pm 0.02^{\text{b}}$	3.26 ± 0.27
-3	-	644	38.7	$0.024 \pm 0.001^{\text{c}}$	0.63 ± 0.10
-3	+	576	47.4	$0.021 \pm 0.001^{\text{c}}$	0.68 ± 0.18

An electronic particle counter was used to track the volume changes of LATA-treated and untreated cells as they were abruptly exposed to 1.5 M dimethyl sulfoxide at indicated temperatures (T). For curve-fitting, isosmotic cell volume (V_{iso}) and osmotically inactive cell volume (V_b) were matched according to LATA treatment or non-treatment, and had been calculated in LATA-treated or untreated cells at room temperature in the absence of cryoprotectant. Superscripts indicate significantly different L_p values ($p<0.05$) at each temperature. There were no significant differences among P_{CPA} values at either temperature.

b. LATA treatment did not significantly affect P_{CPA}

There was no significant effect of LATA-treatment on P_{CPA} . Please refer to Table 5.3 for a list of P_{CPA} values at 22°C and -3°C.

Discussion

One aim of this study was to investigate the mechanisms associated with discrepant extrapolated and observed V_b values of the C57BL/6 mESC line. A second aim was to identify whether controlled cytoskeleton disruption by reversible methods such as Latrunculin A could contribute to improved cryopreservation methods of mESC, either by directly preventing cytoskeleton-associated cell stress during cell cooling and warming, or by improving the accuracy of sub-zero measurement of V_b and permeability parameters by enabling uniform, spherical cell shrinkage during cryomicroscopy. For the latter purpose, it was necessary to show that the use of LATA does not alter cell osmotic response and permeability parameters.

The concentration of LATA required for F-actin depolymerization varies per cell type, reportedly from 0.1-0.2 $\mu\text{g/mL}$ (0.2-0.4 μM) in mouse neuroblastoma cells and hamster fibroblasts [7], to 6.25 μM in human ESCs [24]. A concentration of 1 μM has been used with mouse oocytes [8]. After 1 hour incubation of C57BL/6 mESC with 1.0 μM (0.5 $\mu\text{g/mL}$) LATA, most actin filaments disappeared and cell boundaries were difficult to discern on fluorescent microscopy. At this concentration, most colonies remained intact and fixed to coverslips, although there was distinct rounding of cells and fragmenting of colony edges by the separation of individual cells from the colony mass. Effects of LATA were evident at lower concentrations, but the change between 0.2 and 0.5 $\mu\text{g/mL}$ was dramatic. At higher concentrations, particularly at LATA concentrations of 2 and 3 $\mu\text{g/mL}$, colonies were more infrequent per high-powered field and markedly reduced in size as cells lifted off the coverslips and were lost into culture media. Thus, at

these concentrations, the effect of LATA was difficult to fully interpret as most of the cells affected were no longer present, and the few remaining in colonies possibly received less exposure due to being deep within colonies or possibly were otherwise more resistant to LATA for unknown reasons. Experiments were originally conducted on mESCs in single cell suspension; however the numerous washes and thus centrifugation steps involved with F-actin staining of the single cell suspension resulted in very low yields of stained cells, therefore staining of fixed colonies on coverslips was more practical.

Latrunculin A showed no detrimental effects in terms of cell quantity or membrane integrity at all concentrations studied. In fact, with all LATA treatments, cell numbers were actually significantly higher, as was percent membrane integrity, relative to controls. The observed quantitative increase seemed to originate in Quadrant III of the flow cytometry FSC/SSC dot plot (Figure 5.4c), a region representing cell aggregates or cells that were approximately double or more the average cell size in the single cell population of interest (which were located in the Quadrant IV, Figure 5.4c). This population existed despite cell suspensions being filtered through a 40 μ mesh prior to incubation with or without LATA. The event count in this region decreased significantly while the event count in the gated population representing single-celled mESCs increased significantly.

Hosu *et al.* [8] studied the effects of LATA-mediated F-actin depolymerization on the survival rate of cryopreserved mouse oocytes and found that survival rate was significantly enhanced when oocytes were incubated with 1 μ M LATA for 45 minutes at 37°C. Similarly, unpublished data revealed that incubation of Chinese Hamster Ovary (CHO) cells with 2 μ M LATA prior to cryopreservation resulted in a post-thaw survival

rate, in the absence of CPA, which was at least as high as survival in the presence of 1.5 M Me₂SO alone. The rationale presented by Hosu *et al.* [8] was that an organized, interconnected F-actin polymer mesh is irreversibly subject to damage during cryopreservation, either through the imposition of intracellular ice crystals on the actin mesh, or through mechanical stress exerted by the plasma membrane on the actin cytoskeleton during osmotic shrinking or swelling. G-actin monomer suspensions do not form organized networks within the cell and thus in theory would not be affected by the stresses of cryopreservation in the same manner or extent. Therefore, dismantling the cytoskeleton in a reversible, orderly manner prior to cryopreservation would prevent damage to the cytoskeletal network and result in improved post-thaw recovery.

Our studies demonstrated no improvements in PTR when mESCs were incubated with LATA prior to cryopreservation. From these results, it can be interpreted that the cytoskeleton is unlikely to be a factor that decreases post-thaw recovery of C57BL/6 mESC. It might be that the mESC cytoskeleton is less rigidly anchored to the plasma membrane, as compared to the relatively strong interaction between these structures that is postulated for mouse oocytes [8] and spermatozoa [25], and this could contribute to the relatively wide range of osmotic tolerance limits displayed by C57BL/6 mESC and perhaps their relatively high post-thaw recovery rate, as compared to oocytes and spermatozoa, under standard freezing protocols (10% Me₂SO, 1°C/minute cooling rate, -80°C plunge temperature).

Both V_{iso} and V_b changed with ambient conditions. Isosmotic cell volume was significantly decreased by lower temperature, the presence of 1.5 M Me₂SO, and treatment with LATA. CPA and temperature significantly affected apparent values of V_b ,

while adjusted V_b revealed significant effects of LATA treatment. The precise mechanisms behind these phenomena are unknown and are likely complex. Changes to the dynamics and structure of the cell membrane and organelles could be induced by all three factors.

Osmotically inactive cell volume is generally assumed to be constant for any given cell type, even under conditions that may differ from those under which it was determined [21]. However, the Boyle Van't Hoff equation used to derive V_b assumes that the cell contents form a thermodynamically ideal, dilute solution [26], and the actual intracellular environment, particularly in the presence of CPA and experiencing intracellular dehydration due to extracellular ice formation during cryopreservation, is not an ideal solute and therefore interpretations of V_b must be made with caution [26]. Armitage and Juss (1996) [21] examined the effects of permeating CPAs on the V_b of rabbit corneal keratinocytes and concluded that while the cells behaved as osmometers under all studied conditions, there was no evidence to suggest that Me₂SO or 1,2-propanediol altered V_b . A previous study by Hempling and White (1984) [27] reported that Me₂SO affected the apparent V_b of rat megakaryocytopoietic cells. Connolly and Hempling (1985) [28] subsequently reported that the effect of Me₂SO on V_b was dependent on temperature, where at 4°C, V_b was only slightly increased, however at 36°C, V_b decreased by 10%. The earlier studies involving rat megakaryocytopoietic cells are similar to our current findings, where the apparent V_b of the C57BL/6 mESCs was significantly increased in the presence of 1.5 M Me₂SO and at -3°C. However, as stated before, when values were adjusted for V_{iso} in corresponding conditions relative to the control isosmotic cell volume (at conditions of 0 M Me₂SO, 0 μM LATA, 22°C), the

main effects of CPA and temperature were no longer significant. That being said, the 22.3% increase in adjusted V_b in the presence of 1.5 M Me₂SO at -3°C remained significant when compared to control V_b , while the increase in adjusted V_b in the presence of 1.5 M Me₂SO at 22°C was not significant.

Hempling and White [27] inferred that Me₂SO had altered the state of intracellular free water (the solvent volume). Our initial interpretation was that the water-binding properties of Me₂SO affect the solvent volume. The binding of water by Me₂SO would have the effect of concentrating the intracellular environment. In isosmotic conditions, the water volume should equilibrate such that, as is generally the assumption, V_{iso} is actually slightly larger than in the absence of Me₂SO (although in fact, our data shows the opposite to be true, where V_{iso} is 10% lower in the presence of 1.5 M Me₂SO). However, in hyperosmotic conditions, the smaller V_w (due to binding properties of Me₂SO) has the effect of decreasing the amount of water required to exit the cell to balance osmotic forces, hence the cell does not shrink as much. This would lower the slope of a Boyle Van't Hoff plot, and extrapolation to infinite osmolality would yield a larger V_b .

With regards to the previous studies on Me₂SO effects on V_b , Armitage and Juss [21] argued that the initial efflux of water induced by the extracellular hypertonic salt concentration would concentrate the intracellular Me₂SO as well as the intracellular electrolytes and that if inadequate time was allowed for Me₂SO equilibration, less cell shrinkage would occur than in the absence of Me₂SO. Indeed, we allowed a minimum of 5 minutes of equilibration time after the addition of cells to anisosmotic solutions containing 1.5 M Me₂SO, at which point the error in volume measurement induced by

equilibration factors would have been approximately 7.4% at 1200 mOsm, 16% at 900 mOsm, and 19% at 600 mOsm, so in this regard, the effects of 1.5 M Me₂SO on V_b at -3°C are likely explained by this (Figure 5.7). Additionally, this extrapolated V_b does not seem to emulate real conditions, since in kinetic studies at -3°C in the presence of 1.5 M Me₂SO, cells were observed to shrink to minimal volumes much lower than the extrapolated V_b .

However, the significantly decreased V_{iso} values in the presence of 1.5 M Me₂SO at both 22 and -3°C support the hypothesis that there is a real effect of Me₂SO on the osmotic response of C57BL/6 mESC, as this CPA-concentrating effect proposed by Armitage and Juss [21] would not occur in isosmotic solution. Additional studies are necessary to determine the mechanism regulating this effect, which also occurred in LATA-treated cells in the absence of Me₂SO as well as at low temperatures, and was exaggerated in the presence of multiple factors (*i.e.* V_{iso} was decreased the most in LATA-treated cells in the presence of 1 M Me₂SO at -3°C). Importantly, the changes that occur in V_{iso} as it equilibrates with Me₂SO have implications for the accuracy of modeling using the two parameter mass transport model, as this model is dependent upon the surface area to volume ratio of the cell. Using the V_{iso} and V_b values estimated at 22°C (Table 5.2), the surface area to volume ratios ranged from 0.91 to 1.67. These numbers are different enough to warrant a future study on the sensitivity of fits to parameters.

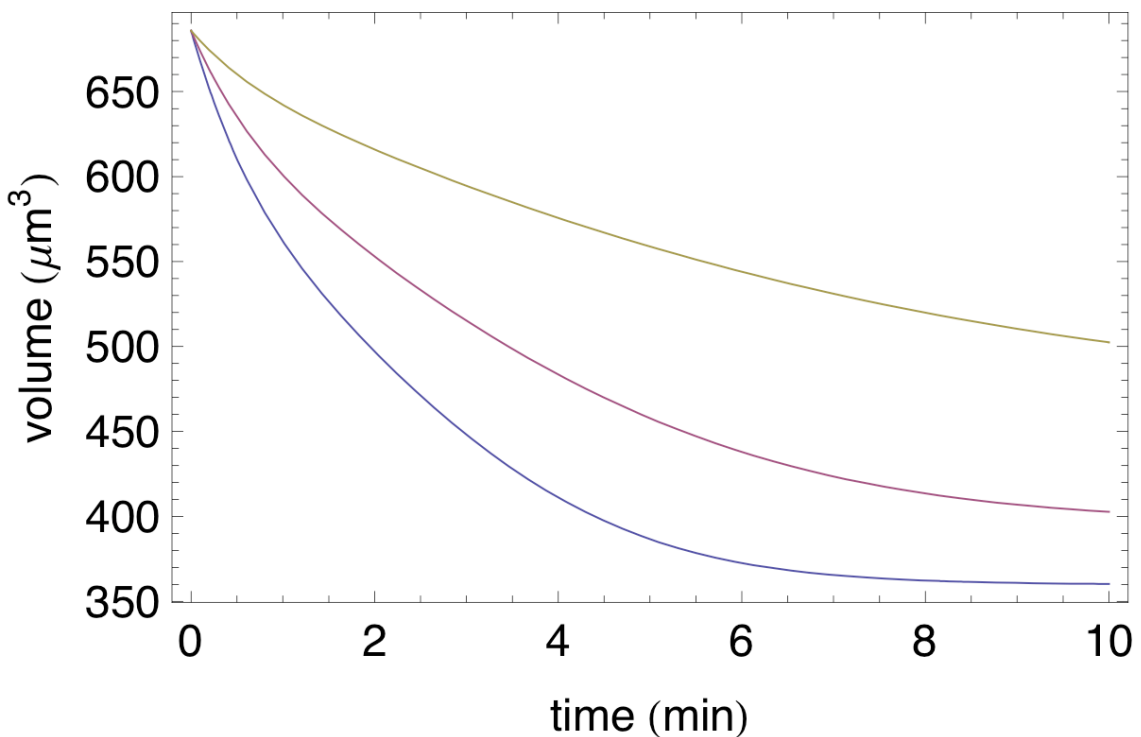


Figure 5.7. Using mean values for -3°C hydraulic conductivity and solute permeability, a plot of the predicted volume response of cells, equilibrated with 1.5 M Me₂SO and exposed to three different osmolalities of PBS, indicates that after 5 minutes equilibration time, the error in volume calculation should be approximately 7.5% in 1200 mOsm Me₂SO, 16% in 900 mOsm Me₂SO, and 19% in 600 mOsm Me₂SO. Yellow line, volume response at 600 mOsm; red line, volume response at 900 mOsm; blue line, osmotic response at 1200 mOsm.

Interestingly, the same phenomenon of increased V_b in the presence of Me₂SO did not occur in LATA-treated cells at -3°C. Since equal equilibration time was allowed for both treatments, the significant difference between LATA-treated and control cells at -3°C suggests that treatment of cells with 1 μM LATA altered their permeability parameters or at least some aspect of their osmotic response in the presence of 1.5 M Me₂SO relative to untreated control cells, and this is an argument against the use of LATA in subzero permeability measurement utilizing cryomicroscopy. As such, when we examined the effects of LATA on L_p and P_{CPA} at 22°C and -3°C, we found that L_p in the presence of 1.5 M Me₂SO was significantly decreased at 22°C relative to control cells in the same conditions. The altered L_p as well as V_{iso} effects invite further study into the cryoprotective mechanisms of LATA that have been observed in other cell types. Additionally, the significant effect of LATA on adjusted V_b values and on L_p is evidence that LATA is inappropriate for use in fundamental cryobiological studies using cryomicroscopy to determine subzero permeabilities of C57BL/6 mESCs. Elucidation of the mechanisms by which LATA treatment significantly decreases adjusted V_b at -3°C, but significantly increases V_b at 22°C requires additional investigation. One possible mechanism could be that removing the interaction of the plasma membrane with the cytoskeleton results in altered membrane function and subsequent altered osmotic response and permeability values. A report by Noiles *et al.* (1997) showed a strong dependence of L_p and its activation energy upon the interaction of the plasma membrane with the mouse spermatozoan cytoskeleton [25], and perhaps these effects extend to the cellular osmotic response and corresponding V_b . Alternatively, actin filaments determine the shape of the cell's surface [29]. It could be possible that LATA-induced

depolymerization of mESC influences membrane shape to either induce or prevent artifacts in the measurement of cell volume using the electronic particle counter.

Finally, it is not surprising that temperature significantly influenced V_{iso} and that it had a significant effect on apparent V_b as well as interactive effect with Me₂SO (apparent V_b) and LATA (adjusted V_b). Tissues, as with materials in general, progressively shrink as they are cooled from physiologic temperatures to lower temperatures [30], and cell shrinkage would be expected to occur as well. Membrane fluidity decreases at low temperatures, where hydrated phospholipid bilayers exist as highly ordered gels with only slight torsional mobility and tightly packed acyl chains [31]. The temperature at which the membrane reversibly changes from fluid to gel, the phase transition temperature, is dependent upon the phospholipid composition of the membrane [31], which varies with cell type and species. Plasma membrane phase transition has been demonstrated to have significant effects on permeability parameters of cells and it is possible that the influence may extend to V_b as well. Additionally, temperature-dependent phase separation of membrane phospholipids into domains influences the distribution of membrane proteins, which can contribute to 40% by weight of intra- and extra-cellular membranes and are usually present in the liquid-crystalline lipid but are excluded from the gel phase [31]. This segregation of proteins can affect the function of the membrane [31]. Temperature also affects protein configuration [32], and perhaps this alters the ratio of up to 10% bound water [26] that exists within a cell and contributes to V_b .

In summary, from the V_{iso} values and the adjusted V_b obtained here, we can glean the following information: first, that treatment of cells with 1 μM LATA alters the cell response such that there is no significant difference with respect to the V_b of untreated

control cells in the presence of 1 M Me₂SO, even at -3°C. Since LATA treatment also induced significant changes in cell permeability parameters, and the mechanism behind the changes in osmotic response in the presence of Me₂SO is unknown, we recommend against the use of LATA in subzero permeability studies, at least for the C57BL/6 mESC line.

Secondly, there is an effect of Me₂SO, LATA, and temperature on V_{iso} , and a main effect of LATA treatment on adjusted V_b . These observed phenomena play a significant role in the assumptions of fundamental cryobiology. Isosmotic cell volume is essential to calculations of surface area to volume ratio in the two parameter mass transport model for determining L_p and P_{CPA} [23]. If V_{iso} is not a static value, then to be accurate, the model should be modified to account for this phenomenon. Accordingly, knowledge of V_b , as it translates into V_w , is also essential for determining permeability parameters using the two parameter mass transport model [23]. The effects on V_b of any pre-treatment of cells, such as LATA-induced cytoskeletal depolymerization or, for example, the addition of intracellular trehalose, a chemical known for its membrane stabilizing properties [33], probably through the replacement of water in hydrogen bonds [34], the trapping of essential hydration water molecules [35], and possibly its role in viscosity [36], should be determined prior to application of the two parameter model, as these treatments have the potential to significantly change V_b and act as a source of error in modeling cell responses during cryopreservation.

Finally, modeling of cell equilibration volumes at -3°C (Figure 5.7) revealed that significant differences in measurements of apparent V_b at -3°C in the presence of 1.5 M Me₂SO were likely due to inadequate equilibration times afforded to C57BL/6 mESCs at

these temperatures. Future studies will be conducted in order to verify whether V_b is significantly affected by CPA at subzero temperatures using adequate equilibration time either through the exposure of CPA-equilibrated cells to salts and room temperature with progressive cooling to -3°C, or through the method previously outlined, in which CPA-equilibrated cells were abruptly exposed to hyperosmotic solutions at -3°C. However, in this case we will increase the equilibration time at -3°C as necessary.

References

1. Kleinhans, F.W. and P. Mazur, *Determination of the water permeability (L_p) of mouse oocytes at -25 degrees C and its activation energy at subzero temperatures*. Cryobiology, 2009. **58**(2): p. 215-24.
2. Agca, Y., et al., *Temperature-dependent osmotic behavior of germinal vesicle and metaphase II stage bovine oocytes in the presence of Me₂SO in relationship to cryobiology*. Mol Reprod Dev, 1999. **53**(1): p. 59-67.
3. Liu, J., et al., *The determination of membrane permeability coefficients of canine pancreatic islet cells and their application to islet cryopreservation*. Cryobiology, 1997. **35**(1): p. 1-13.
4. Verkman, A.S., *Water permeability measurement in living cells and complex tissues*. J Membr Biol, 2000. **173**(2): p. 73-87.
5. Kashuba Benson, C.M., J.D. Benson, and J.K. Critser, *An improved cryopreservation method for a mouse embryonic stem cell line*. Cryobiology, 2008. **56**(2): p. 120-30.
6. Spector, I., et al., *Latrunculins: novel marine toxins that disrupt microfilament organization in cultured cells*. Science, 1983. **219**(4584): p. 493-5.
7. Spector, I., et al., *Latrunculins--novel marine macrolides that disrupt microfilament organization and affect cell growth: I. Comparison with cytochalasin D*. Cell Motil Cytoskeleton, 1989. **13**(3): p. 127-44.

8. Hosu, B.G., et al., *Reversible disassembly of the actin cytoskeleton improves the survival rate and developmental competence of cryopreserved mouse oocytes*. PLoS One, 2008. **3**(7): p. e2787.
9. Liu, X., et al., *Trisomy eight in ES cells is a common potential problem in gene targeting and interferes with germ line transmission*. Dev Dyn, 1997. **209**(1): p. 85-91.
10. Sugawara, A., et al., *Current status of chromosomal abnormalities in mouse embryonic stem cell lines used in Japan*. Comp Med, 2006. **56**(1): p. 31-4.
11. Doetschman, T., *Gene Targeting in Embryonic Stem Cells: I. History and Methodology*, in *Transgenic Animal Technology: A Laboratory Handbook, Second Edition*, C.A. Pinkert, Editor. 2002, Academic Press: San Diego.
12. Gordeeva, O.F., et al., *[Expression of regulatory genes Oct-4, Pax-6, Prox-1, Ptx-2 at the initial stages of differentiation of embryonic stem cells in vitro]*. Ontogenet, 2003. **34**(3): p. 174-82.
13. *Preparation of ES Cells for Injection*, in *Manipulating the Mouse Embryo: A Laboratory Manual*, A. Nagy, et al., Editors. 2003, Cold Spring Harbor Laboratory Press: Cold Spring Harbor, New York. p. 469.
14. Schenke-Layland, K., et al., *Collagen IV induces trophoectoderm differentiation of mouse embryonic stem cells*. Stem Cells, 2007. **25**(6): p. 1529-38.
15. Benson, J.D., et al., *Mercury free operation of the Coulter counter MultiSizer II sampling stand*. Cryobiology, 2005. **51**(3): p. 344-7.
16. McGann, L.E., A.R. Turner, and J.M. Turc, *Microcomputer interface for rapid measurements of average volume using an electronic particle counter*. Med Biol Eng Comput, 1982. **20**(1): p. 117-20.
17. Benson, C.T., et al., *Determination of the osmotic characteristics of hamster pancreatic islets and isolated pancreatic islet cells*. Cell Transplant, 1993. **2**(6): p. 461-5.
18. Fedorow, C., et al., *Osmotic and cryoprotectant permeation characteristics of islet cells isolated from the newborn pig pancreas*. Cell Transplant, 2001. **10**(7): p. 651-9.

19. Phelps, M.J., et al., *Effects of Percoll separation, cryoprotective agents, and temperature on plasma membrane permeability characteristics of murine spermatozoa and their relevance to cryopreservation*. Biol Reprod, 1999. **61**(4): p. 1031-41.
20. Ebertz, S.L. and L.E. McGann, *Cryoprotectant permeability parameters for cells used in a bioengineered human corneal equivalent and applications for cryopreservation*. Cryobiology, 2004. **49**(2): p. 169-80.
21. Armitage, W.J. and B.K. Juss, *Osmotic response of mammalian cells: effects of permeating cryoprotectants on nonsolvent volume*. J Cell Physiol, 1996. **168**(3): p. 532-38.
22. Nobel, P.S., *The Boyle-Van't Hoff relation*. Journal of Theoretical Biology, 1969. **23**(3): p. 375-9.
23. Katkov, II, *A two-parameter model of cell membrane permeability for multisolute systems*. Cryobiology, 2000. **40**(1): p. 64-83.
24. Gerecht, S., et al., *The effect of actin disrupting agents on contact guidance of human embryonic stem cells*. Biomaterials, 2007. **28**(28): p. 4068-77.
25. Noiles, E.E., K.A. Thompson, and B.T. Storey, *Water permeability, L_p , of the mouse sperm plasma membrane and its activation energy are strongly dependent on interaction of the plasma membrane with the sperm cytoskeleton*. Cryobiology, 1997. **35**(1): p. 79-92.
26. Muldrew, K., et al., *The Water to Ice Transition: Implications for Living Cells*, in *Life in the Frozen State*, B.J. Fuller, N. Lane, and E.E. Benson, Editors. 2004, CRC Press LLC: Boca Raton, Florida. p. 67-108.
27. Hempling, H.G. and S. White, *Permeability of cultured megakaryocytopoietic cells of the rat to dimethyl sulfoxide*. Cryobiology, 1984. **21**(2): p. 133-43.
28. Connolly, A. and H.G. Hempling, *The effects of dimethyl sulfoxide on the osmotic properties of a rat megakaryocytopoietic cell line*. Cryobiology, 1985. **22**(4): p. 351-8.
29. *Molecular Biology of the Cell*. 4 ed, ed. B. Alberts, et al. 2002, New York, NY: Garland Science, Taylor & Francis Group. 1616.
30. Taylor, M.J., Y.C. Song, and K.G.M. Brockbank, *Vitrification in Tissue Preservation: New Developments*, in *Life in the Frozen State*, B.J. Fuller, N. Lane, and E.E. Benson, Editors. 2004, CRC Press: New York, NY. p. 672.

31. Wahle, K.W., *Fatty acid modification and membrane lipids*. Proc Nutr Soc, 1983. **42**(2): p. 273-87.
32. Somero, G.N., *Proteins and temperature*. Annu Rev Physiol, 1995. **57**: p. 43-68.
33. Gutierrez-Perez, O., et al., *Boar spermatozoa cryopreservation in low glycerol/trehalose enriched freezing media improves cellular integrity*. Cryobiology, 2009. **58**(3): p. 287-92.
34. Eroglu, A., M. Toner, and T.L. Toth, *Beneficial effect of microinjected trehalose on the cryosurvival of human oocytes*. Fertil Steril, 2002. **77**(1): p. 152-8.
35. Patist, A. and H. Zoerb, *Preservation mechanisms of trehalose in food and biosystems*. Colloids Surf B Biointerfaces, 2005. **40**(2): p. 107-13.
36. Sampedro, J.G. and S. Uribe, *Trehalose-enzyme interactions result in structure stabilization and activity inhibition. The role of viscosity*. Mol Cell Biochem, 2004. **256-257**(1-2): p. 319-27.

CHAPTER 6

GENERAL DISCUSSION AND FUTURE DIRECTIONS

Overview

The research in this dissertation explored the fundamental cryobiology of mouse embryonic stem cells (mESCs) in order to establish improved approaches to cryopreservation, especially for banking purposes. We determined the fundamental cryobiological parameters, including osmotic tolerance limits (OTL) with respect to membrane integrity, osmotically inactive cell volume (V_b), hydraulic conductivity (L_p), and permeability of cryoprotectant (P_{CPA}) as well as temperature dependence of L_p and P_{CPA} ($E_a^{L_p}$, $E_a^{P_{CPA}}$) for the C57BL/6, BALB/c, CBA, FVB, and 129R1 mESC lines, predicted optimal cooling rates and plunge temperatures for all five lines, and conducted experimental validation for experimental protocols that resulted in significantly improved post-thaw recovery for each line. Finally, we worked to improve existing methods of modeling by examining the effects of CPA, temperature, and Latrunculin A (LATA) on mESC osmotic response and permeability parameters.

A method for the systematic characterization of fundamental cryobiological parameters of mESC lines to create cryopreservation protocols for improved post-thaw recovery

In the first phase of this research, outlined in Chapter 2, an approach was established for optimizing mESC cryopreservation protocols that could be applied to different mESC lines in a relatively high throughput fashion, relying strictly on cell membrane integrity as an indicator for post-thaw recovery and for osmotic tolerance, to efficiently generate useful information for predicting optimal cooling rates and plunge temperatures for cell lines from widely differing genetic backgrounds that one encounters in a banking situation such as the Mutant Mouse Regional Resource Center (MMRRC) mESC repository (<http://www.mmrrc.org>). This method, based on principles of the Boyle-Van't Hoff relation [1], the Arrhenius relation [2], a two parameter mass transport model [3][4], and Mazur's two factor hypothesis [5], was successfully applied to the C57BL/6 mESC line, with a resulting two-fold improvement in percent post-thaw recovery (PTR) from a protocol utilizing both the predicted optimal cooling rate and predicted optimal plunge temperature for 1 M 1,2-propanediol (PG).

A comparative study of the fundamental cryobiology of four mESC lines

The next phase, outlined in Chapter 3, was to apply this method to four additional mESC lines (BALB/c, CBA, FVB, and 129R1 mESC lines) of different genetic backgrounds in a comparative fundamental cryobiological study. To confirm anecdotal reports and the trend observed with published values [6][7] (personal communication, Deanna Nielsen, Stem Cell Technologies technical support, 2004; personal communication, Xin Yu, University of California-Davis, 2004) suggesting wide variation in mESC PTR across different genetic backgrounds, the standard cryopreservation method (1.0 M dimethyl sulfoxide (Me₂SO), a 1°C/minute cooling rate to -80°C, plunge into liquid nitrogen, then warming in a 37°C water bath) was applied to all four mESC lines. As expected, post-thaw recovery under these conditions significantly differed by genetic background. We then analyzed how fundamental cryobiological parameters differ from one mESC line to the next, and how this information translated into predicted optimal cooling rates and plunge temperatures across cell lines. Osmotic tolerance limits differed significantly among mESC lines at both upper and lower limits as well as by range of OTL. However, these differences were not great enough to warrant changing the standard cryopreservation media CPA concentration of 10% (roughly 1 M), for any individual line as the addition of 1 M CPA, especially drop-wise, should not have a damaging effect. Our research also determined that genetic background significantly influenced V_b , permeability parameters, and E_a , and there were significant effects of CPA (Me₂SO, PG, ethylene glycol (EG), and glycerol) on permeability parameters and $E_a^{P_{CPA}}$.

Taken together, these significant differences suggested that a “one-size fits all” protocol would not be applicable to mESC lines of different genetic backgrounds.

A comparison of predicted optimal cooling rates and plunge temperatures across four mESC lines and empirical validation of predicted optima

With these data in hand, we subsequently (Chapter 4) defined optimal cooling rates, warming rate, and plunge temperatures for use in a two-step freezing protocol by conducting theoretical simulations based on Mazur’s two factor hypothesis [5]. Across the four mESC lines, predicted optimal cooling rates ranged from 1.1 to 1.9°C/minute for 1.0 M EG, 1.0 to 3.3°C/minute for 1.0 M PG, and 1.3 to 6.5°C/minute for 1.0 M Me₂SO, with predicted optimal plunge temperatures of -41°C (EG), -40 to -41°C (PG), and -32 to -33°C (Me₂SO). These predicted optima were empirically validated, as with the C57BL/6 mESC line. What emerged from these data and that of the previous C57BL/6 mESC study [7] is that with the exception of the CBA mESC line, a protocol utilizing 1 M PG, a cooling rate of 1°C/minute, and plunge temperature of -41°C, while not always the predicted optimal, would yield improved PTR relative to standard methods for most mESC lines. For the FVB line in particular, the improvement in PTR was considerable (a nearly five-fold improvement from the 3.6% PTR using the standard method).

Propylene glycol is currently used as a permeating CPA for human embryos and for oocytes of several mammalian species [8]. There are many studies examining its use

as a CPA, for example in human platelets [9][10], human pancreatic islets [11], and human placental/umbilical cord blood CD34+ cells [12]. Recently, it was studied for its effectiveness in vitrification of R1 mESCs, with the results indicating that vitrification at a low concentration (2 M) of intracellular cryoprotectants might be an effective approach for mESC cryopreservation [13]. One advantage that PG may have over Me₂SO in mESC cryopreservation protocols is that it is a more stable glass former, *i.e.* vitrifies more easily, than Me₂SO [14], and thus devitrification resulting in intracellular ice formation during either cooling or warming is less likely with PG than with Me₂SO.

It thus seems probable that this optimized protocol could be applied to all mESC lines to generate improved PTR relative to the current standard method. It was concluded that enough differences exist between mESC lines and enough mESC lines exist such that exceptions to this universal protocol will occur, and these exceptional lines can be approached on a case-by-case basis using similar methods to what we have described in this dissertation.

Investigating basic fundamental cryobiological assumptions in order to improve existing methods

The prior phases of this dissertation research indicated that current methods of fundamental cryobiology did not always accurately predict cell response to predicted optimal protocols. Since one source of error could be due to the extrapolation of suprazero measurements of permeability parameters and osmotic response to subzero

conditions, preliminary subzero measurements of permeability parameters were conducted for the C57BL/6 mESC line. From these studies, it was noted that the measured minimal volume achieved by mESCs was markedly lower than the extrapolated V_b value for the C57BL/6 mESC line. Accordingly, in the final phase of this dissertation, we decided to investigate key assumptions regarding the temperature independence and effects of 1 M Me₂SO on V_b and permeability parameters. We also wished to investigate the use of Latrunculin A (LATA), a reversible cytoskeleton disruptor, to avoid possible errors in measurement that could lead to the observed minimal volume discrepancy with the idea that Latrunculin A could potentially enable spherical shrinkage of cells by removing the restrictive interactions between the cell membrane and the cytoskeleton. LATA was also intriguing as it has been found to have a cryoprotective effect on at least two cell types: mouse oocytes [15] and Chinese Hamster Ovary cells (unpublished data). Prior to its use in subzero permeability studies, it was necessary to examine whether use of LATA directly altered permeability parameters and osmotic response of mESC, therefore LATA treatment was included in our experimental design in addition to temperature and CPA.

From the V_{iso} and adjusted V_b values we obtained, we concluded that treatment of cells with 1 μ M LATA altered the cell osmotic response in the presence of Me₂SO and significantly affected permeability parameters of C57BL/6 mESC and was therefore inappropriate for use in subzero permeability studies. Secondly, there was an effect of Me₂SO, LATA, and temperature on V_{iso} , and a main effect of LATA treatment on adjusted V_b , phenomena that have a significant role in the assumptions of the two parameter mass transport model for determining L_p and P_{CPA} [4].

Conclusion

The research projects described within this dissertation have provided significant advances with regards to mESC cryopreservation, and have raised important questions to be explored in future research as well. Fundamental cryobiological parameters for mESCs from five different inbred genetic backgrounds were determined, which allowed an analysis of how these parameters vary according to genetic background, and led to the construction of theoretically optimized cryopreservation protocols and the empirical validation of these protocols. Importantly, we accomplished our overall goal in defining a single protocol (utilizing 1.0 M PG, a cooling rate of 1°C/minute, plunge temperature of -41°C, and subsequent warming in a room temperature water bath) that significantly improves PTR of most mESC lines, and we present a straightforward method by which PTR of cell lines exceptional to this application can be systematically optimized. From our studies with LATA, we provided evidence that cytoskeletal damage is unlikely to be responsible for poor PTR, at least with the C57BL/6 mESC line, as treatment with LATA to reversibly depolymerize the cytoskeleton prior to cryopreservation did not improve PTR. Additionally, we established that LATA is inappropriate for subzero permeability parameter measurement in C57BL/6 mESC, as it significantly affects these values. Finally, the significant effects of Me₂SO, LATA, and temperature on V_{iso} challenge the previous assumption that V_{iso} is a static parameter, a finding that has implications for the accuracy of modeling using the two parameter mass transport model. The corresponding

changes in surface area to volume ratio induced by these effects warrants a future study on the sensitivity of fits to parameters.

Future Studies

Through the research presented in this dissertation, considerable advances were made with regards to our understanding of the fundamental cryobiology of mESCs. Ultimately, our systematic analysis of five mESC lines provided strong evidence that a single protocol, utilizing 1.0 M PG, a cooling rate of 1°C/minute, and plunge temperature of -41°C can be applied to most mESC lines with substantial improvement in PTR. Mouse ESC lines that cryopreserve poorly using this method can be approached on a case-by-case basis using the methods outlined in Chapters 2, 3, and 4. However, also in the course of this research, several key areas emerged in which future studies would be of great benefit.

Three constraints of current fundamental cryobiological models could affect the accuracy in prediction of optimal cooling rates and plunge temperatures, and these were discussed in Chapter 4. There are opportunities for future studies in each area with regards to the fundamental cryobiology of mESCs. For one thing, error may occur when one is applying assumptions made under relatively dilute, physiological conditions to predict cell osmotic behavior under nonphysiologic, nondilute conditions that occur during cryopreservation. As new models become available, they can be incorporated into

our analysis of fundamental cryobiological parameters to increase their predictive value. An example is the recent proposal by Elmoazzen *et al.* with respect to a nondilute solute transport model that does not make the previous dilute solution or near-equilibrium assumption [16].

A second constraint is the potential error in extrapolating suprazero E_a to subzero temperatures. In our studies, the assumption was made that suprazero measurement of permeability parameters can be applied to subzero conditions. Nonlinearities in the Arrhenius relationship involving L_p , arising from heterogeneity in water transport properties and temperature-dependent changes in the fluidity of the lipid membrane [17], may lead to inaccuracies in this assumption. While subzero permeability measurements are technically difficult, it will be worthwhile to perform these measurements in order to refine our method for optimizing mESC cryopreservation protocols.

The third constraint outlined in Chapter 4 was that of warming rate interactions. The effects of a particular warming rate are strongly dependent on the cooling rate, and for cells that are slowly cooled (slowly enough that sufficient dehydration occurs, with resulting avoidance of intracellular ice formation), the effects of warming rate are rather unpredictable, to the extent that empirical studies of different warming rates on the PTR of mESCs could reveal areas where further improvement in PTR is possible.

The insights gained in Chapter 5 with our studies on the effects of CPA, temperature, and LATA on C57BL/6 mESC osmotic response and permeability parameters revealed areas for future research. Our studies with LATA did not support its role as a CPA in mESC cryopreservation. However, the significant effect of LATA

treatment on V_b , V_{iso} , and permeability parameters opened doors to future studies exploring the role of the cytoskeleton in osmotic response and the maintenance of cell volume. These LATA studies could extend to mouse oocytes and Chinese Hamster Ovary cells, where LATA has a cryoprotective effect, to ascertain whether the protective effect is strictly due to removal of mechanical stressors during cryopreservation, or whether, in fact, it is due to altered permeability parameters and osmotic response.

Importantly, the changes outlined in Chapter 5 that occurred in V_{iso} as it equilibrated with 1.5 M Me₂SO have implications for the accuracy of modeling using the two parameter mass transport model, as this model is dependent upon the surface area to volume ratio of the cell [4][3]. Using the V_{iso} and V_b values estimated at 22°C (Table 5.2), the surface area to volume ratios ranged from 0.91 to 1.67. These numbers were similar, but different enough to warrant a future study on the sensitivity of fits to parameters.

Additionally, modeling of cell equilibration volumes at -3°C (Figure 5.7) revealed that significant differences in measurements of apparent V_b at -3°C in the presence of 1.5 M Me₂SO were likely due to inadequate equilibration times afforded to C57BL/6 mESCs at these temperatures. In order to verify whether V_b is significantly affected by CPA at subzero temperatures, we will re-visit our approach, allowing adequate equilibration time either through the exposure of CPA-equilibrated cells to salts and room temperature with progressive cooling to -3°C, or through the method outlined in Chapter 5, in which CPA-equilibrated cells were abruptly exposed to hyperosmotic solutions at -3°C, however in this case we will increase the equilibration time at -3°C as necessary.

Finally, to fully analyze the utility of PG as a CPA for a universally applied cryopreservation protocol, it is advisable for studies to be conducted on the effects of PG on the maintenance of mESC growth characteristics in culture, mESC gene expression, and germ-line transmissibility. The new cryopreservation protocol can be rigorously tested through standard mESC techniques such as population doubling and maintenance of mESC morphology in culture, chimera formation, teratoma formation, and germ-line transmission through the breeding of chimeric mice. Additionally, gene expression of individual mESC lines can be monitored by the use of real-time RT-PCR and microarrays to determine whether cryopreservation protocols induce inappropriate selective pressures on mESC lines resulting in altered cell line qualities. During cryopreservation, mESCs undergo selective pressure that favors their ability to be frozen and thawed that may not correlate to the distinct characteristics of that cell line in terms of ESC-related gene expression. The retention of mESC viability, pluripotency, germ-line transmissibility, and the unique gene expression “signature” of each cell line is vital to effective banking of mESCs.

References

1. Nobel, P.S., *The Boyle-Van't Hoff relation*. Journal of Theoretical Biology, 1969. **23**(3): p. 375-9.
2. Mazur, P., W.F. Rall, and S.P. Leibo, *Kinetics of water loss and the likelihood of intracellular freezing in mouse ova. Influence of the method of calculating the temperature dependence of water permeability*. Cell Biophys, 1984. **6**(3): p. 197-213.

3. Jacobs, M.H., *The simultaneous measurement of cell permeability to water and to dissolved substances*. Journal of Cellular and Comparative Physiology, 1933. **2**(4): p. 427-444.
4. Katkov, II, *A two-parameter model of cell membrane permeability for multisolute systems*. Cryobiology, 2000. **40**(1): p. 64-83.
5. Mazur, P., S.P. Leibo, and E.H. Chu, *A two-factor hypothesis of freezing injury. Evidence from Chinese hamster tissue-culture cells*. Exp Cell Res, 1972. **71**(2): p. 345-55.
6. Miszta-Lane, H., et al., *Effect of slow freezing versus vitrification on the recovery of mouse embryonic stem cells*. Cell preservation technology, 2007. **5**(1): p. 16-24.
7. Kashuba Benson, C.M., J.D. Benson, and J.K. Critser, *An improved cryopreservation method for a mouse embryonic stem cell line*. Cryobiology, 2008. **56**(2): p. 120-30.
8. Karow, A.M. and J.K. Critser, *Reproductive tissue banking : scientific principles*. 1997, San Diego: Academic Press. xviii, 472 p.
9. Arnaud, F.G. and D.E. Pegg, *Permeation of glycerol and propane-1,2-diol into human platelets*. Cryobiology, 1990. **27**(2): p. 107-18.
10. Woods, E.J., et al., *Determination of human platelet membrane permeability coefficients using the Kedem-Katchalsky formalism: estimates from two- vs three-parameter fits*. Cryobiology, 1999. **38**(3): p. 200-8.
11. Woods, E.J., et al., *Water and cryoprotectant permeability characteristics of isolated human and canine pancreatic islets*. Cell Transplant, 1999. **8**(5): p. 549-59.
12. Woods, E.J., et al., *Osmometric and permeability characteristics of human placental/umbilical cord blood CD34+ cells and their application to cryopreservation*. J Hematother Stem Cell Res, 2000. **9**(2): p. 161-73.
13. He, X., et al., *Vitrification by ultra-fast cooling at a low concentration of cryoprotectants in a quartz micro-capillary: a study using murine embryonic stem cells*. Cryobiology, 2008. **56**(3): p. 223-32.
14. Baudot, A., L. Alger, and P. Boutron, *Glass-forming tendency in the system water-dimethyl sulfoxide*. Cryobiology, 2000. **40**(2): p. 151-8.

15. Hosu, B.G., et al., *Reversible disassembly of the actin cytoskeleton improves the survival rate and developmental competence of cryopreserved mouse oocytes*. PLoS One, 2008. **3**(7): p. e2787.
16. Elmoazzen, H.Y., J.A. Elliott, and L.E. McGann, *Osmotic transport across cell membranes in nondilute solutions: a new nondilute solute transport equation*. Biophys J, 2009. **96**(7): p. 2559-71.
17. Verkman, A.S., *Water permeability measurement in living cells and complex tissues*. J Membr Biol, 2000. **173**(2): p. 73-87.

APPENDIX A

LIST OF ABBREVIATIONS

<i>A</i>	Cell surface area
ANOVA	Analysis of variance
B6	C57BL/6 mouse strain
CHO	Chinese hamster ovary
CPA	Cryoprotective agent
DPBS	Dulbecco's phosphate buffered saline
<i>E_a</i>	Activation energy
<i>E_a^{Lp}</i>	Activation energy of hydraulic conductivity
<i>E_a^{Pcpa}</i>	Activation energy of solute permeability
EG	Ethylene glycol
EPC	Electronic particle counter
ESC	Embryonic stem cell
EUCOMM	European Conditional Mouse Mutagenesis Program
FBS	Fetal bovine serum
FSC	Forward scatter
GLY	Glycerol
KOMP	Knockout Mouse Project
LATA	Latrunculin A

L_p	Hydraulic conductivity
L_p^{CPA}	Hydraulic conductivity in the presence of cryoprotectant
mESC	Mouse embryonic stem cell
Me ₂ SO	Dimethyl sulfoxide
mOsm	Milliosmoles
OTL	Osmotic tolerance limits
PG	Propylene glycol (1,2-propanediol)
PMEF	Primary mouse embryonic fibroblast cells
PTR	Percent post-thaw recovery
R	The universal gas constant
R1	129R1 mouse strain
SEM	Standard error of the mean
SSC	Side scatter
T	Temperature
t	Time
V	Cell volume
V_b	Osmotically inactive cell volume
V_{iso}	Isotonic cell volume
V_w	Intracellular water volume

VITA

Corinna Mary Kashuba Benson was born on December 30, 1971 to her Irish mother, Anna (nee Gow), and Canadian father, David Kashuba - both teachers - and grew up in Rumsey, Alberta, Canada. She was seven years old when her father died of a ruptured brain aneurysm. Along with her brother, Sheldon, and sister, Shauna, Corinna attended Rumsey, Murroe, and Morrin public schools, was valedictorian at her high school graduation in 1989, and graduated from the University of Alberta in 1993 with a Bachelor of Science with Specialization in Zoology. In 1999, she graduated from the University of Illinois at Urbana-Champaign with her Doctor of Veterinary Medicine degree. Following Chagas Disease research, part-time small animal veterinary practice, and employment as Veterinary Inspector for the Canadian Food Inspection Agency, Corinna attended the University of Missouri-Columbia. Here she gained a husband, James, and a son, Jonathan, and completed a residency in Comparative Medicine. She will complete her Ph.D. in the Pathobiology Area Program at the University of Missouri in August 2009.